Department of Biosciences and Bioengineering

Indian Institute of Technology Guwahati

Guwahati-781039 Assam, India

Understanding the mechanism of action of cytochalasin D against TNBC cell line MDA-MB-231 and a nano-carrier based drug delivery system

A THESIS

Submitted for the partial fulfilment of requirement for the award of

DOCTOR OF PHILOSOPHY

Under the guidance of

Prof. Gurvinder Kaur Saini

by

Arman Mohanty

Dedicated to

My Parents, Loved ones and the Almighty

INDIAN INSTITUTE OF TECHNOLOGY GUWAHATI

Department of Biosciences and Bioengineering

DECLARATION

I do hereby declare that the content embodied in this thesis is the result of investigations carried out by me in the **Department of Biosciences and Bioengineering, Indian Institute of Technology Guwahati, Guwahati, India**, under the supervision of **Prof. Gurvinder Kaur Saini.**

In keeping with the general practice of reporting scientific observations, due acknowledgements have been made wherever the work of other investigators are referred.

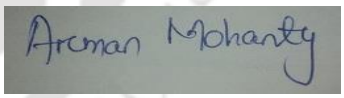

Date: 13/09/2024 **Arman Mohanty**

Place: Guwahati **176106018**

INDIAN INSTITUTE OF TECHNOLOGY GUWAHATI

Department of Biosciences and Bioengineering

CERTIFICATE

It is certified that the work described in this thesis entitled **"Understanding the mechanism of action of cytochalasin D against TNBC cell line MDA-MB-231 and a nano-carrier based drug delivery system"** by **Mr. Arman Mohanty (Roll no. 176106018)** for the award of degree of Doctor of Philosophy is an authentic record of the results obtained from the research work carried out under my supervision at the Department of Biosciences and Bioengineering, Indian Institute of Technology Guwahati, Guwahati, India and this work has not been submitted elsewhere for a degree.

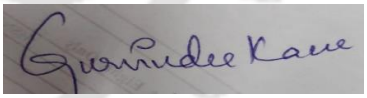

Date: 13/09/2024 **Prof. Gurvinder Kaur Saini**

Place: Guwahati **(Thesis supervisor)**

ACKNOWLEDGEMENT

I would like to express my deepest gratitude to all those who have supported and guided me throughout the course of my Ph.D. journey.

First and foremost, I wish to express my deepest gratitude to my supervisor, **Prof. Gurvinder Kaur Saini.** Her unwavering guidance, advice and continuous encouragement have been invaluable throughout this journey. I have greatly benefited from her expertise, wisdom and experience. I am truly fortunate to have had the opportunity to learn under her mentorship.

I would also like to extend my sincere thanks to the members of my thesis committee, *Prof. Senthilkumar Sivaprakasm, Prof. Selvaraju Narayanasamy, Dr. Biplab Bose* and *Prof. Gopal Das*. I would also like to thank my former committee members *Prof. Aiyagiri Ramesh* and *Prof. Sanjukta Patra*. Their constructive criticism, thoughtful suggestions, and challenging questions pushed me to refine my work and approach problems from different angles.

My heartfelt appreciation goes to my colleagues and friends in IIT Guwahati. The collaborative spirit, and mutual support we shared have been integral to my research experience. I am especially grateful to Dr. Dhana Singh, Dr. Balwant Singh, Dr. Neha Maurya, Arupam Patra and Sujisha S. Nambiar for their constant motivation and help across the duration of my Ph.D.

My deepest gratitude goes to my family, whose unconditional love and support have been my foundation throughout this journey. To my parents, thank you for instilling in me the values of hard work and perseverance. Your unwavering belief in my abilities has been a constant source of strength, and I am forever grateful for your sacrifices and encouragement.

I am also deeply thankful to my friends. Special thanks to Yangzing Lhamu Lepcha, Rajesh K. Shasani, Abhishek Mishra, Alok Senapati, Suraj K. Panda, Alok K. Pandey, Pratik Das Gupta, Siddharth Neog, Dr. Rafi Uz Zama Khan, Ajeet Kumar, Nikhil Kulkarni and Sahil Dhull, who provided me with much-needed balance and perspective. Your encouragement, humor, and understanding helped me navigate the challenges with doctoral research.

Finally, I am immensely grateful to the technical and administrative staff of IIT Guwahati for their assistance. The smooth running of experiments, availability of resources, and efficient handling of administrative tasks were made possible through their hard work and dedication.

This thesis is dedicated to everyone who has believed in me, supported me, and contributed to my journey. Your faith in my abilities and your contributions to this work are deeply appreciated.

Arman Mohanty

September, 2024

CONTENTS

ABSTRACT

Cancer remains one of the leading causes of mortality worldwide, with breast cancer being the most common malignancy affecting women. Breast cancer is a heterogeneous disease characterized by its complex biological behaviour and diverse clinical manifestations. The etiology of breast cancer is multifactorial, involving genetic predisposition, hormonal influences, and environmental factors. Advances in molecular biology have led to the identification of key oncogenes and tumor suppressor genes, which play crucial roles in the pathogenesis of breast cancer. The molecular subtyping of breast cancer into categories such as hormone receptor-positive, HER2-positive, and triple-negative has revolutionized treatment approaches, allowing for more personalized and targeted therapies.

Natural compounds have emerged as promising agents in the treatment of breast cancer, offering potential therapeutic benefits through their diverse mechanisms of action. Derived from plants, marine organisms, and other natural sources, these compounds exhibit anti-cancer properties, including the inhibition of cell proliferation, induction of apoptosis, and suppression of metastasis. But traditional drug discovery methods relied heavily on textbooks of the old world and is a cumbersome process.

Network pharmacology has become a powerful tool in anti-cancer drug discovery by providing a holistic approach to understanding the complex interactions between drugs, targets, and biological pathways. By integrating data from genomics, proteomics, and other omics technologies, network pharmacology aids in the identification of novel drug candidates and the repurposing of existing drugs, thereby accelerating the development of more effective and personalized anti-cancer therapies.

The present thesis focuses on employing network pharmacology to decipher the molecular targets of cytochalasin D in TNBC cell line MDA-MB-231. It also covers the *in vitro* therapeutic effects of cytochalasin D and cytochalasin D loaded PLGA nanoparticles

against MDA-MB-231 cells. The thesis has been divided into six chapters which have been briefed as follows.

Chapter 1 titled as '**Introduction and review of literature'** provides a detailed overview about the current global scenario of cancer, with focus on breast cancer. It discusses the current therapeutic strategies and also the challenges associated with it. Furthermore, it sheds light on the role of natural compounds from microbial origin in the ongoing fight against cancer. It also emphasizes on the role of network pharmacology in the discovery and development of novel drugs in cancer treatment. Further the chapter focuses on the use of nanocarriers to facilitate the delivery of anti-cancer agents. Finally, it delineates the scope of research and objectives of the thesis.

Chapter 2 titled **'Materials and Methods'** provides a comprehensive overview of the resources utilized and the experimental procedures employed to achieve the research objectives outlined in the previous chapter. This section meticulously details all the materials involved, including the specific software, cell lines, chemicals, and reagents used throughout the study. The chapter further elaborates on the methodologies adopted for conducting various experiments. Detailed protocols are provided for each experimental procedure. Additionally, the chapter includes a thorough description of the calculations and statistical analyses performed, offering insight into the data interpretation methods used to draw meaningful conclusions from the experimental results.

Chapter 3 titled **'*In*-silico identification of molecular targets of cytochalasin D in breast cancer cells'** focuses on identifying protein targets that may be involved in cancer progression through network analysis. Compounds structurally similar to cytochalasin D, along with their corresponding protein targets, were identified from three separate databases and mapped using Cytoscape software. The protein-protein interactions of all identified targets were examined using STRING software, and the resulting network was analyzed within the

Cytoscape-STRING software. Targets with the highest degree of centrality within the network were selected for further investigation. Gene Ontology (GO) and Kyoto Encyclopaedia of Genes and Genomes (KEGG) enrichment analyses were performed using DAVID software to gain insights into the biological processes and pathways associated with these targets. The shortlisted protein targets were then subjected to molecular docking and molecular dynamics simulations to evaluate their binding affinity with cytochalasin D. The results indicated a stable protein-ligand complex over a 100ns simulation with members of the Mitogen-Activated Protein Kinase (MAPK) family, specifically MAPK1, MAPK3, MAPK8, and MAPK14. In contrast, the other two candidates, JAK1 and c-SRC, did not demonstrate the same level of stability in binding with cytochalasin D.

Chapter 4 titled as **'*In vitro* therapeutic effects of Cytochalasin D against MDA-MB-231 cells'** focuses on the *in vitro* experiments conducted to determine the IC_{50} value of cytochalasin D against the TNBC cell line MDA-MB-231, assess its impact on cell monolayer progression, identify the phase of cell cycle arrest, and perform immunoblotting assays on the selected MAP kinase family targets. The results revealed that cytochalasin D induced 50% cell mortality at a concentration of 28.9 µg/mL. Furthermore, the anti-migratory effects of the compound were evident, as only 54% of the wound area healed in drug-treated cells, compared to complete healing in untreated cells, underscoring its ability to inhibit cell migration. Cytochalasin D also caused a significant disruption in cell cycle progression, with an accumulation of cells arrested in the S-phase. The treated cells also exhibited a 4-fold increase in intracellular ROS population. Western blot analysis showed a decrease in the expression levels of all four MAPKs (MAPK1, MAPK3, MAPK8, and MAPK14), demonstrating a direct correlation between higher drug concentrations and reduced protein expression levels.

Chapter 5 titled as **'Nano-carrier mediated delivery of cytochalasin D'** centred on developing a nano-carrier system for drug delivery that minimized immune response.

Nanoparticles were synthesized using PLGA as the primary polymer, PVA as the co-polymer, and TPGS as the surfactant. The emulsification of the aqueous and organic phases was achieved through sonication. The resulting nanoparticles were collected by ultracentrifugation, thoroughly washed, and then subjected to lyophilization. The lyophilized nanoparticle powders were characterized using ζ potential analysis, Field Emission Scanning Electron Microscopy (FESEM), and Field Emission Transmission Electron Microscopy (FETEM). Additionally, the cytotoxicity of both the unloaded (void) and drug-loaded nanoparticles was assessed against the MDA-MB-231 breast cancer cell line. The drug loaded NPs exhibited an average size of 54±21nm with an encapsulation efficiency of 60%. They also showed cytotoxicity against MDA-MB-231 cells at low concentrations of 1.056mg/mL and generated 2-fold more ROS compared to untreated cells.

The final chapter, **chapter 6** titled as **'Conclusion and Future prospects'** outlines the major findings of the thesis and viable applications of the research in improving the current scenario against cancer. The thesis focuses on better understanding of the molecular aspects of the cytotoxic activities of cytochalasin D against breast cancer. The results show the ability of the drug to be accepted widely as a chemotherapeutic drug.

ABBREVIATIONS

Term	Description
Akt	Ak strain transforming
AMPs	Antimicrobial peptides
APS	Ammonium persulphate
AR	Androgen Receptor
BL	Basal-Like
BP	Biological Processes
BSA	Bovine serum albumin
CAR T	Chimeric Antigen Receptor T
CC	Cellular Component
CRC	Colorectal cancer
DAVID	Database for Annotation, Visualization and Integrated Discovery
DCFDA	Dichlorodihydrofluorescein diacetate
DEPC	Diethyl pyrocarbonate
DMEM	Dulbecco's Modified Eagle's Medium
DMSO	Dimethylsulphoxide
DNA	Deoxyribonucleic acid
EDTA	Ethylenediamine tetraacetic acid
EGF	Epidermal growth factor
EGF	Epidermal growth factor
EMT	Epithelial-Mesenchymal Transition
EPR	Enhanced Permeability and Retention
ER	Estrogen Receptor

EtBr	Ethidium Bromide
FBS	Fetal bovine serum
FESEM	Field Emission Scanning Electron Microscopy
FETEM	Field Emission Transmission Electron Microscopy
GO	Gene Ontology
HER2	Human epidermal growth factor receptor 2
HPV	Human Papillomavirus
hr	highly reducing
IM	Immunomodulatory
IPTG	Isopropyl β- d-1-thiogalactopyranoside
KEGG	Kyoto Encyclopedia of Genes and Genomes
LAR	Luminal Androgen Receptor
LPS	Lipopolysaccharides
M	Mesenchymal
MD	Molecular dynamics
MDA-MB	M. D. Anderson Metastatic Breast cancer
MDR	Multi-drug resistance
MF	Molecular Function
MMPBSA	Molecular Mechanics Poisson-Boltzmann Surface Area
MSL	Mesenchymal Stem-Like
MTCs	Microbial tryptophan catabolites
mTOR	Mammalian target of rapamycin
MTT	3-(4, 5-dimethylthiazolyl-2)-2, 5-diphenyltetrazolium bromide
NCCS	National Centre for Cell Sciences

NPs	Nanoparticles
nr	non-reducing
NRPs	Non-ribosomal peptides
NRPSs	Non-ribosomal peptide synthetases
PBS	Phosphate-buffered saline
PCL	Polycaprolactone
PCR	Polymerase chain reaction
PDA	Potato dextrose agar
PDB	Protein Data Bank
PEG	Polyethylene glycol
PI	Propidium Iodide
PI3K	Phosphoinositide 3 kinase
PKS	Polyketide synthases
PLA	Polylactic acid
PLGA	Poly (lactic-co-glycolic acid)
PMSF	Phenylmethylsulfonyl fluoride
PPI	Protein-Protein Interaction
PR	Progesterone Receptor
pr	partially reducing
PVDF	Polyvinylidene difluoride
RIPA	Radioimmunoprecipitation assay
RMSD	Root Mean Square Deviation
RMSF	Root Mean Square Fluctuation
ROS	Reactive Oxygen Species

SCFAs	Short chain fatty acids
SDS	Sodium dodecyl sulphate
SDS-PAGE	Sodium Dodecyl Sulfate Polyacrylamide Gel Electrophoresis
SIDER	Side Effect Resource
SMs	Secondary metabolites
STITCH	Search Tool for Interactions of Chemicals
STRING	Search Tool for the Retrieval of Interacting Genes/Proteins
TBST	Tris-buffered saline with Tween 20
TCM	Traditional Chinese Medicine
TCMSP	Traditional Chinese Medicine Systems Pharmacology
TEMED	Tetra methyl ethylene diamine
TNBC	Triple-Negative Breast Cancer
TPGS	d-alpha-tocopheryl polyethylene glycol 1000 succinate
VEGF/MMP	Vascular Endothelial Growth Factor/ Matrix Metalloprotease
WHO	World Health Organization

LIST OF SCHEMES

LIST OF FIGURES

LIST OF TABLES

Chapter 1

Introduction and Review of literature

1.1. Cancer

The human body, composed of approximately 30 trillion cells, functions as a highly complex and interconnected system, where each cell type plays a specific role in maintaining overall health (Weinberg, n.d.). These cells exist in a finely tuned balance, working in harmony to regulate each other's growth, division, and function. Through various signaling pathways and feedback mechanisms, cells can monitor and control each other's behavior, preventing uncontrolled growth and ensuring that damaged or unnecessary cells are removed (Schwartzman & Cidlowski, 1993). This cellular regulation is essential for maintaining homeostasis. However, when these mechanisms fail, it can lead to the unchecked proliferation of cells leading to formation of tumors, which can be either cancerous (malignant) or non-cancerous (benign). Cancerous tumors invade nearby tissues and can travel to distant places in the body via the lymphatic or circulatory system, a process known as metastasis.

A multifaceted disease such as cancer is associated with various risk factors that can increase the likelihood of its development. These can be broadly categorized into lifestyle (use of tobacco, alcohol consumption, obesity, physical inactivity, diet), environmental (pollution, exposure to sunlight for long durations, carcinogens), genetic (family history, inherited genetic mutations), biological factors (age, hormonal changes, chronic inflammation) and Human Papillomavirus (HPV) infection (Danaei et al., 2005).

Cancer cells exhibit several key differences compared to normal cells. They grow in the absence of signals, ignore vital checkpoints during cell cycle progression, evade apoptosis, promote angiogenesis and accumulate multiple changes in their chromosomes (Amin et al., 2015). They can be categorized into two sub-groups:

- Hematologic (Blood) Cancers: Leukemia (cancer of the bone marrow), Lymphoma (cancer of the lymphatic system), Multiple myeloma (cancer affecting plasma cells in the bone marrow)
- Solid Tumor Cancers: Carcinoma (cancer of skin or tissues lining other organs), Sarcoma (originates in connective tissues)

1.2. Breast cancer: Tackling the complex landscape of a global health challenge

The global cancer landscape is a cause for concern, with breast cancer emerging as the second most prevalent cancer type worldwide, in terms of incidence. Annually, there are approximately 2.2 million new cases of breast cancer, placing it just behind lung cancer, which leads with around 2.4 million cases each year. It is also the fourth leading cause of cancer related morbidity, accounting for nearly 0.7 million (6.8%) deaths (Bray et al., 2024).

Despite progress in medical technology and increased awareness, breast cancer continues to be a leading cause of cancer-related deaths among women. The incidence of breast cancer varies globally, with developed regions reporting higher rates due to more effective screening programs and longer life expectancies. Conversely, low- and middle-income countries are seeing a rise in breast cancer cases as they experience lifestyle changes and increased urbanization. Global estimates by the World Health Organization (WHO) suggests that the mortality rate is higher in less developed countries, where 1 in 48 women will succumb to breast cancer, as opposed to 1 in 71 women in highly developed countries (Bray et al., 2024).

Considering the heterogeneity of breast cancer, its classification into molecular subtypes has significantly advanced the understanding and treatment of the condition. These molecular subtypes are identified based on the expression of hormone receptors and the human epidermal growth factor receptor 2 (HER2).

- **Luminal A** breast cancer is characterized by its positive status for hormone receptors, specifically estrogen receptor-positive (ER+) and/or progesterone receptor-positive (PR+), while lacking HER2 overexpression (Creighton, 2012). These tumors are usually exhibit slower growth rate and typically a more favorable outcome following treatments. Due to their hormone receptor status, Luminal A cancers are commonly treated with hormone therapies such as tamoxifen or aromatase inhibitors, which can be effective in managing the disease.
- **Luminal B,** like Luminal A, is also hormone receptor-positive but may be HER2-positive or HER2-negative. Luminal B tumors are typically higher grade, grow faster, and have a worse prognosis compared to Luminal A. They may require a combination of hormone therapy and chemotherapy (Ades et al., 2014).
- **HER2-Enriched** subtype is characterized by being HER2-positive and hormone receptor-negative (ER- and PR-). HER2-enriched tumors are often more aggressive and have a poorer prognosis. Treatment involves HER2-targeted therapies, such as trastuzumab (Agus et al., 2002; Ghosh et al., 2011) and pertuzumab (Agus et al., 2002), has significantly improved outcomes for patients with this subtype.
- **Triple-Negative Breast Cancer (TNBC)** is negative for ER, PR, and HER2. It is considered to be the most aggressive subtype with a higher likelihood of recurrence and poorer prognosis. Because it lacks the targets for hormone therapy and HER2-targeted treatments, chemotherapy remains the main treatment option despite advancements in targeted and biological therapies (Isakoff, 2010).

Breast cancer treatment has evolved significantly with the advent of molecular profiling, enabling a more personalized approach tailored to the specific characteristics of each patient's tumor. Traditionally, breast cancer treatment was based on clinical features such as tumor size, grade, and lymph node involvement. The advances in

molecular biology helped understand that breast cancer is not a single disease but a group of distinct subtypes, each with its own biological behavior, prognosis, and response to treatment. This has revolutionized the way breast cancer is treated, moving towards a more individualized strategy that improves outcomes and reduces unnecessary side effects (Klocker et al., 2022; Malone et al., 2020).

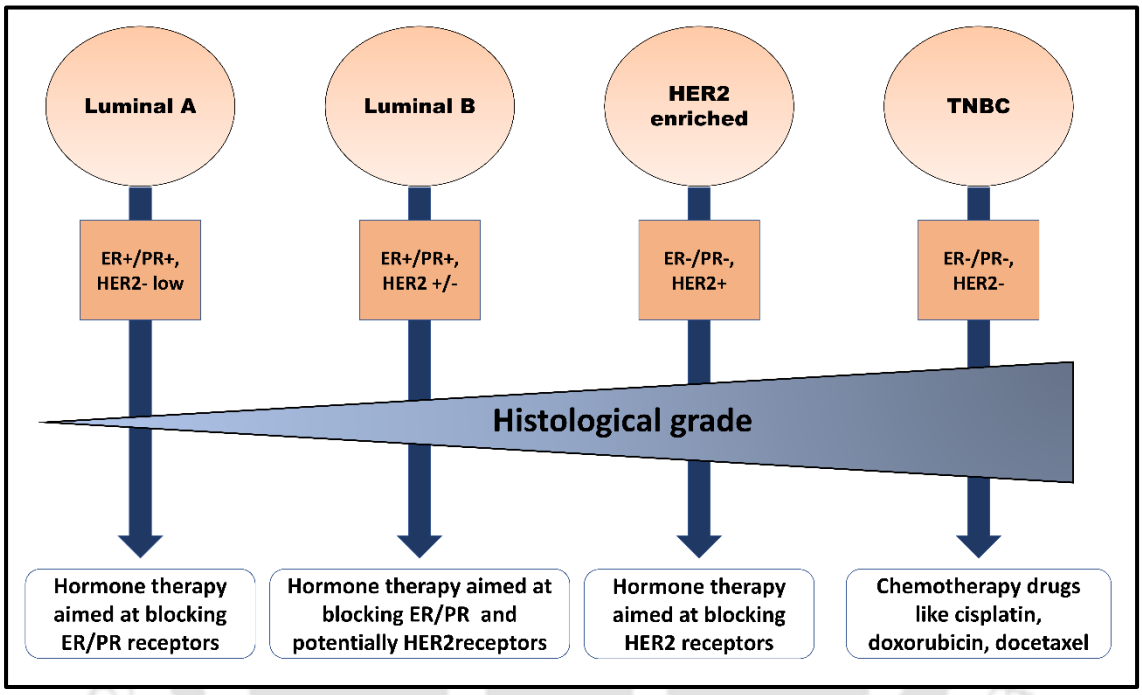

Scheme 1.1. Schematic representation of molecular subtypes of breast cancer (ER- Estrogen Receptor, PR- Progesterone Receptor, HER2- Human Epidermal Growth Receptor factor 2). (*Illustrated using Biorender*)

1.3. TNBC: Current global scenario and available treatments

Triple-negative breast cancer (TNBC) is recognized as one of the most aggressive forms of breast cancer, characterized by the absence of three key receptors: estrogen receptors (ER), progesterone receptors (PR), and human epidermal growth factor receptor 2 (HER2). These receptors are commonly targeted in other breast cancer subtypes for treatment, but their absence in TNBC makes the tumors non-responsive to hormone therapy and HER2-targeted treatments (Kumar & Aggarwal, 2016; Mani et al., 2022).

The aggressive nature of TNBC is partly due to its high grade, rapid proliferation rate, and its tendency to metastasize early in the disease course (Bianchini et al., 2022). It accounts for 10-15% of all breast cancer incidences globally and is most commonly seen in African- American and pre-menopausal women (Zagami & Carey, 2022).

Molecular subtyping has been pivotal in unravelling the heterogeneity of TNBC and designing of therapeutic strategies. Four major subtypes have been listed basing on the expression or absence of characteristic genes among the tumor cells. Basal-Like (BL) subtype is the most common and well-studied subtype of TNBC. It is often associated with high grade tumors, exhibits high proliferation rates and a poor prognosis (Espinosa Fernandez et al., 2020). The Immunomodulatory (IM) subtype is distinguished by the presence of immune cell signaling pathways and genes related to immune responses. This subtype has a better prognosis compared to other TNBC subtypes (Garrido-Castro et al., 2019). The Mesenchymal (M) and Mesenchymal Stem-Like (MSL) subtypes are characterized by gene expression profiles related to epithelial-mesenchymal transition (EMT), cell motility, and stem cell-like features. This subtype is often very aggressive, highly likely to metastasize and develop drug resistance (S. Zhu et al., 2023). The Luminal Androgen Receptor (LAR) subtype is characterized by the expression of androgen receptor (AR) and genes typically associated with luminal breast cancer. It usually has a slower growth rate and a better prognosis compared to other subtypes (Y.-M. Lee et al., 2020).

Present-day treatment approaches for TNBC are diverse, encompassing traditional therapies, novel targeted treatments, and continuous clinical research efforts. The inherently aggressive behavior of TNBC, combined with its non-expression of hormone receptors and HER2, narrows the scope of available treatments relative to other breast cancer subtypes (M. A. Medina et al., 2020; Obidiro et al., 2023).

- **Chemotherapy** is the use of anti-cancer drugs to treat or control cancerous cells. Usually administered following surgery in a "dose dense" fashion (Citron, 2008), it is also sometimes used prior to surgery (neoadjuvant) to assist in reducing the size of the tumor (Colleoni et al., 1998). Most commonly used chemotherapy agents include anthracyclines, taxanes, platinum chemo-drugs, etc (Y. Li et al., 2022).
- **Radiotherapy** or **radiation therapy** is often employed as a crucial part of the multimodal treatment approach for TNBC. It reduces the likeliness of local reoccurrence following surgery (Haussmann et al., 2020). Advances in radiation oncology has paved path for newer combinatorial approaches such as radiogenomics (Grimm & Mazurowski, 2020) and radiotherapy coupled with immunotherapy (Tsoutsou et al., 2018).
- **Surgery** is employed depending on the stage of the cancer. Usually one of the two methods i.e. breast-conserving surgery (lumpectomy and quadrantectomy) or mastectomy (surgical removal of the entire breast) is performed (Cotlar et al., 2003). It is often integrated with other treatments to maximize the chances of cure, improve survival rates and limit the chances of recurrence.
- **Targeted therapy** found its way into cancer treatment following the advent of molecular subtyping. It has been thoroughly helpful in treatment of HER2-amplified subtypes. Alongside the existing drugs such as trastuzumab and pertuzumab, many new agents are being regularly tested, hence widening the range of therapeutic options (Higgins & Baselga, 2011).
- **Immunotherapy** is one of the most recent advancements in cancer therapy. Immune checkpoint inhibitors such as pembrolizumab, atezolizumab, etc. help the body to generate T-cells, that can actively kill off cancerous cells. A combination

of immune checkpoint inhibitors with conventional therapies and other immunotherapeutic strategies such as cancer vaccines, CAR-T (Chimeric antigen receptor T) cells, bispecific antibodies, and oncolytic viruses are undergoing clinical trials (Debien et al., 2023).

The diverse range of therapies available for breast cancer, tailored to its various molecular subtypes, underscores the importance of personalized treatment approaches. Combination of targeted therapies, surgery, chemotherapy, and radiotherapy, along with emerging biologic agents, offers more effective and individualized care, improving outcomes and quality of life for patients battling this complex disease.

1.4. Nature: Exploring the reservoir of anticancer agents

Nature has long been a rich source of novel anticancer agents, providing a diverse array of compounds that have significantly contributed to the advancement of cancer therapy (Moraes et al., 2017). Secondary metabolites (SMs) are such organic compounds produced by plants, fungi, and other microorganisms. Unlike primary metabolites (essential for growth and development), secondary metabolites serve various ecological functions, such as defense against herbivores, pathogens, and environmental stressors (Zeeshan Bhatti et al., 2022). These compounds exhibit diverse chemical structures and biological activities. For generations, plants have served as the primary sources of therapeutic SMs which include alkaloid (Nitrogen-containing compounds), flavonoids (Polyphenolic compounds with antioxidant properties), terpenoids (Derived from isoprene units and include essential oils), tannins (Polyphenols that bind to proteins and inhibit enzymes), coumarins (Benzopyrone derivatives with diverse biological effects), quinones (Compounds involved in redox reactions), carotenoids (Pigments responsible for color in fruits and vegetables), steroids (Lipid-based compounds with hormonal

roles). Many plant-derived metabolites have shown promising anti-carcinogenic properties and are used in the current approaches for treatment of cancer. To list a few:

- **Paclitaxel (Taxol):** Derived from the bark of the Pacific yew tree (*Taxus brevifolia*), is one of the most commonly used chemotherapy drugs. It works as a microtubule inhibitor, thereby arresting the cells in G2/M phase and preventing cell division and growth (Das & Agarwal, 2024).
- **Vincristine and Vinblastine:** Originally sourced from the Madagascar periwinkle (*Catharanthus roseus*), these alkaloids have been used in cancer treatment. Vincristine disrupts microtubule formation, while vinblastine inhibits cell division (Das & Agarwal, 2024).
- **Topotecan:** Derived from a chemical found in the Chinese tree (*Camptotheca acuminata*), topotecan is an anticancer drug that targets topoisomerase I, an enzyme involved in DNA replication and repair (M. Huang et al., 2021).
- **Irinotecan:** Another topoisomerase I inhibitor, irinotecan is used in colorectal cancer treatment. It is derived from the same plant as topotecan (M. Huang et al., 2021).
- **Etoposide:** Obtained from the American mayapple (*Podophyllum peltatum*), etoposide inhibits topoisomerase II and is used against various cancers (M. Huang et al., 2021).

Today, approximately 47 anticancer drugs have been approved by regulatory authorities and are directly derived from plants. These plant-based compounds represent a significant portion of the arsenal used in modern cancer therapy. The natural compounds isolated from plants have not only demonstrated potent anticancer activity but have also served as templates for the development of synthetic derivatives and analogs. These synthetic versions are often engineered to enhance efficacy, reduce

toxicity, and improve pharmacokinetic properties, making them more effective and safer for patient use. The success of these plant-derived drugs underscores the importance of natural products in drug discovery and highlights the ongoing need to explore the vast biodiversity of plants for new therapeutic agents. As research advances, the potential for discovering even more effective treatments from plant sources remains a promising area in the fight against cancer.

1.5. Bacteria as allies in the fight against cancer

Historically, bacteria have been primarily recognized as pathogens, responsible for causing a wide range of diseases. Certain bacterial strains have also been implicated in the development of cancer, highlighting a complex relationship between microbes and human health. Although most bacteria are harmless or even beneficial to their hosts, specific strains have been identified as contributors to carcinogenesis, either by directly inducing mutations, promoting chronic inflammation, or altering the host's immune response (Song et al., 2018). For example, *Helicobacter pylori* is associated with gastric cancer (Correa et al., 1990), *Salmonella typhi* is associated with hepatobiliary carcinoma (Upadhayay et al., 2022), *Campylobacter jejuni* is associated with small intestinal lymphomas (Mesnard et al., 2012), *Chlamydia psittaci* is associated with ocular lymphomas (Ferreri et al., 2004), *Mycobacterium tuberculosis* is associated with lung cancer (P. K. Gupta et al., 2016), and *Citrobacter rodentium* is associated with human colorectal cancer (De Spiegeleer et al., 2015).

Although some bacterial strains are implicated in the onset and progression of cancer, numerous bacterial metabolites have been identified as potent chemotherapeutic agents. These natural compounds have shown significant promise in the fight against cancer, offering new avenues for treatment. Anticancer metabolites of bacterial origin exhibit

their effects through various mechanisms, targeting multiple pathways crucial for cancer development and progression.

- **Inhibition of cell proliferation:** Anthracyclines, such as doxorubicin, inhibit DNA synthesis by intercalating into DNA strands, halting replication and transmission in rapidly dividing cells (Tacar et al., 2012). Another mechanism of doxorubicin involves the generation of reactive oxygen species within the cells leading to apoptosis via oxidative stress (H. Zhu et al., 2016). Actinomycin D inhibits the DNA unwinding mechanism of the enzyme topoisomerase II leading to DNA damage and cell death (Onishi et al., 1993).
- **Induction of apoptosis:** Antimicrobial peptides (AMPs) alter the membrane permeability of mitochondria, leading to the release of pro-apoptotic factors, such as cytochrome c. this in-turn leads to the activation of caspase 9 and subsequent activation of caspase 3 ultimately driving the cells to apoptosis (H. Wang et al., 2022; Weber-Stiehl et al., 2022). Short chain fatty acids (SCFAs) (Rangan & Mondino, 2022), Microbial tryptophan catabolites (MTCs) (Liu et al., 2023) and Lipopolysaccharides (LPS) (Reis-Sobreiro et al., 2021) can enhance expression of death receptors on the surface of cancer cells, making them easy targets for apoptosis via cells of the host immune system.
- **Microtubule dynamics disruption:** Epothilones work on the same principle as the first generation taxanes (Paclitaxel and Docetaxel), i.e. stabilization and depolymerization of microtubules. This disrupts the cytoskeletal framework of the cancer cells hence hindering cell division (Bollag, 1997; Kowalski et al., 1997).
- **Angiogenesis inhibition:** Cell-free supernatants from *Lactobacillus plantarum* prevents metastasis of colorectal cancer (CRC) by hindering the formation of blood vessels around tumor microenvironment. This is achieved by the downregulation

of VEGF/MMPs (Vascular Endothelial Growth Factor/ Matrix Metalloprotease) signaling pathway (Yue et al., 2020).

- **Blocking oncogenic pathways:** Several probiotic bacteria belong to the genus *Lactobacillus*, *Bifidobacterium*, *Lactococcus*, and *Enterococcus* spp have been found to interfere with key signal transduction pathways that are often upregulated in cancer cells, such as the PI3K/AKT/mTOR (Phosphoinositide 3 kinase/Ak strain transforming/Mammalian target of rapamycin) pathway (Gulhati et al., 2011; Porta et al., 2014; Roulin et al., 2010).

1.6. Power of fungal alchemy

Fungal secondary metabolites are a diverse group of bioactive compounds produced often in response to environmental stresses or during specific stages of their lifecycle. These compounds, however, not involved in basic cellular processes, serve other critical roles such as defense against predators, help in competition against other microorganisms and as agents of communication in symbiotic relationships (Roy et al., 2021). Fungal metabolites exhibit a wide range of biological activities, including antibiotic, antifungal, antiviral, and anticancer effects, underscoring their significant role in pharmaceutical development (Abdel-Wareth, 2021). A well-developed secondary metabolism coupled with the ability of fungi to colonize various habitats, serves as an added advantage over plants, for the synthesis and production of multiple life-saving drugs (Yogeswari et al., 2023).

Although fungi produce a large number of mycotoxins, that are harmful to plants, crops and humans, the beneficial aspects of fungi cannot be left unnoticed. Fungal SMs are categorized thoroughly on the basis of their chemical structures, but can be broadly classified into four major families:

- **Terpenoids,** also known as isoprenoids, are a diverse group of naturally occurring organic compounds derived from the 5-carbon compound isoprene and its derivatives. Often referred to as adaptogens as they help the fungal body to cope with stress and maintain balance (González-Hernández et al., 2023). Fungal terpenoids are fascinating to medicinal chemists due to their biological activities, such as antimicrobial (Grifolin from fungus *Grifola frondosa*) (Goto et al., 1963), antitumor (Cordycepin from *Cordyceps militaris*) (Nakamura et al., 2015), cytotoxic (Fumagilin from *Aspergillus fumigatus*) (Okrój et al., 2005), and anti-inflammatory properties (Ganoderic acid from *Ganoderma lucidum*) (J.-Q. Ma et al., 2021).
- **Polyketides** originate from the condensation of simple acyl CoA thioesters. Biosynthesized by Type I iterative polyketide synthases (PKS), these enzymes can be further defined as non-reducing (nr), partially reducing (pr) and highly reducing (hr) PKS. Some of the notable fungal polyketides that have been in use for decades are, penicillin (antibiotic and antifungal properties) (Spratt, 1980), epithilones (anticancer compounds) (Bollag, 1997), cyclosporin A (immunosuppressive agent) (Borel et al., 1994), lovastatin (cholesterol lowering agent) (Garg & Grundy, 1988) and many more.
- **Non-ribosomal peptides (NRPs)** are secondary metabolic compounds mainly composed of specific or modified amino acids and hydroxyl acids. These are synthesized by non-ribosomal peptide synthetases (NRPSs) and are important pathogenic factors in entomogenous fungi (Berg et al., 1965). NRPs exhibit a wide array of biological activities, including insecticidal, antibiotic, antiviral, and antitumor properties (Jakubczyk & Dussart, 2020).

- **Hybrids:** PKS–NRPS hybrid systems combine elements of both PKS and NRPS pathways to produce hybrid natural products that incorporate features of both polyketides and nonribosomal peptides (Du et al., 2001). These complex natural products exhibit diverse bioactivities, including antimicrobial, antifungal (Prado-Alonso et al., 2022), antiviral, and anticancer (Shen et al., 2001) properties.

1.6.1. Anticancer agents from entomopathogenic fungi

Entomopathogenic fungi are a unique group of microorganisms that primarily infect and kill insects (Sabbahi et al., 2022). These fungi have evolved specialized mechanisms to invade, colonize, and eventually destroy their insect hosts, making them valuable in biological control of pest populations. Beyond their role in entomology, these fungi are garnering attention for their potential in medicine, particularly in cancer research. Their complex life cycles and interactions with hosts have led to the production of a diverse array of bioactive compounds, some of which exhibit potent anticancer properties (Quiñonero et al., 2024; Rai et al., 2022). These secondary metabolites, produced as part of their survival strategy, are now being explored for their ability to target cancer cells, offering new avenues for the development of novel anticancer therapies.

The unique ecological niche of entomopathogenic fungi drives the production of diverse and structurally complex compounds that can target cancer cells in various ways. Many fungal metabolites have been found to trigger apoptosis in cancer cells by activating specific cellular pathways, such as the intrinsic (mitochondrial) and extrinsic (death receptor) pathways. For example, compounds like cytochalasins, produced by certain entomopathogenic fungi, can disrupt the actin cytoskeleton in cancer cells, leading to cell cycle arrest and apoptosis (Brown & Spudich, 1981). Other metabolites such as epithilones (primarily obtained from soil-dwelling bacteria, but also found in

endophytic fungi) inhibit mitosis by interfering with key enzymes and proteins involved in cell division (Bollag, 1997). Other mechanisms of action involve disruption of key cell signaling pathways, inhibition of angiogenesis and immune modulation, much like as seen in their microbial counter parts i.e. bacteria, which has been discussed in detail in the previous sections. As research in this field progresses, entomopathogenic fungi are gaining recognition as a valuable reservoir of natural products with potential applications in cancer therapy while offering lesser side effects compared to conventional chemotherapy.

1.7. Cytochalasins

Cytochalasins are a fascinating and diverse group of fungal metabolites that have captured the attention of researchers across various scientific fields due to their unique biological activities and potential therapeutic applications. Originally discovered in the late 1960s from the fungus *Helminthosporium dematioideum* (C Aldridge et al., 1967)(now classified under the genus *Phoma*), cytochalasins have since been identified in several other fungal species, including *Metarhizium anisopliae* (Vilcinskas et al., 1997) and *Aspergillus clavatus* (Qiao et al., 2011). These compounds are part of a larger class of secondary metabolites known as mycotoxins, which fungi produce to deter predators and compete with other microorganisms in their environment.

Characterized extensively based on their complex molecular structures, over 20 different cytochalasins analogs such as cytochalasin A, B, C, D, E, F and G (Binder & Tamm, 1973; Goddette & Frieden, 1986) have been identified the most notable ones being cytochalasin B (Bogyo et al., 1991) and D (F. Y. Huang et al., 2012). These analogs have also inspired the chemical synthesis of various derivative compounds with similar activities.

Malignant cells are marked by significant alterations in the cytoskeleton, leading to changes in cell shape, movement, and adhesion properties (Hayot et al., 2006; Stehn et al., 2006). These cytoskeletal disruptions contribute to the aggressive behavior of cancer cells, enabling them to invade surrounding tissues and metastasize to distant sites, thus playing a critical role in the progression of malignancy. Hence, targeting microfilaments offers a more promising therapeutic approach. The primary mechanism of action of cytochalasins revolves around their ability to bind to actin filaments. Cytochalasins bind to the barbed end of actin filaments, inhibiting the polymerization of actin monomers (G-actin) into filaments (F-actin). This disruption of actin polymerization leads to a cascade of effects, including altered cell morphology, inhibition of cell division, and induction of apoptosis (programmed cell death) (Brown & Spudich, 1979, 1981). Apart from their ability to disrupt the cytoskeletal framework, cytochalasins also inhibit angiogenesis which creates a nutrition-deprived environment in cancer cells (F.-Y. Huang et al., 2012; J. Lee et al., 2014; Y. Ma et al., 2019).

1.7.1. Cytochalasin B

Cytochalasin B was first isolated from the mold *Helminthosporium dematioideum* and has since been extensively studied for its unique biological activities. Most importantly, it is known for its ability to inhibit various types of cellular movement by interacting with the actomyosin complex, a key contractile protein structure in striated muscle. Its primary mode of action is through a direct interaction with the actin component of the actomyosin complex (Spudich & Lin, 1972). This selective targeting of actin by cytochalasin B disrupts essential cellular functions, such as cell motility and division, making it a critical tool in studies of cytoskeletal dynamics and a potential candidate for therapeutic applications, such as in cancer treatment. It also inhibits contractile ring and central spindle formation during cell division in mammalian cells (Cimini et al.,

1998). Cytochalasin B has also been reported to exhibit cytotoxicity against HeLa human cervical carcinoma cells at IC_{50} concentrations of 7.9 µM by ROS (Reactive oxygen species) generation and inhibition of actin filament elongation (Hwang et al., 2013; Su et al., 2018).

1.7.2. Cytochalasin D

Cytochalasin D is a structural isomer of cytochalasin B. It has been isolated from the molds of *Metarhizium anisopliae* (Fujii et al., 2000) and *Zygosporium mansonii* (Hädener et al., 1989). Although similar in action, it exhibits higher efficacy in achieving actin depolymerization when compared to cytochalasin B (Brown & Spudich, 1979) although this enhanced affinity towards actin filaments has resulted in limiting its use as a commercial drug. The disruption of the cytoskeleton can result in the inhibition of cell migration and invasion, which are critical processes in cancer metastasis. Furthermore, cytochalasin D has been shown to induce apoptosis, or programmed cell death, in various cancer cell lines. This is achieved by triggering a cascade of molecular events that lead to the activation of apoptotic pathways, including the release of cytochrome c from mitochondria and the activation of caspases (Małecki et al., 2010). In another study, it was observed that cytochalasin D affects the cell cycle machinery by elevating levels of p53 and preventing entry of cells into S-phase (Rubtsova et al., 1998). p53 is essential in regulating cell growth and maintaining cellular integrity (Hansen & Oren, 1997; Levine, 1997). It orchestrates cellular responses to various stressors including DNA damage (Kuerbitz et al., 1992), inhibition of nucleic acid synthesis (Chernova et al., 1995) and upregulation of oncogenes (Serrano et al., 1997).

While cytochalasin D shows significant promise as an anticancer agent, its therapeutic application is not without challenges (Trendowski, 2015). Its potent effects on normal

cells can lead to toxicity and side effects. Hence, its effects in synergy with compounds have been of great interest. A brief (1-hour) treatment with latrunculin A and cytochalasin D at specific concentrations disrupts the subcortical actin filaments, leading to the breakdown of these structures and a temporary halt in cytoplasmic streaming in Characean internodal cells (Foissner & Wasteneys, 2007). Another study involving cytochalasin congeners including cytochalasin D with three other clinically approved drugs doxorubicin, paclitaxel and vinblastine, showed cytochalasins to inhibit the efflux mechanism of ABC transporters in human ovarian carcinoma cells (Trendowski, Christen, et al., 2015). Notable works of cytochalasin D has been listed in the following table

Effects	Research article	Output
Inhibition of cytokinesis	Puszkin et al. 1973	Cytochalasin D disrupts cytokinesis, leading to the formation of multinucleated cells, as the actin cytoskeleton is essential for the formation of the contractile ring during cell division.
Cell morphology	Brown and Spudich 1981	Treated cells exhibit altered morphology, including loss of lamellipodia and filopodia, and rounding up of cells, indicating cytoskeletal reorganization
Actin polymerization inhibition	Cooper 1987	Cytochalasin D binds to the barbed (fast-growing) ends of actin filaments, inhibiting their polymerization and leading to the disruption of the actin cytoskeleton.
Gene expression profiling	Loty et al. 1995	Cytochalasin D alters the expression of numerous genes involved in cytoskeletal organization, cell cycle regulation, and apoptosis.
Induction of apoptosis	White et al. 2001	Cytochalasin D induces apoptosis in respiratory epithelial cell, possibly through the disruption of the cytoskeleton and subsequent activation of apoptotic pathways.
Anti-tumor activity	Huang et al. 2012	Cytochalasin D exhibits cytotoxic effects on cancer cells, reducing cell viability and tumor growth, partly by disrupting the actin cytoskeleton and inhibiting essential cellular processes.
Cell migration and invasion	Shankar and Nabi 2015	Cytochalasin D significantly inhibits cell migration and invasion by disrupting the actin cytoskeleton which results in inhibition of EMT, which is crucial for cell motility.
Impact on signaling pathways	Glaviano et al. 2023	Cytochalasin D modulates various signaling pathways, such as the MAPK and PI3K/Akt pathways, affecting cell survival, proliferation, and apoptosis.

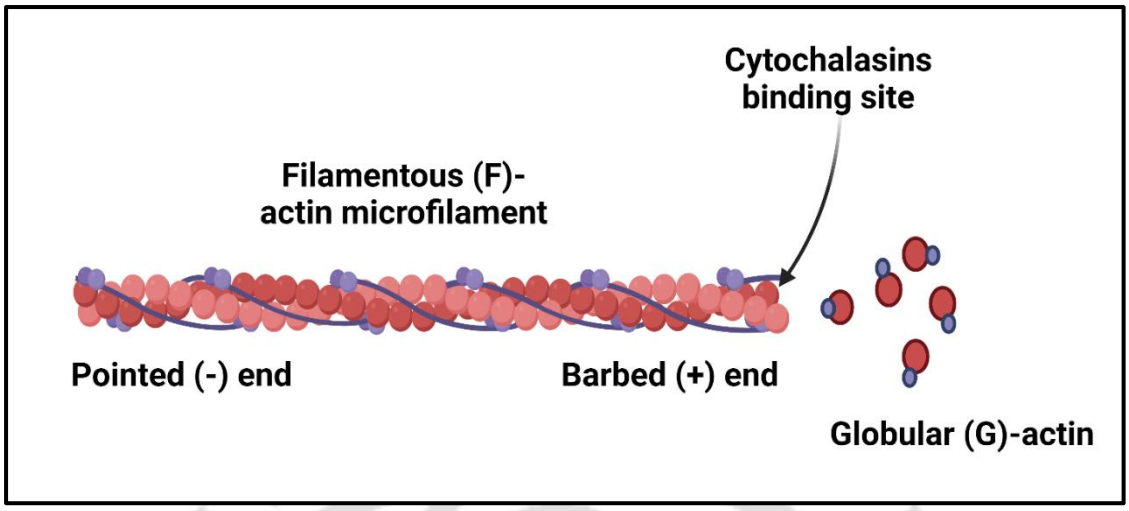

Scheme 1.2. Schematic representation of mode of action of cytochalasin B and D on actin filament (*Conceptualized and illustrated based on* (Trendowski, 2015) *using Biorender*)

1.8. Network pharmacology

The advent of network pharmacology has helped tackle the challenges associated with one-drug/one-target/one-disease conventional approach. It is a multidisciplinary study that integrates systems biology, polypharmacology and network science together to decipher the interconnectivity between several disease targets and drugs, simultaneously highlighting the role of a single drug in multiple diseases (Chandran et al., 2017).

Traditionally, drug discovery relied heavily on the *materia medica* written by priests and traditional healers in classical and early mediaeval periods. These scripts usually contained lists of various natural products from plants, animals and mineral sources that showed therapeutic effects against various physiological diseases. The practice is still prevalent in many aspects of medical biology such as in Ayurveda (Touwaide & Appetiti, 2013), Homoeopathy (Riley, 2022) and Traditional Chinese Medicine (TCM) (*Shennong Ben Cao Jing*) (Z. Zhao et al., 2018). These books paved the paths for

modern day pharmacopoeias and drug formularies that contain details about therapeutic drugs, their pharmacodynamics, pharmacokinetics and potential side effects.

The core of network pharmacology is the concept that diseases are rarely caused by a single molecular defect but rather by disturbances in multiple interconnected pathways. Similarly, the therapeutic effects of drugs are often the result of their influence on various molecular targets within these networks. By mapping out these interactions, network pharmacology aims to identify key nodes or hubs in the network that can be targeted to achieve the most effective therapeutic outcomes (S. Zhao & Li, 2010).

Various tools such as databases and repositories, network construction and visualization tools, data mining tools, pathway analysis tools and molecular docking and dynamics tools have shaped network pharmacology to be an effective and comparatively easier approach in drug discovery.

1.8.1. Databases

1.8.1.1.DrugBank

Launched in 2006, DrugBank is a comprehensive online database that combines drug data with drug target information (Knox et al., 2024). It is a unique bioinformatics and cheminformatics resource that integrates data on drugs (approved, experimental, nutraceuticals, etc.) with comprehensive information on their corresponding targets (proteins, enzymes, receptors, etc.). The database provides details on the chemical, pharmacological, and pharmaceutical properties of drugs (Wishart, 2008), as well as their mechanisms of action, metabolic pathways, and potential interactions. It is used to explore drug repurposing opportunities, understand drug-drug interactions, and investigate the molecular basis of drug effects (Masoudi-Sobhanzadeh et al., 2020). It serves as a crucial tool in drug discovery and precision medicine.

1.8.1.2.BindingDB

BindingDB is an open-access database that stores measured binding affinities, focusing primarily on protein-ligand interaction (Gilson et al., 2016). It contains data on interactions between proteins (including drug targets like enzymes, receptors, and ion channels) and small molecule ligands (Wassermann & Bajorath, 2011). This database provides essential insights into the strength of binding between a drug and its target, which is a key determinant of the drug's efficacy and specificity.

1.8.1.3.SwissTargetPrediction

SwissTargetPrediction is a web-based tool designed to predict the most likely protein targets for small molecules (Daina et al., 2019). Using a combination of 2D and 3D similarity measures, SwissTargetPrediction compares the input molecule with known ligands in the database to predict potential targets. This tool is particularly useful for drug repurposing, identifying off-target effects, and understanding the polypharmacology of compounds (X. Ren et al., 2023). By providing insights into the possible biological activities of a molecule, SwissTargetPrediction aims at exploring new therapeutic opportunities and minimizing adverse effects. It is widely used in network pharmacology, toxicology, and drug discovery to predict how a drug or chemical compound might interact with various targets in the human body.

Other databases such as STITCH (Search Tool for Interactions of Chemicals) (Integrates information on chemical-protein interactions (Kuhn et al., 2007)), CheMBL (Database of bioactive molecules (Gaulton et al., 2012)), PubChem (Repository of chemical molecules (Kim et al., 2016)), TCMSP (Traditional Chinese Medicine Systems Pharmacology Database) (Integrates pharmacokinetic properties and active ingredients from TCM (Ru et al., 2014)), SIDER (Side Effect Resource) (Information on commercial medicines and their adverse reactions (Kuhn et al., 2016)), BioCarta

(information on gene pathways and interactions (ADRIAENS et al., 2008)) and canSAR (Integrates cancer-specific data (Halling-Brown et al., 2012)) have been pivotal in the advancement of drug discovery.

1.8.2. Data mining tools

STRING (Search Tool for the Retrieval of Interacting Genes/Proteins) is a tool that predicts complex protein-protein interactions within a biological system (Szklarczyk et al., 2015). By integrating both known and predicted interactions, STRING provides insights into the functional associations between proteins, helping to elucidate the underlying molecular mechanisms of various biological processes and diseases. It also helps in identification of interactions between proteins involved in disease pathways, hence helping in the discovery of novel drug targets.

1.8.3. Mapping tools

Cytoscape allows construction, visualization and analysis of biological networks (Shannon et al., 2003). It helps in studying molecular interaction networks, such as protein-protein, gene-gene, and metabolic pathways, in a visual manner. Additional plugins, such as BiNGO (Offers ontology and enrichment analysis), MCODE (Facilitates clustering and graph analysis), MiMIplugin (Helps in network generation), etc. make this tool indispensable in network pharmacology (Saito et al., 2012).

1.8.4. Enrichment tools

1.8.4.1. Gene Ontology (GO)

GO annotations link genes or proteins to GO terms, helping understand gene functions, discover potential gene relationships, and explore the roles of genes in broader biological contexts. With the ever-changing and growing knowledge of genes and proteins, GO aims at providing a dynamic language that can be applied across all eukaryotes (Ashburner et al., 2000). The classification of gene functions is majorly

done under three important domains i.e. Biological Processes (BP), Molecular Function (MF) and Cellular Component (CC) (Gene Ontology Consortium, 2004).

1.8.4.2. The Kyoto Encyclopaedia of Genes and Genomes (KEGG)

KEGG is a comprehensive bioinformatics resource that bridges the gap between genomes and biological systems. It integrates molecular-level information, including pathways, genes, proteins, compounds, diseases, and drugs (Kanehisa, 2000). It is used to explore cellular functions, organismal processes, and genomic data. Its comprehensive approach makes it valuable for bioinformatics research, systems biology modeling, and drug development.

1.8.5. Molecular docking and dynamics

1.8.5.1. Molecular docking

Molecular docking plays a pivotal role in drug discovery and computational biology. It involves predicting the binding mode and affinity of a small molecule (ligand) to a target protein (Pinzi & Rastelli, 2019). Understanding binding sites and energetics, can help design molecules that fit comfortably into these sites, thus inhibiting or modulating protein function. Docking enables large-scale screening of compound libraries, prioritizing those with favorable docking scores. It also reveals how ligands interact with proteins by predicting the number of hydrogen bonds, van der Waals forces, and hydrophobic interactions. Some well-known examples of docking software are AutoDock (Morris et al., 1998), AutoDock Vina (Trott & Olson, 2010), FlexX (Rarey et al., 1996), Molegro Virtual Docker (Bitencourt-Ferreira & de Azevedo, 2019), etc.

1.8.5.2. Molecular dynamic (MD) simulation

Molecular dynamics (MD) is a powerful computational simulation technique used to study the physical movements of atoms and molecules over time in a simulated biological environment (Karplus & McCammon, 2002). MD provides detailed insights

into the behavior of molecules at the atomic level, how they interact, fold, and change conformation. This technique is particularly valuable in understanding complex biological processes, such as protein folding, enzyme function, and ligand-receptor interactions, which are crucial in drug discovery and development. It also helps predict how molecules respond to different environmental conditions, such as temperature and pressure, and how they behave in different states, such as in solution (Hollingsworth & Dror, 2018). As a result, molecular dynamics has become an essential tool in modern biophysics, chemistry, and drug design, providing a deeper understanding of molecular mechanisms and aiding in the rational design of new therapeutics.

A combination of all these bioinformatics tools has made novel drug discovery relatively easier. Alongside, they have also improved the understanding of drug-target interactions involved in a disease.

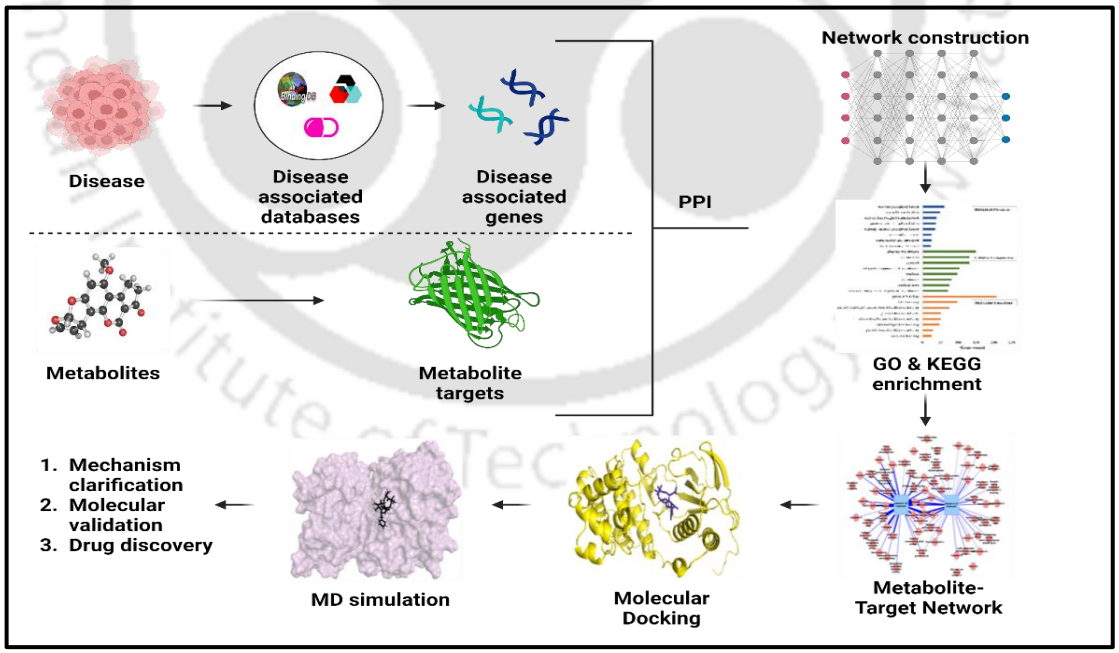

Scheme 1.3. Schematic depiction of general workflow of network pharmacology (*Conceptualized and illustrated based on* (W. Ren et al., 2020) *using Biorender*)

1.9. Nanocarriers: Shaping drug delivery scenario

Nanocarriers are an advanced and versatile vehicle in drug delivery systems, designed to enhance the efficacy and safety of therapeutic agents. These nanoscale capsules, typically ranging from 1 to 100nm in size, can encapsulate drugs, protecting them from degradation, improving their solubility, and ensuring controlled and targeted release (Balogh, 2020). Therapeutic drugs are usually administered via the enteral route (Magnuson et al., 2005) (oral, rectal or sublingual) or parenteral route (Guy, 2010) (intravenous, intramuscular or subcutaneous), with enteral routes being more preferred. This however faces challenges such as reduced bioavailability of drugs and non-specificity leading to side effects. Nanocarriers ability to deliver drugs specifically to diseased tissues reduces off-target effects and minimizes the adverse side effects often associated. The targeted delivery is achieved through passive targeting, where the nanocarriers accumulate in tumor tissues via the enhanced permeability and retention (EPR) effect (Gabizon, 1995), or through active targeting, where ligands on the surface of nanocarriers bind specifically to receptors on target cells (Vitetta et al., 1983).

While surgery, chemotherapy, and radiotherapy are effective in treating cancer, they come with significant challenges. The invasiveness of surgery, the systemic toxicity of chemotherapy, and the collateral damage caused by radiotherapy highlight the need for advancements in cancer treatment (Chabner & Roberts, 2005). Encapsulating or conjugating biomolecules in suitable delivery systems helps overcome the hurdles associated with the traditional approaches. The ability to modify the surface properties and functionalize them with targeting moieties makes them a powerful tool in personalized medicine. The following is a list of various nanocarriers in use today for delivery of chemotherapy drugs.

1.9.1. Organic NPs

Organic nanoparticles are a versatile and promising class of nanocarriers used in drug delivery, particularly in cancer therapy. They are composed of organic materials, primarily polymers, lipids, or proteins, and offer several advantages, including biocompatibility, biodegradability, and the ability to be engineered for targeted and controlled drug release (Horn & Rieger, 2001). Organic nanoparticles can be prepared using the following methods (i) Emulsification, (ii)Nano-precipitation and (iii) By drying process (Shatrohan Lal, 2014).

- **Polymer-based nanocarriers** are made from various polymers such as poly(lactic-co-glycolic acid) (PLGA) (Alvi et al., 2022), polylactic acid (PLA) (D. Zhu et al., 2016), polyethylene glycol (PEG) (CHENG et al., 2007), and polycaprolactone (PCL) (L. Zhang et al., 2016). These materials are chosen for their biodegradability, biocompatibility, and ability to degrade into non-toxic byproducts. These nanoparticles can encapsulate a wide range of drugs, including hydrophilic and hydrophobic molecules, proteins, and nucleic acids. They also offer sustained release over longer durations ensuring stable drug titer in tumors. The use of biodegradable and biocompatible polymers ensures that the NPs break down into non-toxic components after fulfilling their drug delivery function, reducing the risk of long-term toxicity in the body.
- **Liposome based NPs** are spherical vesicles with a lipid bilayer structure that can encapsulate both hydrophilic and hydrophobic drugs (Cavalli et al., 1993; Souto et al., 2007). Liposomes enhance drug stability, protect the encapsulated drug from degradation, and can be modified for targeted delivery (O. Medina et al., 2004). They are well known for their biocompatibility and low toxicity and are suitable carrier systems for chemotherapy drugs as well as vaccines (Ferreira et al., 2013).

- **Dendrimers** are highly branched, tree-like structures made from synthetic polymers. These NPs have multiple functional groups that can be used to attach drugs, targeting ligands, or imaging agents. They are excellent delivery systems for hydrophobic chemotherapy drugs and nucleic acid delivery in cancer therapy (Palmerston Mendes et al., 2017).

1.9.2. Inorganic NPs

Inorganic NPs offer several advantages over organic materials, including being non-toxic, hydrophilic, biocompatible, and highly stable. They possess distinctive physicochemical properties, such as a high surface area relative to volume and unique optical and magnetic characteristics. These NPs can be functionalized with specific ligands to increase their affinity for target cells or molecules. For example, targeted drug delivery using the folate-modified iron oxide-mesoporous silica nanoparticles were found be useful for treating cancer with minimal toxicity surrounding tissues. Additionally, inorganic NPs provide controlled drug release, protect drugs from degradation, and can decrease the frequency and dosage required for administration. This leads to a significant reduction in drug toxicity, particularly in cancer treatments (Paul & Sharma, 2020). Several inorganic NPs are currently in use in the fight against cancer including, gold NPs (Connor et al., 2005), silver NPs (Chugh et al., 2018), iron oxide NPs (Albukhaty et al., 2024; A. K. Gupta & Gupta, 2005), silica NPs (Koohi Moftakhari Esfahani et al., 2022) and quantum dots (H. Zhang et al., 2008).

1.9.3. Hybrid NPs

Hybrid nanoparticles combine the benefits of both organic and inorganic materials, creating versatile platforms for drug delivery and other biomedical applications. These nanoparticles integrate the unique properties of both materials, such as the biocompatibility and biodegradability of organic components with the stability and

functional capabilities of inorganic elements (Mokri et al., 2022). Hybrid nanoparticles can be engineered to enhance drug loading capacity, improve targeted delivery, and provide controlled release profiles. Additionally, they often exhibit multifunctional properties, such as the ability to combine therapeutic and diagnostic functions, making them highly promising for advanced medical treatments, particularly in cancer therapy (Della Rocca & Lin, 2010; Lin et al., 2009).

Nanocarrier drug delivery systems have advanced cancer treatment by enhancing precision and efficacy, but they face challenges such as complexity in design and manufacturing, stability issues, and difficulties in achieving precise targeting. Potential toxicity eliciting immune responses add further complications. Additionally, regulatory hurdles, high costs, and limited accessibility pose significant barriers to widespread adoption of these innovative therapies.

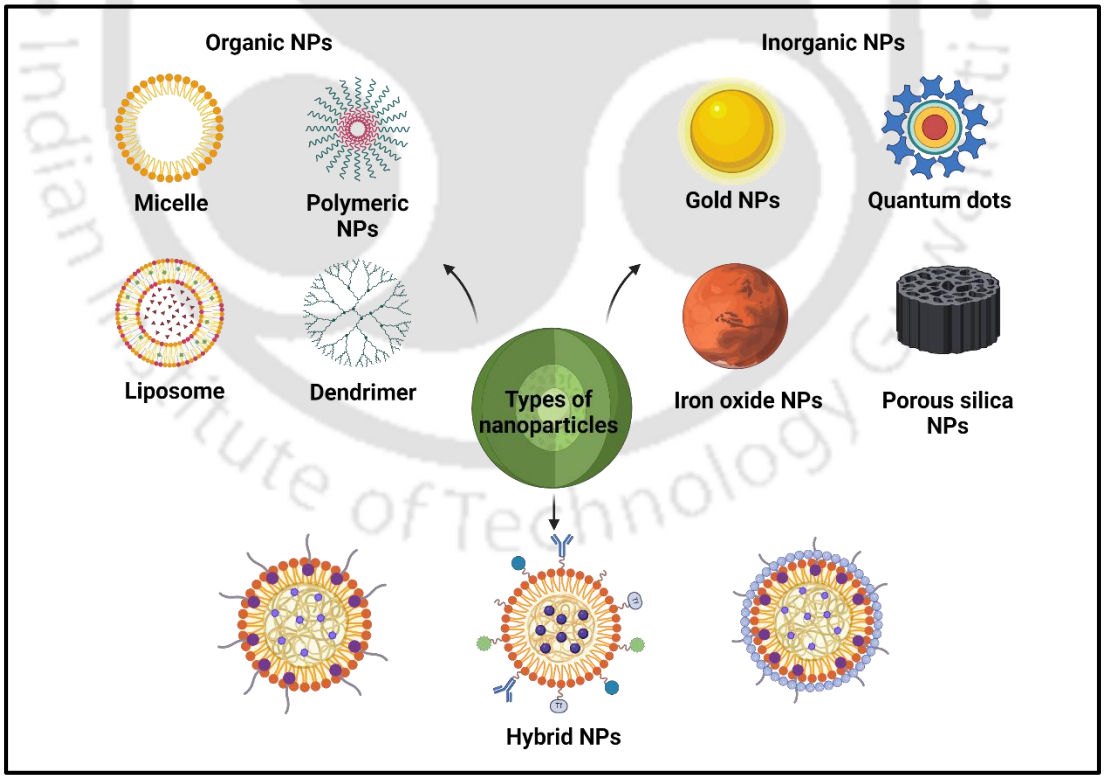

Scheme 1.4. Schematic representation of different categories of nanoparticles in use against cancer therapy (*Prepared using Biorender*)

1.10. Scope of research

The exponential rise in global breast cancer incidence, coupled with the absence of universally effective therapeutic solutions, underscores the urgent need for focused research efforts. Traditional chemotherapy, though an important pillar in combating the issue, faces challenges such as non-specific targeting, toxicity, drug resistance, limited efficacy and relapse. Fungal metabolites, like cytochalasin D, provides a promising avenue in the current battle against breast cancer. Cytochalasin D is primarily known for disrupting actin polymerization by binding to actin filaments. However, the molecular pathways disrupted by the metabolite has not been studied in details and hence provides an avenue to further explore the mode of action. This thesis investigates the therapeutic effects of cytochalasin D against the TNBC cell line MDA-MB-231. With the help of network pharmacology, the molecular mechanism of action of cytochalasin D has also been highlighted. Simultaneously, a biocompatible PLGA nanocarrier has been utilized to achieve a more efficient delivery of cytochalasin D into the cancer cells.

1.11. Objectives

- In-silico identification of molecular targets of cytochalasin D in breast cancer cells
- In-vitro therapeutic effects of Cytochalasin D against MDA-MB-231 cells
- Nano-carrier mediated delivery of Cytochalasin D

Chapter 2

Materials and Methods

2.1. Materials

2.1.1. Chemicals and Reagents

Following chemicals were procured to conduct the experiments –

Sigma Aldrich - Agarose, Cytochalasin D (purity ≥98%), Dulbecco's Modified Eagle's Medium (DMEM) supplemented with L-glutamine and sodium pyruvate, Sodium bicarbonate, Formamide, 3-(4, 5-dimethylthiazolyl-2)-2, 5-diphenyltetrazolium bromide (MTT), dichlorodihydrofluorescein diacetate (DCFDA) Acridine orange, Epidermal growth factor (EGF), Propidium Iodide (PI), RIPA (Radioimmunoprecipitation assay) cell lysis Buffer, Tetra methyl ethylene diamine (TEMED), Ammonium persulphate (APS), Dimethylsulphoxide (DMSO), Epidermal growth factor (EGF), Phosphate-buffered saline (PBS) for cell culture, PVDF (polyvinylidene fluoride) membrane.

HiMedia Laboratories: Luria Bertani media, Agar powder, Potato dextrose agar media (PDA), triton-X-100, Tris base, Tween-20, Diluent for DNA extraction (100% ethanol), Glycerol, Tris base, Glacial acetic acid, Ethylenediamine tetraacetic acid (EDTA), Sodium dodecyl sulphate (SDS), Bromophenol blue, Xylene cyanol FF, ethidium bromide (EtBr), Calcium chloride ($CaCl_2$), Magnesium chloride ($MgCl_2$), Ampicillin, Diethyl pyrocarbonate (DEPC), Isopropyl β- d-1-thiogalactopyranoside (IPTG), Tris-HCL, Sodium hydroxide (NaOH), Potassium acetate, Glycine, Sodium chloride (NaCl), Maltose, disodium hydrogen phosphate (Na_2HPO_4), Potassium dihydrogen phosphate (KH_2PO_4), Bovine serum albumin (BSA).

BioRad Laboratories: Prestained protein molecular weight marker, ECl western blotting substrate.

Merck: Chloroform, phenol-chloroform-isoamyl alcohol mixture, isopropanol.

ThermoFisher Scientific: Acetonitrile, dimethyl sulfoxide (DMSO), JC-1 assay kit, Annexin-V-Alexa flour 488- propidium iodide apoptosis kit, Protein molecular weight marker, DNA molecular weight marker.

Gibco: Fetal bovine serum (FBS), antibiotic solution (100 units/mL penicillin + 0.1 mg/mL streptomycin + 0.025 mg/mL amphotericin B).

2.1.2. Glassware and Plasticwares

Following glassware and plasticwares were used to conduct the experiments –

Borosil: Test tubes, conical flasks, beakers etc.

Tarsons Products Pvt. Ltd: Petri-dishes, microtips, spreaders, microcentrifuge tubes, centrifuge tubes, cryo-chill vials, PCR (Polymerase chain reaction) tubes etc.

ThermoFisher Scientific: Cell culture dishes, cell culture T-flasks, 96-well plates, 6-well plates etc.

Cell Signaling Technology (CST):

Table 2.1.2.1. The list of antibodies used to study the expression profile of the enlisted genes.

Antibodies	Product code
p-42/44 (MAPK1/3)	9926T
p-38 (MAPK14)	9926T
JNK (MAPK8)	9926T
Caspase 8	4987
Cleaved Caspase 8	9496
β-actin	8457S

2.1.3. Software

Cytoscape (Shannon et al., 2003), STRING (Search Tool for the Retrieval of Interacting Genes/Proteins) (Szklarczyk et al., 2015), DAVID (Database for Annotation, Visualization, and Integrated Discovery) (Sherman et al., 2022), AutoDock Tools (Trott & Olson, 2010), CHARMM-GUI, Param-Ishan Computing Facility.

2.2. Cell Lines, culture conditions and maintenance

The MDA-MB-231 triple-negative breast cancer cell line was obtained from the National Centre for Cell Sciences (NCCS) cell repository in Pune, India. These cells were cultured in high glucose Dulbecco's Modified Eagle Medium (DMEM) enriched with L-glutamine, sodium pyruvate, 10% fetal bovine serum (FBS), sodium bicarbonate, and a 1% (v/v) antibiotic solution containing 100 units/mL penicillin, 0.1 mg/mL streptomycin, and 0.025 mg/mL amphotericin B. The cells were maintained in a humidified incubator set at 37°C with a 5% CO_2 atmosphere to ensure optimal growth conditions. The culture medium was regularly refreshed with new medium every 2 to 3 days to maintain cell health and promote consistent growth. For all experimental procedures, cell culture plates with a confluence exceeding 80% were utilized. This high confluence ensures that the cells are in a similar phase of growth, which is crucial for obtaining reliable and reproducible experimental results.

2.3. Experimental Methodologies

2.3.1. *In silico* prediction of targets involved in breast cancer pathology

2.3.1.1. Collection and mapping of Cytochalasin D related targets

Cytochalasin D-related targets were identified using three distinct databases: DrugBank (Knox et al., 2024), BindingDB (Gilson et al., 2016), and SwissTargetPrediction (Daina et al., 2019). These databases were selected for their comprehensive coverage of drug-target interactions and predictive capabilities. From these sources, only compounds

with a probability value of 0.5 or higher were considered to ensure a high level of confidence in the predicted interactions. The corresponding targets in Homo sapiens, along with their UniProt IDs, were then compiled to create a robust dataset. To visualize and analyse the interactions between cytochalasin D and its potential human targets, the data were imported into Cytoscape version 3.9.1, a powerful network analysis software. In this visualization, the compounds were designated as source nodes, while the UniProt IDs represented the target nodes. This approach allowed for the creation of an interaction network that highlights the connections between cytochalasin D and its predicted targets. The use of Cytoscape facilitated a deeper understanding of the molecular interactions and potential pathways influenced by cytochalasin D. By mapping these relationships, researchers can identify key targets and pathways that may be relevant for therapeutic interventions or further experimental investigations. This comprehensive network analysis not only aids in elucidating the mechanism of action of cytochalasin D but also provides a valuable resource for identifying novel drug targets and understanding the broader implications of cytochalasin D's interactions within human biology.

2.3.1.2.Protein-protein interaction (PPI) data

The Search Tool for the Retrieval of Interacting Genes (STRING version 11.5) was employed to analyse the protein-protein interaction data of the selected targets. This analysis was restricted to Homo sapiens to ensure species-specific relevance and was conducted with a high confidence score of 0.9 to guarantee the reliability of the interactions. The resulting network from the STRING database provided a comprehensive overview of the interactions among the selected protein targets. To gain deeper insights into the network's structure and the significance of individual nodes, the data from STRING were further analysed using Cytoscape version 3.9.1. Cytoscape's

powerful visualization and analytical capabilities allowed for an in-depth examination of the network. One key measure used in this analysis was the degree of centrality, a graph-theoretic index that quantifies the importance of each node within the network. Nodes with higher degree centrality values were identified as being more central and influential in the network, indicating their greater significance in the protein-protein interaction landscape. This integrated approach, combining STRING and Cytoscape, enabled a detailed exploration of the protein-protein interactions of the selected targets. By focusing on nodes with high degree centrality, researchers could pinpoint critical proteins that play pivotal roles in the network, potentially highlighting key targets for therapeutic intervention or further biological investigation. This method not only enhances the understanding of the molecular interactions and pathways associated with the selected targets but also provides a robust framework for identifying and prioritizing significant proteins within complex biological networks.

2.3.1.3. Gene Ontology (GO) and KEGG enrichment analysis

Gene ontology and KEGG enrichment analysis were achieved using Database for Annotation, Visualization and Integrated Discovery (DAVID 2021) bioinformatics database (Sherman et al., 2022) including biological processes (BP), molecular functions (MF), cellular components (CC) and KEGG signalling pathways. DAVID 2021 facilitated the integration and visualization of the enrichment results, providing a comprehensive overview of the functional annotations associated with the target proteins. The enriched GO terms and KEGG pathways were systematically categorized and visualized, enabling researchers to identify significant patterns and relationships. By leveraging DAVID 2021 for GO and KEGG enrichment analysis, the study aimed to uncover the functional roles and biological significance of the selected protein targets. This approach not only enhanced the understanding of the molecular

mechanisms underlying cytochalasin D interactions but also identified potential pathways and processes that could be targeted for therapeutic interventions. The integrated analysis provided a robust framework for interpreting the complex biological data, thereby contributing to the advancement of molecular biology and pharmacology research.

2.3.1.4.Molecular docking studies

The chemical structure of Cytochalasin D was retrieved from PubChem (Kim et al., 2023) in SDF format. This structure provided the necessary molecular data to proceed with further computational analyses. The 3D structures of the target proteins were obtained from the RCSB Protein Data Bank (PDB) (Zardecki et al., 2022) by using their respective UniProt IDs, ensuring accurate and up-to-date structural information. These structures were saved in PDB format to facilitate compatibility with molecular docking software. Molecular docking studies were conducted using Autodock Tools-1.5.6, a widely used software suite for simulating the interaction between small molecules and target proteins. The 3D structures of the target proteins were prepared by removing water molecules and adding hydrogen atoms to optimize the structures for docking. The chemical structure of Cytochalasin D was converted into a format compatible with Autodock and optimized for docking simulations. The grid box, which defines the search space for the docking simulation, was positioned to enclose the entire catalytic domain of each target protein. This ensures that the docking simulation comprehensively explores the potential binding sites within the catalytic region. Autodock performed the docking simulations, predicting the most favourable binding orientations and interactions between Cytochalasin D and the target proteins. The software evaluated the binding affinities and scored the interactions based on factors such as hydrogen bonding, hydrophobic interactions, and van der Waals forces.

The results from the molecular docking simulations were analysed to determine the binding affinities and interaction patterns between Cytochalasin D and the target proteins. Key binding residues and interaction types were identified, providing insights into the potential mechanisms of action. PyMOL (The PyMOL Molecular Graphics System, version 2.5.4) was used to generate high-quality visualizations of the docking results. It provided detailed images of the binding interactions, highlighting key residues and interactions within the catalytic domain. The software allowed for the creation of detailed 3D representations of the protein-ligand complexes, facilitating a clear understanding of the binding modes. BIOVIA Discovery Studio was utilized to further analyse and visualize the docking results. It provided additional tools for exploring the molecular interactions and generating publication-quality images. By combining molecular docking with advanced visualization tools, this study provided a detailed examination of the interactions between cytochalasin D and its target proteins. The use of Autodock Tools-1.5.6 facilitated accurate predictions of binding affinities and interaction patterns, while PyMOL and BIOVIA Discovery Studio enabled the creation of insightful visual representations. This integrated approach enhanced the understanding of the molecular mechanisms by which Cytochalasin D interacts with its targets, offering valuable insights for future drug development and therapeutic strategies.

2.3.1.5.MD simulation study

Molecular dynamics (MD) simulation is a powerful computational technique used to study the dynamic behaviour of particles, such as atoms and molecules, over time. By simulating the temporal evolution of a system's configuration and energy, MD simulations provide detailed insights into the structural and functional dynamics of biological macromolecules. In this study, the dynamics of target proteins in complex

with cytochalasin D were investigated using the GROMACS 2023 software package. The 3D structures of the target proteins and the cytochalasin D ligand were prepared for MD simulations. This included the addition of hydrogen atoms and the optimization of the structures to ensure accurate simulation conditions. The CHARMM-GUI all-atom force field was utilized to parameterize the system. This force field is known for its accuracy in simulating biological molecules, ensuring reliable interactions between the protein and ligand. The prepared protein-ligand complexes were solvated in a water box to mimic a physiological environment. Appropriate counterions were added to neutralize the system, ensuring proper electrostatic conditions for the simulation. An initial energy minimization step was performed to remove any steric clashes or unfavourable interactions within the system. This step is crucial for stabilizing the system before commencing the dynamics simulations. The system was equilibrated in two phases: first, with position restraints on the protein and ligand to allow the solvent molecules to equilibrate, and second, without restraints to equilibrate the entire system. This process ensures that the system reaches a stable state before the production run. The final MD simulation was conducted for a duration of 100 nanoseconds (ns). During this period, the system's atomic positions and velocities were updated at each time step to simulate the natural movements and interactions of the molecules. The RMSD (Root Mean Square Deviation) was calculated to measure the structural stability and conformational changes of the protein-ligand complex over time. This metric indicates how much the structure deviates from the initial configuration. RMSF (Root Mean Square Fluctuation): The RMSF was analysed to assess the flexibility of individual residues within the protein. Higher RMSF values indicate regions of the protein that are more flexible and potentially involved in binding interactions. The number and stability of hydrogen bonds between the protein and ligand were evaluated throughout the

simulation. Hydrogen bonds play a crucial role in the stability and specificity of protein-ligand interactions. The bond lengths between specific atoms of the protein and ligand were monitored to understand the nature and stability of the interactions. The MM-PBSA (Molecular Mechanics Poisson-Boltzmann Surface Area) method was used to calculate the binding free energy of the protein-ligand complexes. This approach combines molecular mechanics energies with solvation energies to provide an estimate of the binding affinity. The binding free energy (ΔGbind) of cytochalasin D with stable targets was computed utilizing the subsequent equation:

$$\Delta G_B = \Delta E_{MM} + \Delta G_{SA} – T\Delta S_{MM}$$

In this context,

ΔG_B = mean binding free energy of the target-inhibitor complex.

ΔE_{MM} = average molecular mechanics energy.

ΔG_{SA} = solvation free energy.

$T\Delta S_{MM}$ = solute configuration entropy (Massova & Kollman, 2000)

The graphs and plots generated from the simulation data were analysed and visualised using QtGrace, a graphical user interface for the Grace plotting tool.

2.3.2. Cytotoxicity of Cytochalasin D against MDA-MB-231 cells

2.3.2.1. Cell viability assay via MTT method

Cells were seeded in a 96-well plate at a concentration of 10,000 cells per well to ensure uniform growth and optimal conditions for the experiment. The plate was then placed in an incubator set at 37°C with 5% CO_2 for 24 hours to allow the cells to adhere and establish themselves on the well surface, ensuring proper cell attachment and initial growth. Following the initial incubation period, the cells were treated with varying concentrations of cytochalasin D. The concentrations used were 10, 20, 30, 50, 75, and 100 µg/mL. These different concentrations were prepared to assess the dose-dependent

effects of cytochalasin D on the cells. To ensure the solvent (DMSO) did not affect the results, the final concentration of DMSO in each well was kept below 0.2%. After 48 hours of cytochalasin D treatment, the viability and proliferation of the cells were assessed using the MTT assay, a colorimetric assay for measuring cellular metabolic activity. 5 µL of MTT solution (3-(4,5-dimethylthiazol-2-yl)-2,5-diphenyl tetrazolium bromide) was added to each well. MTT is a yellow tetrazole that is reduced to purple formazan in living cells, indicating the presence of metabolically active cells. The plate was incubated for an additional 2 hours at 37°C with 5% CO_2. During this period, the MTT is taken up by the cells and reduced by mitochondrial dehydrogenase enzymes to form insoluble formazan crystals, which accumulate in the cells. After the 2-hour incubation with MTT, the media in each well was carefully removed to discard the unreacted MTT. 100 µL of DMSO was added to each well to dissolve the formazan crystals. DMSO acts as a solvent, facilitating the solubilization of the purple formazan crystals, resulting in a homogeneous solution. The absorbance of each well was measured using a Thermo Fisher Scientific Multiskan SkyHigh microwell plate reader. The primary absorbance was read at 590 nm, which corresponds to the absorbance maximum of the dissolved formazan. A reference wavelength of 630 nm was used to account for any background absorbance or optical imperfections in the plate. The absorbance values at 590 nm, after subtracting the reference values at 630 nm, provided a measure of the viable cell count. Cell viability percentages were determined from the absorbance values based on the equation:

$$\text{Cell viability (\%)} = \frac{\text{Average absorbance of treated wells}}{\text{Average absorbance of untreated wells}} \times 100$$

Higher absorbance indicates higher metabolic activity and, consequently, a higher number of viable cells. The results were analysed to determine the effect of different concentrations of cytochalasin D on cell viability and proliferation. By using a range of

concentrations and the MTT assay, the study aimed to establish a dose-response relationship, providing valuable insights into the compound's potential therapeutic effects and cytotoxicity.

2.3.2.2.Cell cycle progression analysis

For the cell cycle analysis, approximately 1 x 10^6 cells were seeded in a 6-well plate the night before the experiment to ensure proper attachment and growth. The next day, the cells were treated with three different concentrations of cytochalasin D: 10 µg/mL, 20 µg/mL, and 30 µg/mL. Following the treatment, the cells were cultured in serum-free media for 24 hours to synchronize the cell cycle and reduce variability. After the incubation period, the cells were harvested and stained with propidium iodide (20 µg/mL). Propidium iodide is a fluorescent dye that binds to DNA, allowing for the quantification of DNA content within each cell. This staining enables the identification of different phases of the cell cycle based on DNA content: G0/G1 phase (low DNA content), S phase (DNA synthesis), and G2/M phase (high DNA content). The stained cells were then analysed using the FCS Express software, which facilitated the identification and quantification of the cell populations in each phase of the cell cycle. By comparing the cell cycle profiles at different cytochalasin D concentrations, the study aimed to elucidate the compound's impact on cellular proliferation and its potential as a therapeutic agent.

2.3.2.3.Wound healing assay

To assess the effects of cytochalasin D on cell migration and wound healing, approximately 1 x 10^6 cells were seeded in a 6-well plate and allowed to adhere and form a monolayer over a 12-hour period. Once a confluent monolayer was established, the cells were washed twice with phosphate-buffered saline (PBS) to remove any residual media and debris. Following the washes, the cells were subjected to a 12-hour

serum starvation period in serum-free media. Serum starvation helps to synchronize the cells and reduce baseline proliferation, thereby highlighting the effects of the treatment on cell migration. After the serum starvation period, a wound was introduced in each well by gently scratching the cell monolayer with a sterile 200 µL micropipette tip. This creates a uniform wound area that serves as a starting point for measuring cell migration. To remove any detached cells and debris resulting from the scratch, the wells were washed twice with PBS. The cells were then treated with cytochalasin D at its IC_{50} concentration, determined from prior experiments, to ensure a physiologically relevant dose. The treatment lasted for 48 hours, allowing sufficient time for the cells to migrate and attempt to close the wound. Throughout the treatment period, images of the wound areas were captured at various time points using a microscope equipped with a camera. These images were analysed using ImageJ software, which facilitated the precise quantification of the wound area at each time point. ImageJ's measurement tools were used to calculate the reduction in wound area, providing a quantitative assessment of cell migration and wound healing. The migration rate of each sample was calculated according to the following formula

$$\text{Migration rate } (\mu m/h) = \frac{\text{Initial distance (0th h)} - \text{Final distance (nth h)}}{\text{Total time (h)}}$$

This assay provided valuable insights into the potential inhibitory effects of cytochalasin D on cell motility, which is crucial for understanding its therapeutic potential in conditions where cell migration plays a key role, such as cancer metastasis and tissue repair.

2.3.2.4.Intra-cellular reactive oxygen species (ROS) detection

The intracellular reactive oxygen species (ROS) generation in MDA-MB-231 cells following cytochalasin D treatment was assessed using 2′,7′-dichlorofluorescein diacetate (DCFDA), a fluorescent probe obtained from Sigma Aldrich. Approximately

1×10^5 MDA-MB-231 cells were seeded per well in a suitable growth medium within a 24-well plate. The cells were allowed to attach and grow for 24 hours to ensure they formed a stable monolayer. After the initial attachment period, the cells were treated with IC_{50} of cytochalasin D. The treatment lasted for 4 hours, allowing sufficient time for cytochalasin D to exert its influence on the cells. Following the cytochalasin D treatment, the cells were incubated with 0.01 mM DCFDA for 30 minutes. DCFDA is a cell-permeable dye that, once inside the cell, is deacetylated by cellular esterases to form 2′,7′-dichlorofluorescein (DCF), which fluoresces upon oxidation by ROS, thereby indicating the level of ROS generation. After the DCFDA incubation, the cells were trypsinized to detach them from the well surface. The cells were then washed with 1× phosphate-buffered saline (PBS) to remove any remaining DCFDA and to prepare the cells for flow cytometry analysis. The washed cells were analysed using a CytoFLEX flow cytometer from Beckman Coulter. Flow cytometry allows for the quantitative measurement of fluorescence intensity in individual cells, providing a detailed assessment of ROS levels within the cell population. The fluorescence intensity of DCF was measured to determine the amount of ROS generated within the cells following cytochalasin D treatment.

2.3.2.5.Immunoblotting

To investigate the protein expression changes in MDA-MB-231 cells following cytochalasin D treatment, a Western blot analysis was performed. MDA-MB-231 cells were treated with three different concentrations of cytochalasin D: 5 µg/mL, 10 µg/mL, and 30 µg/mL. This range of concentrations was selected to evaluate the dose-dependent effects of cytochalasin D on protein expression. After treatment, the cells were lysed using a 1× RIPA (Radioimmunoprecipitation Assay) lysis buffer containing 1% PMSF (Phenylmethylsulfonyl fluoride) to inhibit protease activity and preserve protein

integrity. The treated cells were subjected to mechanical stress to ensure complete cell lysis. The lysate was then collected by centrifugation, which separates the cellular debris from the protein-containing supernatant. The protein concentration in the lysates was quantified to ensure equal loading of samples. Subsequently, 25 µL of each sample was loaded onto a 10% SDS-PAGE (Sodium Dodecyl Sulfate Polyacrylamide Gel Electrophoresis) gel for separation based on molecular weight. The proteins were resolved by electrophoresis, which separates them according to their size. Following electrophoresis, the separated proteins were transferred from the gel to a PVDF (Polyvinylidene Difluoride) membrane. This transfer process allows for the subsequent detection of specific proteins using antibodies. The PVDF membrane was blocked with 5% BSA (Bovine Serum Albumin) in TBST (Tris-buffered saline with Tween 20) for 2 hours to prevent non-specific binding of antibodies. After blocking, the membrane was incubated overnight at 4°C with primary antibodies specific to the target proteins. The primary antibodies bind to their respective target proteins on the membrane. The membrane was then incubated with anti-rabbit secondary antibodies conjugated with peroxidase for 4 hours. The secondary antibodies bind to the primary antibodies, allowing for the detection of the target proteins via chemiluminescence. The protein bands were visualized using the ChemiDoc imaging system (Bio-Rad). The images captured by the ChemiDoc system were analysed to quantify the expression levels of the target proteins. This detailed Western blot protocol enabled the study to assess the impact of cytochalasin D on protein expression in MDA-MB-231 cells, providing insights into the molecular mechanisms underlying its effects.

2.3.2.6.Statistical analysis

A statistical analysis was conducted on all acquired data using GraphPad Prism (v9.0) software. The standard error of the mean (SEM) was expressed as the mean ±. When

comparing three or more groups, a one-way ANOVA was carried out to evaluate differences between the experimental groups; when comparing two groups, an unpaired t-test was employed. A statistically significant p-value was one that was less than 0.05, and an insignificant p-value was one that was more than 0.05. The following symbols were used to indicate statistical significance: * for $p < 0.05$, ** for $p < 0.01$, *** for $p < 0.001$, and **** for $p < 0.0001$.

2.3.3. Delivering Cytochalasin D using a suitable nano-carrier for hydrophobic drugs

2.3.3.1. Preparation of cytochalasin D loaded PLGA nanoparticles

Cytochalasin D-loaded nanoparticles were prepared using the single emulsion solvent evaporation method (P. Singh & Sahoo, 2022). The organic phase was prepared by dissolving 100 mg of PLGA (poly (lactic-co-glycolic acid)) and 200 µL of cytochalasin D stock solution (5 mg/mL) in 3 mL of chloroform. PLGA serves as the polymer matrix for the nanoparticles, while cytochalasin D is the active drug to be encapsulated. The aqueous phase was prepared by dissolving 2% PVA (polyvinyl alcohol) and 0.1% TPGS (d-alpha-tocopheryl polyethylene glycol 1000 succinate) in water. PVA acts as a stabilizer, and TPGS improves the emulsification process. The organic phase solution was emulsified into the aqueous phase to form an oil-in-water emulsion. This was achieved by adding the organic phase to the aqueous phase under constant stirring. To enhance emulsification, the mixture was sonicated using a microtip probe sonicator set at 33% amplitude for 4 minutes. The sonication was performed over an ice bath to prevent overheating and degradation of the components. The emulsion was subjected to overnight stirring on a magnetic stir plate at room temperature. This allowed the chloroform to evaporate, leading to the formation of solid nanoparticles encapsulating cytochalasin D. To remove excess PVA and purify the nanoparticles, the suspension was ultra-centrifuged at 40,000 rpm for 20 minutes at 4°C (Thermo Fisher). This high-

speed centrifugation step helps in pelleting the nanoparticles. The collected nanoparticles were washed three times with double-distilled water to remove any residual PVA and other impurities. The retrieved nanoparticle suspension was then sonicated again for 4 minutes at 33% amplitude over an ice bath. This step ensured uniform dispersion of the nanoparticles and prevented aggregation. Finally, the nanoparticle suspension was lyophilized (freeze-dried) for 72 hours to obtain dry, stable nanoparticles. Lyophilization helps in long-term storage and handling of the nanoparticles without compromising their stability and efficacy. Void nanoparticles (void NPs), which do not contain cytochalasin D, were prepared using the same procedure. The only difference was the omission of cytochalasin D during the initial dissolution step in chloroform. The lyophilized cytochalasin D-loaded nanoparticles and the void nanoparticles were then ready for further characterization and experimental studies.

2.3.3.2. Characterisation of PLGA nanoparticles

To ensure a comprehensive understanding of the poly (lactic-co-glycolic acid) (PLGA) nanoparticles (PL-NPs), their zeta potential and surface morphology were thoroughly characterized using state-of-the-art analytical techniques. The zeta potential of the PLGA nanoparticles was measured using a Zetasizer (Zetasizer Nano ZS, ZEN3600, Malvern instrument, UK). This technique provides crucial information about the surface charge of the nanoparticles. The surface characteristics and detailed morphology of the formulated PLGA nanoparticles were analysed using field emission scanning electron microscopy (FESEM) and field emission transmission electron microscopy (FETEM). The PLGA nanoparticles were examined using the Sigma 3000 FESEM (Carl Zeiss, Germany). FESEM provides high-resolution images by scanning the nanoparticle

surface with a focused beam of electrons. FETEM was employed to obtain even more detailed insights into the internal structure and morphology of the nanoparticles.

2.3.3.3. Drug encapsulation efficiency and *in-vitro* release kinetics of cytochalasin D loaded PLGA nanoparticles

Following centrifugation of cytochalasin D loaded PLGA nanoparticles, the supernatant was collected. The absorbance of this supernatant was measured using a spectrophotometer (Varioskan, Thermo Fisher). The measured absorbance values were compared against a standard curve of cytochalasin D, prepared using known concentrations. This comparison allowed for the calculation of the amount of cytochalasin D not encapsulated in the nanoparticles, thereby determining the entrapment efficiency. The *in vitro* release profile of cytochalasin D from the PLGA nanoparticles was evaluated under different pH conditions to simulate various environments in the body. The release studies were conducted at acidic pH (pH 4) and physiological pH (pH 7.4) using phosphate-buffered saline (PBS) as the medium. These conditions were chosen to mimic the acidic environment found in tumor tissues, as well as the neutral pH of normal physiological conditions respectively.

2.3.3.4. Cytotoxicity of cytochalasin D loaded PLGA nanoparticles

The cytotoxic effect of cytochalasin D-loaded nanoparticles was evaluated using the MTT assay, a standard method for assessing cell viability and proliferation. A total of 5,000 cells were seeded into each well of a 96-well plate and allowed to adhere for 24 hours. Following the initial incubation period, the cells were treated with varying concentrations of cytochalasin D-loaded nanoparticles (0.5 mg/mL, 1 mg/mL, 2 mg/mL, 2.5 mg/mL, 3 mg/mL) and void nanoparticles (nanoparticles without cytochalasin D). The treated cells were incubated for 48 hours at 37°C in a 5% CO_2 atmosphere to allow for the effects of the nanoparticles to manifest. After the 48-hour

treatment period, 5 µL of MTT reagent was added to each well. The MTT reagent interacts with metabolically active cells to produce formazan crystals. The plate was incubated for an additional 2 hours at 37°C with 5% CO_2 to ensure sufficient formation of formazan crystals. To dissolve the formazan crystals, 100 µL of DMSO was added to each well. The absorbance of each well was measured using a Thermo Fisher Scientific Multiskan SkyHigh microwell plate reader. The primary absorbance was read at 590 nm. A reference wavelength of 630 nm was used to account for any background absorbance or optical imperfections in the plate, ensuring accurate measurement of cell viability. The cell viability percentages were calculated from the absorbance values using the following equation:

$$\text{Cell viability (\%)} = \frac{\text{Average absorbance of treated wells}}{\text{Average absorbance of untreated wells}} \times 100$$

2.3.3.5. Generation of ROS in MDA-MB-231 cells treated with cytochalasin D loaded PLGA NPs

The intracellular reactive oxygen species (ROS) generation in MDA-MB-231 cells following cytochalasin D loaded PLGA NPs treatment was assessed using 2′,7′-dichlorofluorescein diacetate (DCFDA) (Sigma Aldrich). Approximately 1×10^5 MDA-MB-231 cells were seeded per well in a suitable growth medium within a 24-well plate. The cells were allowed to attach and grow for 24 hours to ensure they formed a stable monolayer. After the initial attachment period, the cells were treated with IC_{50} of cytochalasin D. The treatment lasted for 4 hours, allowing sufficient time for cytochalasin D to exert its influence on the cells. Following the cytochalasin D loaded PLGA NPs treatment, the cells were incubated with 0.01 mM DCFDA for 30 minutes. After the DCFDA incubation, the cells were trypsinized to detach them from the well surface. The cells were then washed with 1× phosphate-buffered saline (PBS) to remove any remaining DCFDA and to prepare the cells for flow cytometry analysis. The washed

cells were analysed using a CytoFLEX flow cytometer from Beckman Coulter. The fluorescence intensity of DCF was measured to determine the amount of ROS generated within the cells following cytochalasin D treatment.

Chapter 3

In-silico prediction of targets involved in breast cancer cells

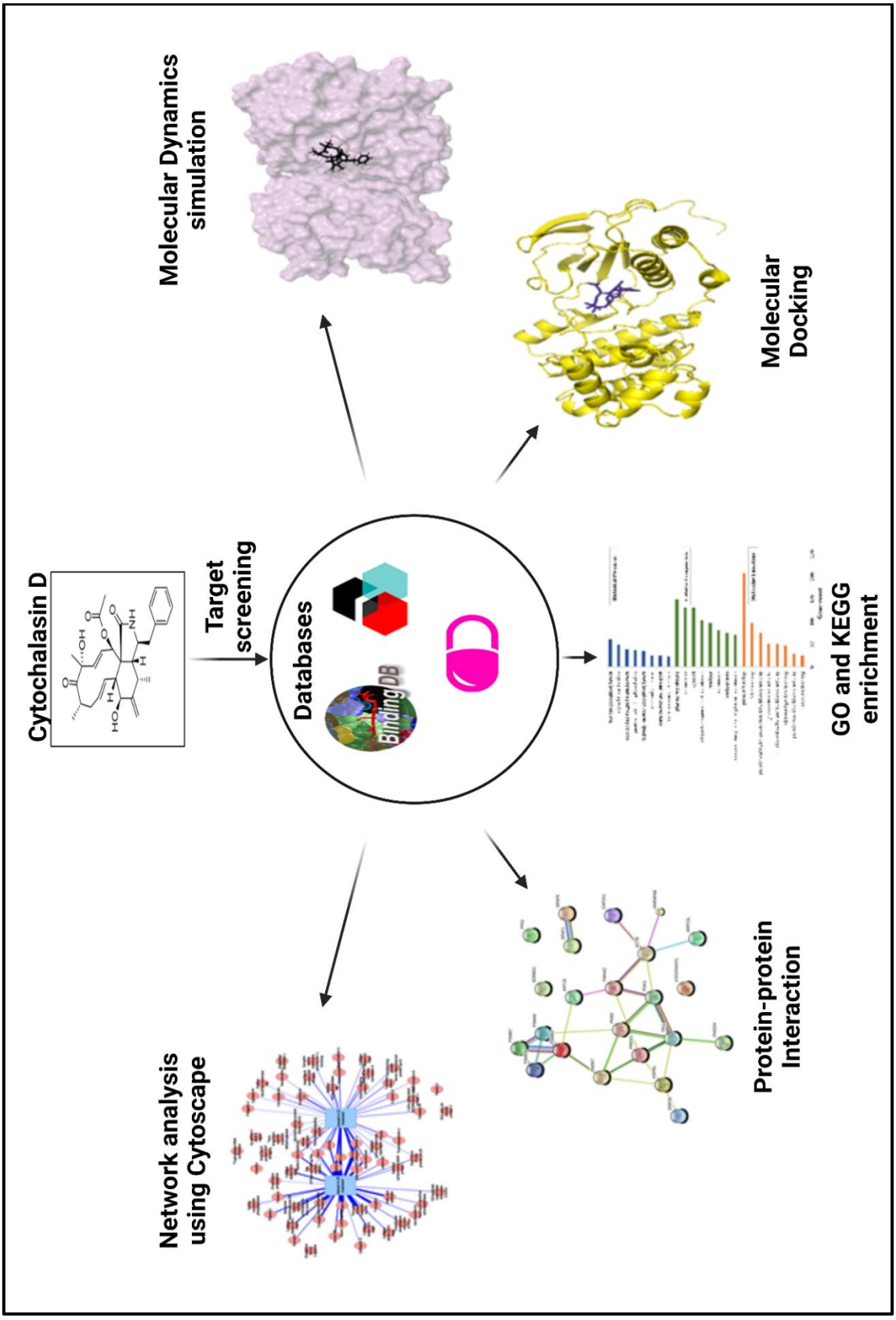

Scheme 3.1. A schematic representation of network pharmacology employed to discover molecular targets of cytochalasin D

Abstract

Network pharmacology is an interdisciplinary field that combines biology, pharmacology, and network science to explore the complex interactions between biological molecules within cellular networks. In the context of traditional medicine, network pharmacology systematically deciphers the relationships between diseases, syndromes, medicinal drugs, and their underlying biological components, such as cells, genes, and proteins. The process involves data integration, network construction, functional analysis, and the identification of key nodes and pathways, followed by experimental validation. By mapping these intricate networks, network pharmacology provides new insights into disease mechanisms, identifies potential therapeutic targets, and supports the development of personalized treatment strategies. This approach bridges the gap between traditional medicine and modern molecular biology, enhancing the drug discovery process and contributing to more effective healthcare solutions. In this study, the molecular targets of cytochalasin D were deciphered using components of network pharmacology such as STRING, GO and KEGG enrichment analysis and mapped using Cytoscape software. Further the protein-ligand stability was analysed using molecular docking and MD simulation to check for potential therapeutic targets of cytochalasin D.

3.1. Introduction

Network pharmacology is a multidisciplinary field that bridges biology, pharmacology, and network science. It systematically investigates the intricate interactions between biological molecules within cellular networks, aiming to understand how drugs affect these networks and how network perturbations lead to therapeutic or adverse effects (S. Li, 2021). The evolution of network pharmacology has enabled a shift from the traditional "one disease-one drug" model to a more versatile "one disease-multiple drugs" paradigm (Federico et al., 2022; Khan & Trivedi, 2023; Noor et al., 2022). This transition is facilitated by the integration of systems biology, multivariate pharmacology, and molecular network analysis, establishing network pharmacology as a pivotal tool for expeditiously uncovering unexplored connections between drugs and diseases (Sen et al., 2022; Yang et al., 2022).

Network pharmacology provides a holistic perspective for understanding traditional medicine (P. Zhang et al., 2023). The process predominantly involves systematically deciphering the complex, multi-layered relationships between higher-level objects, such as diseases, syndromes, and traditional medicinal drugs, and lower-level biological components, such as cells, genes, and proteins. This approach seeks to identify and map out the network elements that can integrally connect these macro-level and micro-level objects. By doing so, it aims to elucidate the underlying biological mechanisms and pathways that link diseases with their molecular and cellular bases, and how traditional drugs exert their effects through these pathways. In detail, this method encompasses several steps:

- **Data integration**: Aggregating vast amounts of biological, pharmacological, and clinical data to establish connections between diseases, drugs, and molecular targets.

- **Network construction**: Building complex networks that depict the interactions between various biological components. This includes constructing protein-protein interaction (PPI) networks, gene regulatory networks, and drug-target interaction networks.
- **Functional analysis**: Employing gene ontology (GO) and pathway enrichment analyses to understand the functional roles of identified genes and proteins within the context of the disease or drug action.
- **Identification of key nodes and pathways**: Pinpointing crucial network elements, such as hub proteins or key signalling pathways, that play significant roles in disease pathology or drug response.
- **Validation**: Experimentally validating the predicted interactions and pathways using various biological assays and techniques.

Through this comprehensive approach, researchers can uncover new insights into disease mechanisms, identify potential therapeutic targets, and develop more effective and personalized treatment strategies. This systematic analysis of multilevel relationships is at the core of network pharmacology, bridging the gap between traditional medicine and modern molecular biology. The integration of various omics-data and tools such as gene ontology (GO), pathway enrichment analysis, PPI and cytoscape helps to understand the interaction between the proteins within the cellular environment and decipher their roles, hence highlighting proteins of importance.

The following sections encompass the findings of network analysis along with the data from molecular docking and molecular dynamic simulation studies conducted with cytochalasin D and its target proteins within the cell. The detailed methodology has been described in the previous chapter (Chapter 2).

3.2. Results

3.2.1. Network analysis of Drug-Protein Interactions and pivotal hub proteins

The principle that ligands with similar structures often target analogous proteins has been well-documented in the literature (Shaikh et al., 2021). This study leveraged this principle by performing a cheminformatics analysis based on the concept that molecules sharing identical chemical functional groups tend to exhibit comparable functionalities. In this context, the study identified 127 drugs with a structural similarity greater than 0.5 from three databases: DrugBank, BindingDB, and SwissTargetPrediction. Alongside cytochalasin D, these drugs and their 278 unique protein targets were mapped using Cytoscape software (version 3.9.1), resulting in a network with 400 nodes and 449 edges (**Fig. 3.2.1**). This network visualization facilitated the examination of the relationships between the drugs and their target proteins. The network analysis revealed two primary modules, also referred to as communities, which are clusters of nodes representing groups of interconnected drugs and proteins. In addition, the network contained 13 distinct motifs and 15 independent drug-protein pairs, illustrating various interactions and patterns within the dataset. The average number of neighbours per node was calculated to be 2.245, providing an indication of the average connectivity within the network. Notably, the protein P62942 (Peptidyl-prolyl cis-trans isomerase FKBP1A) emerged as a central node with the highest degree of connectivity, possessing an in-degree of 30. This was followed by P08684 (Cytochrome P450 3A4), which had an in-degree of 20. Among the drugs, cytochalasin D was the most prominent node with an out-degree of 104, indicating its extensive interaction with various target proteins. It was followed by cocaine (out-degree = 28) and minocycline (out-degree = 23). These metrics highlight the significant

role of cytochalasin D and other compounds in the network, showcasing their potential as key players in drug-target interactions.

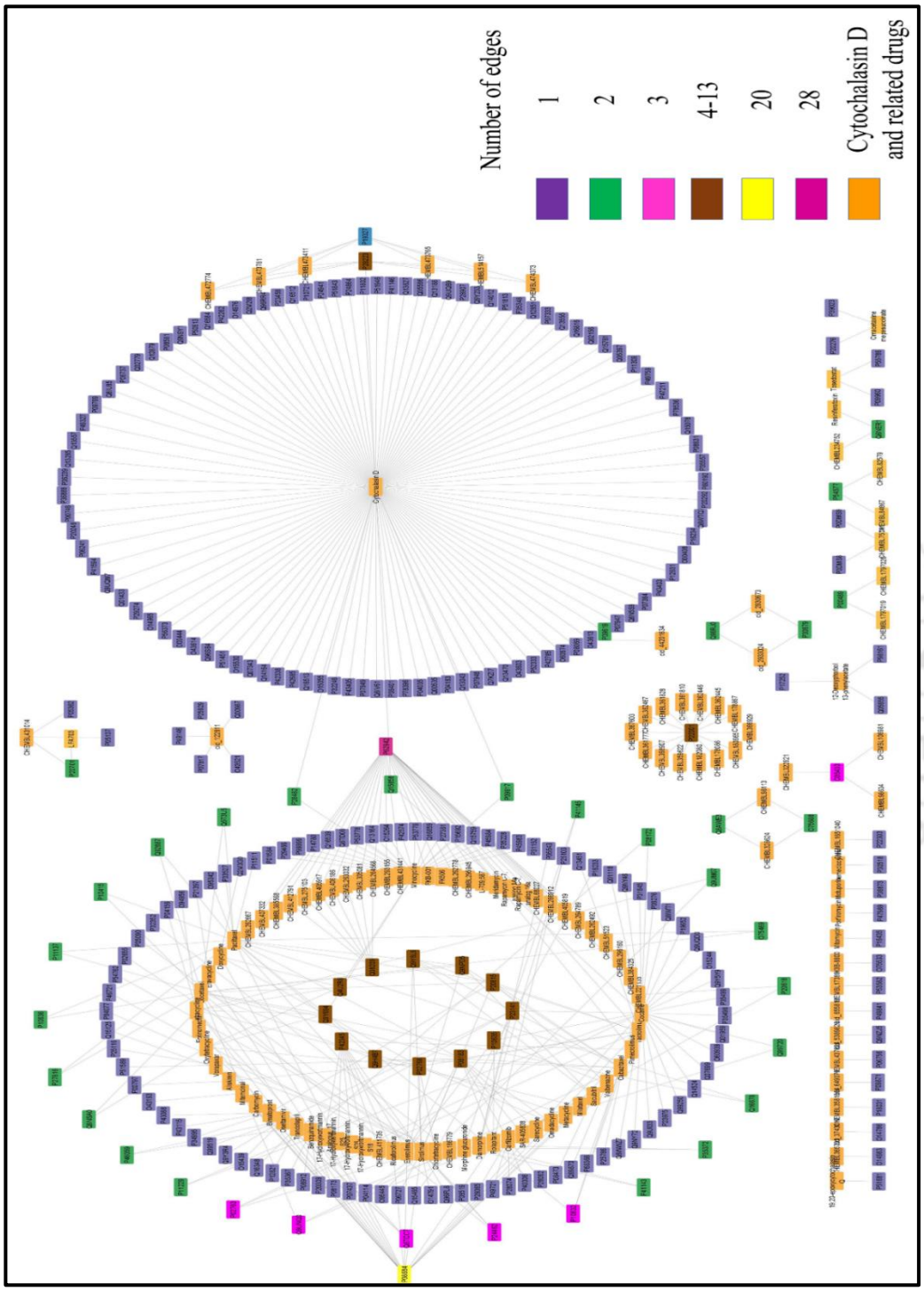

Figure 3.2.1. Cytoscape network of cytochalasin D and related drugs with the target proteins (Nodes- 400; Edges -449)

The protein targets identified from the cytochalasin D-protein interaction network were further analysed to identify key hub proteins critical for maintaining network integrity. This analysis involved constructing a protein-protein interaction (PPI) network using STRING, a tool designed to predict and visualize interactions among proteins. Homo sapiens was selected as the organism of interest. The interaction score threshold was set to 0.9, indicating a high confidence level for the interactions depicted in the network. The resulting PPI network (**Fig. 3.2.2(A)**) comprised 265 nodes (representing proteins) and 407 edges (representing interactions between proteins). The network exhibited a PPI enrichment p-value of less than 1.0e-16, underscoring the statistical significance of the observed interactions. The PPI network was further analysed using Cytoscape version 3.9.1, which facilitated the visualization and interpretation of protein interactions. Cytoscape enabled the identification of central proteins and the examination of their roles within the network. Proteins were evaluated based on their degree, which measures the number of direct interactions a protein has with other proteins. Higher degree values indicate greater centrality and potential importance within the network. Based on degree centrality, the top 11 proteins were selected for detailed analysis (**Table 3.2.1**). These proteins were identified as pivotal hubs due to their extensive interaction profiles, suggesting their significant roles in the PPI network. A specialized PPI hub network for these 11 proteins was generated using STRING (**Fig. 3.2.2(B)**). This focused network highlights the interactions among the key hub proteins, providing insights into their functional relationships and potential impact on the network.

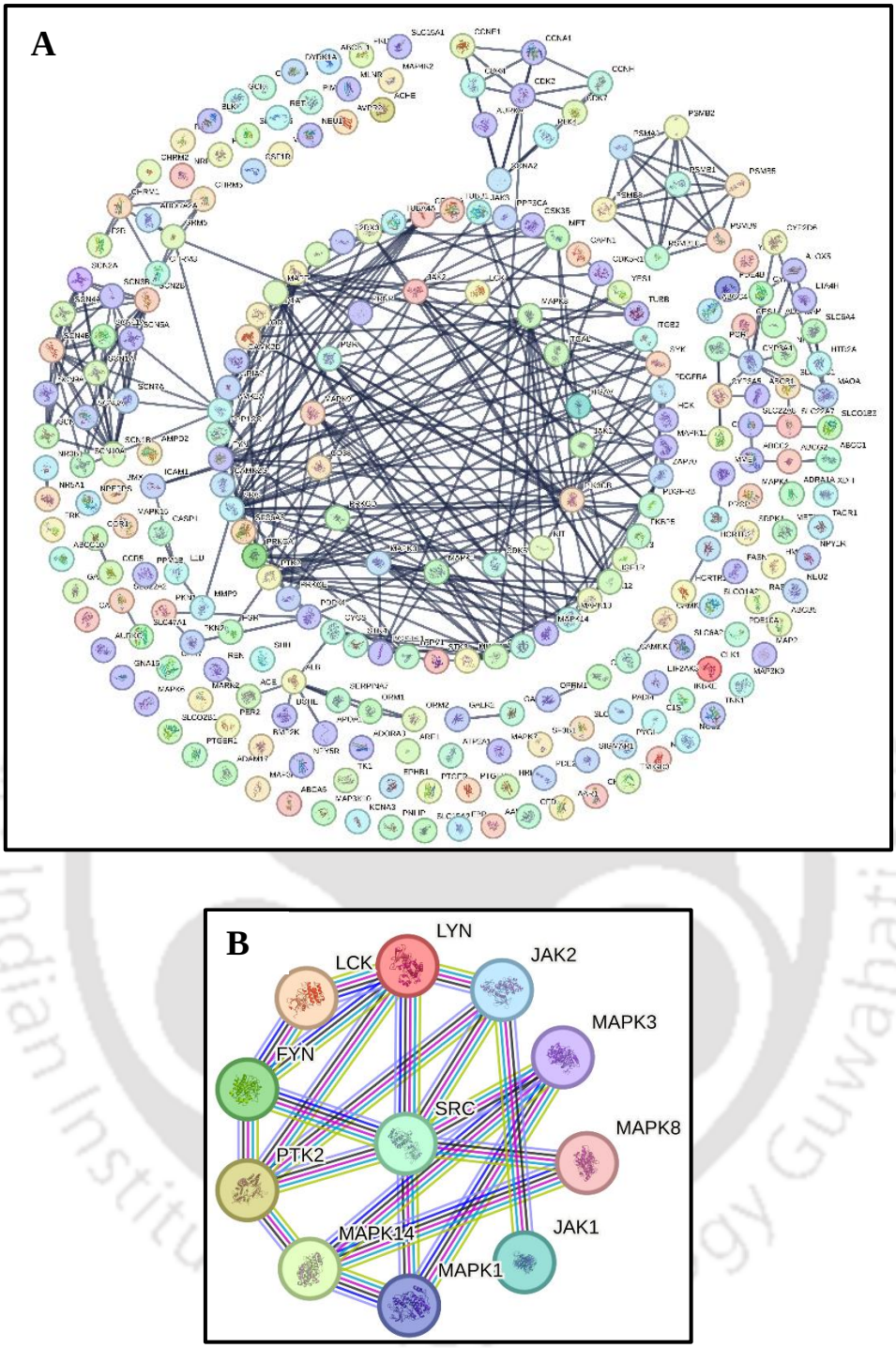

Figure 3.2.2. (A) PPI network using STRING software; **(B)** Hub of the top 11 proteins on the basis of degree of freedom

Table 3.2.1. Top 11 proteins from PPI network on the basis of degree of centrality

Uniprot ID	Protein	Degree
P12931	SRC	40
P06241	FYN	30
P28482	MAPK1	27
P06239	LCK	25
P27361	MAPK3	24
P07948	LYN	22
P23458	JAK1	21
O60674	JAK2	21
Q05397	PTK2	21
Q16539	MAPK14	21
P45983	MAPK8	19

3.2.2. Functional Insights from Enrichment Analysis of Protein Targets: GO Terms and KEGG Pathways

The DAVID database was used to perform enrichment analysis for biological processes (BP), cellular components (CC), molecular functions (MF), and KEGG pathways. The top eight enriched terms in BP, CC, and MF, based on their frequency of occurrence, were selected for Gene Ontology (GO) analysis with a significance threshold of $p < 0.05$ (**Fig. 3.2.3**). The analysis revealed that the enriched biological processes were predominantly associated with protein phosphorylation (61 targets), signal transduction (49 targets), apoptotic processes (26 targets), and transmembrane transport (25 targets). The majority of proteins were localized in the plasma membrane (150 targets), followed by the cytoplasm (132 targets) and cytosol (131 targets). This distribution highlights the cellular compartments where these proteins are most active. The targets were involved in several critical molecular functions, including protein binding (207 targets), ATP binding (97 targets), protein kinase activity (52 targets), and enzyme binding (25

targets), among others (**Fig. 3.2.4**). Out of 153 total pathways analysed, 142 were found to be statistically significant ($p < 0.05$) (see Fig. 3.5). The analysis identified that many genes were involved in key pathways related to tumorigenesis, such as the calcium signalling pathway, PI3-Akt signalling pathway, and MAPK pathway. A detailed list of the target genes associated with the top eight pathways (based on count) is provided in **Table 3.2.2.**

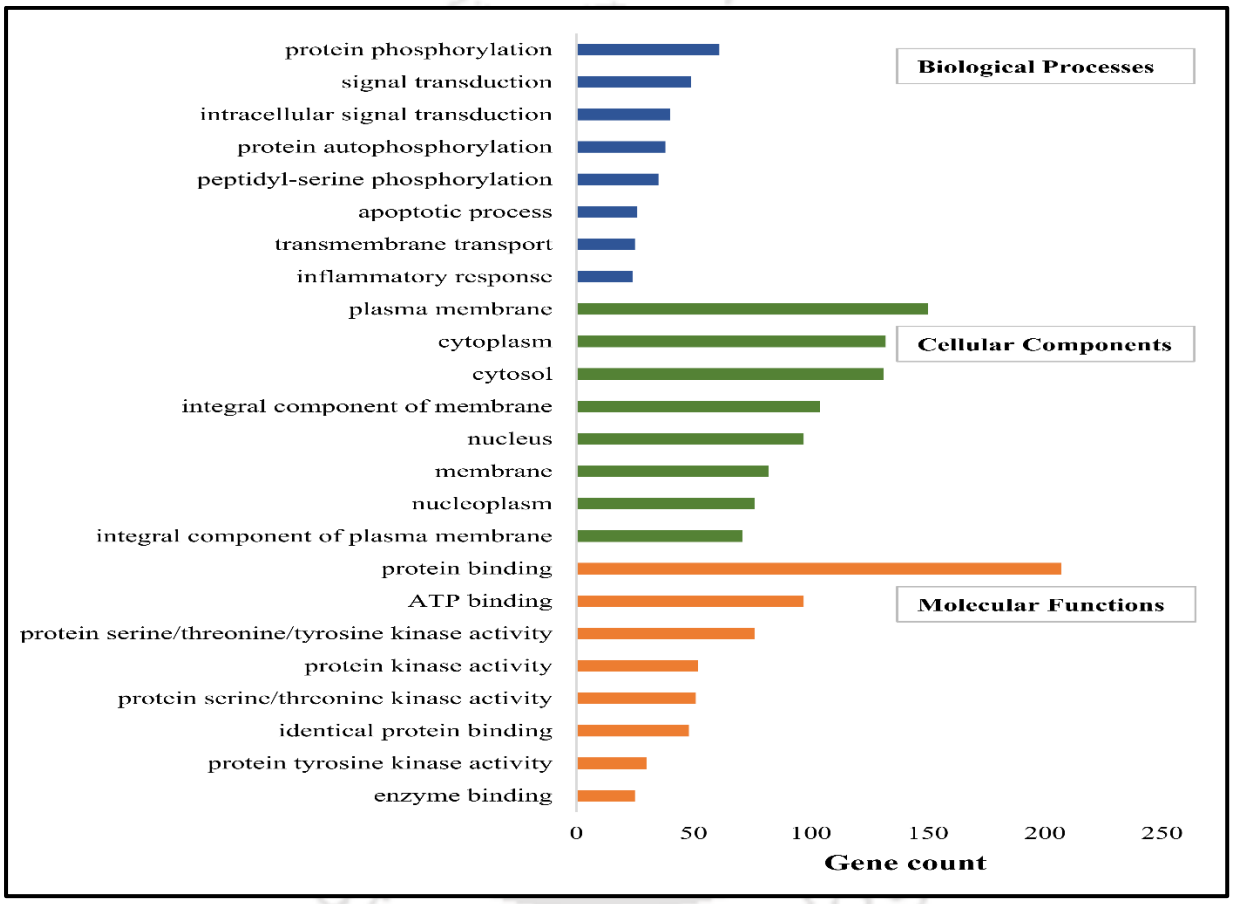

Figure 3.2.3. Gene Ontology showing involvement of the proteins in Biological processes (BP), Cellular Components (CC) and Molecular Functions (MF)

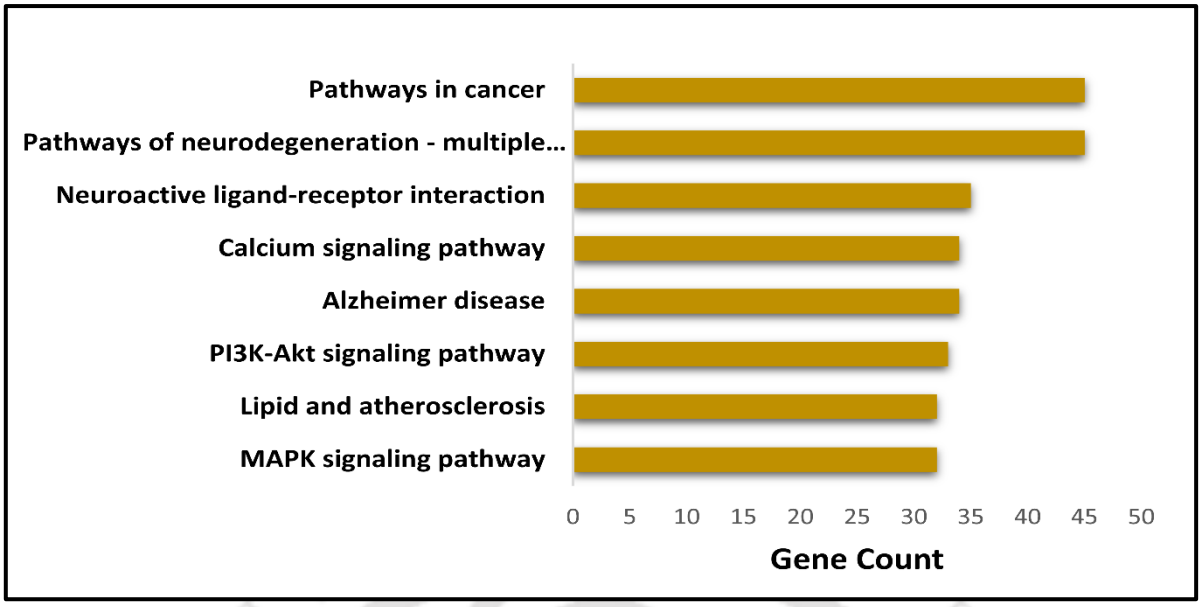

Figure 3.2.4. KEGG enrichment analysis of the target proteins showing the involvement in various diseases and physiological pathways

Table 3.2.2. Potential target genes and the pathways they are involved in on the basis of KEGG enrichment analysis

Term	Genes	P-Value
Pathways in cancer	BCL2, BCL2L11, JAK1, JAK2, JAK3, KIT, MDM2, MET, PIM1, RASGRP3, CAMK2A, CAMK2D, CAMK2G, CASP3, F2R, CSF1R, CCNA1, CCNA2, CCNE1, CDK2, CDK4, CYCS, FLT3, GSK3B, IGF1R, ITGAV, MMP9, MTOR, MAPK1, MAPK10, MAPK3, MAPK8, MAPK9, NOS2, PIK3CB, PDGFRA, PDGFRB, PTGER1, PTGER3, PRKCA, PTK2, RET, STK4, SHH, VEGFA	3.7E-12
Pathways of neurodegeneration-multiple diseases	ATP2A1, BCL2, CAMK2A, CAMK2D, CAMK2G, CAPN1, CASP3, CHRM1, CHRM3, CHRM5, CDK5R1, CDK5, EIF2AK3, GRIA2, GRIN1, GRIN2A, GRM5, GSK3B, IL1B, MTOR, MAPT, MAPK1, MAPK10, MAPK11, MAPK12, MAPK13,	8.1E-14

	MAPK14, MAPK3, MAPK8, MAPK9, MAP3K10, NOS2, PRNP, PSMA1, PSMB1, PSMB2, PSMB5, PRKCA, PPP3CA, SIGMAR1, SLC6A3, TUBA4A, TUBB1, TUBB	
Neuroactive ligand-receptor interaction	HTR2A, ADORA2A, ADORA3, ADRA1A, AVPR2, CHRM1, CHRM2, CHRM3, CHRM4, CHRM5, F2R, GALR1, GALR2, GRIA2, GRIN1, GRIN2A, GRM5, HRH1, HCRTR1, HCRTR2, MLNR, NPY1R, NPY2R, NPY5R, OPRD1, OPRK1, OPRM1, OPRL1, PTGER1, PTGER3, PTGFR, P2RX3, TACR1, TAAR1, TRPV1	7.7E-11
Calcium signalling pathway	HTR2A, ATP2A1, CD38, GNA15, MET, ADORA2A, ADRA1A, CAMK1, CANK1D, CAMK2A, CAMK2D, CAMK2G, CHRM1, CHRM2, CHRM3, CHRM5, F2R, GRIN1, GRIN2A, GRM5, HRH1, NOS2, PHKG1, PDGFRA, PDGFRB, PTGER1, PTGER3, PTGFR, PRKCA, PPP3CA, P2RX3, RET, TACR1, VEGFA	9.8E-15
Alzheimer disease	ADAM17, ATP2A1, CAPN1, CASP3, CHRM1, CHRM3, CHRM5, CDK5R1, CDK5, CYCS, EIF2AK3, GRIN1, GRIN2A, GRM5, GSK3B, IL1B, MTOR, MME, MAPT, MAPK1, MAPK10, MAPK3, MAPK8, MAPK9, NOS2, PIK3CB, PSMA1, PSMB1, PSMB2, PSMB5, PPP3CA, TUBA4A, TUBB1, TUBB	1.1E-9
PI3K-Akt signalling pathway	PDPK1, BCL2, BCL2L11, JAK1, JAK2, JAK3, KIT, MDM2, MET, CHRM1, CHRM2, F2R, CSF1R, CCNE1, CDK2, CDK4, FLT3, GSK3B, IGF1R, ITGAV, MTOR, MAPK1,	7.9E-10

	MAPK3, PIK3CB, PDGFRA, PDGFRB, PRKCA, PKN1, PKN2, PTK2, RET, SYK, VEGFA	
Lipid and atherosclerosis	PDPK1, BCL2, JAK2, LYN, SRC, APOA1, CAMK2A, CAMK2D, CAMK2G, CASP1, CASP3, CYP2J2, CYCS, EIF2AK3, GSK3B, IKBKE, ICAM1, IL1B, MMP9, MAPK1, MAPK10, MAPK11, MAPK12, MAPK13, MAPK14, MAPK3, MAPK8, MAPK9, PIK3CB, PRKCA, PPPECA, PTK2	4.1E-15
MAPK signalling pathway	KIT, MET, RASGRP3, CASP3, CSF1R, FLT3, IGF1R, IL1B, MAPT, MAPK1, MAPK10, MAPK11, MAPK12, MAPK13, MAPK14, MAPK3, MAPK7, MAPK8, MAPK9, MAPK3K10, MAPK3K11, MAPK3K9, MAP4K2, PDGFRA, PDGFRB, PRKCA, PPP3CA, PPM1B, RET, STK3, STK4, VEGFA	3.9E-11

3.2.3. Molecular docking studies highlighted Cytochalasin D's binding efficacy against key protein targets

Among the 11 targets initially identified through the comprehensive analysis of the core STRING Protein-Protein Interaction (PPI) network, six were deemed pivotal for further investigation. These include c-SRC, JAK1, MAPK1, MAPK3, MAPK8, and MAPK14. Notably, the selection process involved a discerning approach. For instance, while SRC, FYN, LYN, and LCK belong to the Src family kinases, only c-SRC was advanced for deeper scrutiny, considering its specific relevance within this kinship. Similarly, from the trio of JAK1, JAK2, and PTK2, JAK1 was singled out for further study, indicating a judicious selection process based on distinctive characteristics and functional roles. Furthermore, the decision to include all four MAPKs (MAPK1, MAPK3, MAPK8, and

MAPK14) was substantiated by insights derived from KEGG enrichment analysis, underscoring their collective importance in the regulatory landscape under investigation. Docking experiments were performed using cytochalasin D in conjunction with established inhibitors specific to each target protein. The selection of binding sites was guided by the locations known to interact with these inhibitors, with the objective of assessing the potential of cytochalasin D as a superior inhibitor across the range of target proteins under investigation. This approach enables a comprehensive evaluation of cytochalasin D's inhibitory capabilities and facilitates a comparative analysis with established inhibitors, thereby offering valuable insights into its potential therapeutic efficacy across various protein targets. A comparative inspection of the binding energies has been listed in **Table 3.2.3**. Cytochalasin D showed most favourable binding with JAK1(-9.49 kcal/mol). More or less similar binding energies were observed in case of the other proteins. Further, protein-ligand interactions for all the proteins with their known inhibitors and cytochalasin D has been illustrated (**Fig. 3.2.5**). Furthermore, **Table 3.2.4** summarizes a comparative analysis between reported interacting amino acid residues and those identified post-docking.

Table 3.2.3. Binding energy after docking the target proteins with cytochalasin D

PDB ID	Protein	Inhibitor	Binding energy(kcal/mol)	Inhibitor	Binding energy(kcal/mol)
3EYG	JAK1	MI1	-8.71	Cyt D	-9.49
2H8H	c-SRC	2H8H	-10.40	Cyt D	-8.35
1TVO	MAPK1	FRZ	-9.46	Cyt D	-8.27
4QTB	MAPK3	38Z	-18.61	Cyt D	-8.46
3V3V	MAPK8	MYU	-8.22	Cyt D	-7.14
3QU3	MAPK14	Skepinone	-9.92	Cyt D	-8.49

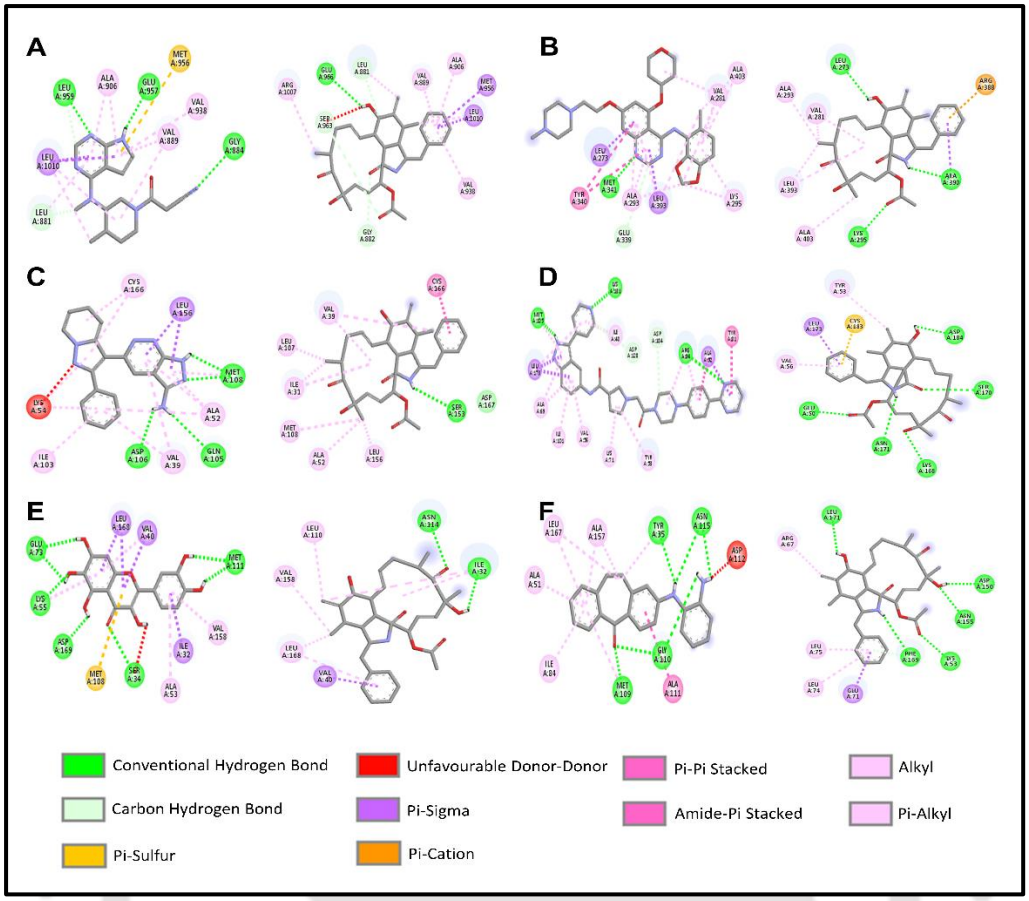

Figure 3.2.5. 2-D interactions between **(A)** JAK1 and MI1 (left), JAK1 and CytD (right); **(B)** c-SRC and 2H8H (left), c-SRC and CytD (right); **(C)** MAPK1 and FRZ, MAPK1 (left) and CytD (right); **(D)** MAPK3 and 38Z (left), MAPK3 and CytD (right); **(E)** MAPK8 and MYU (left), MAPK8 and CytD (right); **(F)** MAPK14 and Skepinone (left), MAPK14 and CytD (right).

Table 3.2.4. Interacting amino acid residues in the binding sites

Protein	Reported Interactions	Docked Interactions with Inhibitor	Docked Interactions with CytD
JAK1 (Inhibitor-MI1)	Leu-881, Gly-884, Val- 889, Ala-906, Lys-908, Val-938, Met-956, Glu-957, Leu-959, Asn-1008, Leu-1010.	Leu-881, Gly-884, Val-889, Ala-906, Val-938, Met-956, Glu-957, Leu-959, Leu-1010.	Leu-881, Gly-882, Val-889, Ala-906, Val-938, Met-956, Ser-963, Glu-966, Arg-1007, Leu-1010.

c-Src (Inhibitor-2H8H)	Leu-273, Val-281, Ala-293, Lys-295, Thr-338, Glu-339, Met-341, Ser-342, Gly-344, Ser-345, Leu-393, Ala-403.	Leu-273, Val-281, Ala-293, Lys-295, Glu-339, Tyr-340, Met-341, Leu-393, Ala-403.	Leu-273, Val-281, Ala-293, Lys-295, Arg-388, Ala-390, Leu-393, Ala-403.
MAPK1 (Inhibitor-FRZ)	Val-39, Ala-52, Lys-54, Gln-105, Asp-106, Met-108, Leu-156, Cys-166.	Val-39, Ala-52, Lys-54, Ile-103, Gln-105, Asp-106, Met-108, Leu-156, Cys-166.	Ile-31, Val-39, Gly-52, Leu-107, Met-108, Ser-153, Leu-156, Cys-166, Asp-167.
MAPK3 (Inhibitor-38Z)	Ile-48, Ala-52, Tyr-53, Val-56, Ala-69, Ile-73, Tyr-81, Arg-84, Thr-85, Asp-123, Met-125, Asp-128, Lys-131, Leu-173, Asp-184.	Ile-48, Ala-52, Tyr-53, Val-56, Ala-69, Lys-71 Tyr-81, Arg-84, Ile-101, Met-125, Asp-128, Lys-131, Leu-173, Asp-184.	Glu-50, Tyr-53, Val-56, Lys-168, Ser-170, Asn-171, Leu-173, Cys-183, Asp-184.
MAPK8 (Inhibitor-MYU)	Ile-32, Val-40, Ala-53, Lys-55, Glu-73, Met-108, Met-111, Val-158, Leu-168.	Ile-32, Ser-34, Val-40, Ala-53, Lys-55, Glu-73, Met-108, Met-111, Val-158, Leu-168, Asp-169.	Ile-32, Val-40, Leu-110, Asn-114, Val-158, Leu-168.
MAPK14 (Inhibitor-Skepinone)	Val-30, Tyr-35, Val-38, Ala-51, Lys-53, Leu-104, Thr-106, Met-109, Gly-110, Ala-111, Asp-112, Leu-167.	Tyr-35, Ala-51, Ile-84, Met- 109, Gky-110, Ala-111, Asp-112, Asn- 115, Ala-157, Leu-167.	Lys-53, Arg-67, Glu-71, Leu-74, Leu-75, Asp-150, Asn-155, Phe-169, Leu-171.

3.2.4. MD simulation studies revealed stable protein-ligand complexes for MAPKs and Cytochalasin D

In order to further validate the molecular docking findings of this study, we performed MD simulation studies because it addresses structural flexibility and entropic effects of a system, enabling a more precise assessment of the thermodynamics and kinetics

involved in the recognition and binding of drugs to their targets. MD simulation of the 6 proteins with their respective inhibitors and cytochalasin D were performed for a period of 100 ns under simulated physiological conditions and the dynamic attributes were analysed based on RMSD (Root mean square deviation), RMSF (Root mean square fluctuation), pair distance, radius of gyration and number of H-bonds. A comparison of the RMSD values between the protein backbone, proteins with their respective inhibitors and proteins with cytochalasin D showed fluctuations within 1Å highlighting the minimal effect on protein stability upon ligand binding (**Fig 3.2.6**). Similar comparison for RMSF values for protein backbone and protein-cytochalasin D complexes showed negligible changes (<0.1) indicating fewer fluctuations in the residues upon cytochalasin D binding. The paired distant plots exhibit a comparative analysis between the proteins in conjunction with their corresponding inhibitors and proteins co-administered with cytochalasin D. Notably, among the four MAPKs investigated (MAPK1, MAPK3, MAPK8, and MAPK14), an average value of 0.125 was observed upon conjugation with cytochalasin D. However, this pattern was not replicated with JAK1 and c-SRC. The average value of pair distance for JAK1-MI1 was 0.18 but for JAK1-CytD it was 0.67. Similarly, c-SRC-2H8H had an average pair distance value of 0.2 as compared to 0.37 in case of c-SRC-CytD (**See appendix**). These findings underscore the differential responses exhibited by distinct protein targets when subjected to cytochalasin D treatment, suggesting potential variations in regulatory mechanisms or downstream signalling pathways. It is readily apparent that for JAK1 and c-SRC interacting with cytochalasin D, the binding exhibited instability. Specifically, in the case of c-SRC, cytochalasin D displayed a propensity to migrate towards an alternate binding site as opposed to the intended one. Examination of hydrogen bonding interactions within the protein-cytochalasin D complexes revealed

an average of approximately one hydrogen bond, with MAPK8 demonstrating an average of approximately two hydrogen bonds (**Fig. 3.2.7**). These observations underscore the dynamic nature of the interactions between cytochalasin D and various protein targets, suggesting potential implications for binding stability and specificity. In order to corroborate these findings, multiple conformations of all six proteins in complex with cytochalasin D were recorded at intervals of 25 nanoseconds (**Fig. 3.2.8**).

Table 3.2.5. Predicted binding energies as per MMPBSA method

Protein	Inhibitor	van der Waal energy (kJ/mol)	Electrostatic energy (kJ/mol)	Polar solvation energy (kJ/mol)	SASA energy (kJ/mol)	Binding energy (kJ/mol)
MAPK1	Frz	-166.141 +/- 13.097	-62.893 +/- 5.612	197.734 +/- 15.021	-17.750 +/- 0.877	-49.050 +/- 17.357
	Cyt D	-124.248 +/- 28.355	-28.651 +/- 28.372	123.849 +/- 49.735	-16.406 +/- 2.866	-45.456 +/- 19.072
MAPK3	38Z	-276.324 +/-29.924	-163.708 +/-22.340	410.303 +/-37.776	-30.132 +/- 1.478	-59.862 +/-25.378
	Cyt D	-104.600 +/-24.734	-35.885 +/- 15.433	108.034 +/-44.875	-14.882 +/- 3.102	-47.333 +/-16.490
MAPK8	Myu	-119.503 +/- 16.800	-79.657 +/- 40.696	177.845 +/- 37.588	-16.001 +/- 1.094	-37.315 +/- 14.265
	Cyt D	-168.552 +/- 18.880	-47.135 +/- 14.911	145.618 +/- 21.771	-20.030 +/- 1.329	-90.100 +/- 19.187
MAPK14	Skepinone	-155.723 +/- 26.065	-28.369 +/- 13.136	133.055 +/- 19.055	-18.173 +/- 1.347	-69.210 +/- 22.162
	Cyt D	-142.419 +/- 27.522	-13.401 +/- 8.641	113.049 +/- 44.497	-18.626 +/- 2.653	-61.396 +/- 19.772

Binding free energy was calculated for the 4 stable complexes (MAPK1, MAPK3, MAPK8 and MAPK14 with cytochalasin D) using MMPBSA (Molecular Mechanics

Poisson-Boltzmann Surface Area). For a comparison study, the binding free energies of the proteins with their respective inhibitors was also calculated (**Table 3.2.5**). There wasn't any major fluctuation in the binding energies for any of the protein-ligand complex but in case of MAPK8 a huge difference was observed. MAPK8-Myu complex had a binding energy value of -37.3kJ/mol whereas, MAPK8-CytD complex had a binding energy of -90.1kJ/mol indicating a more favourable binding compared to the reported inhibitor.

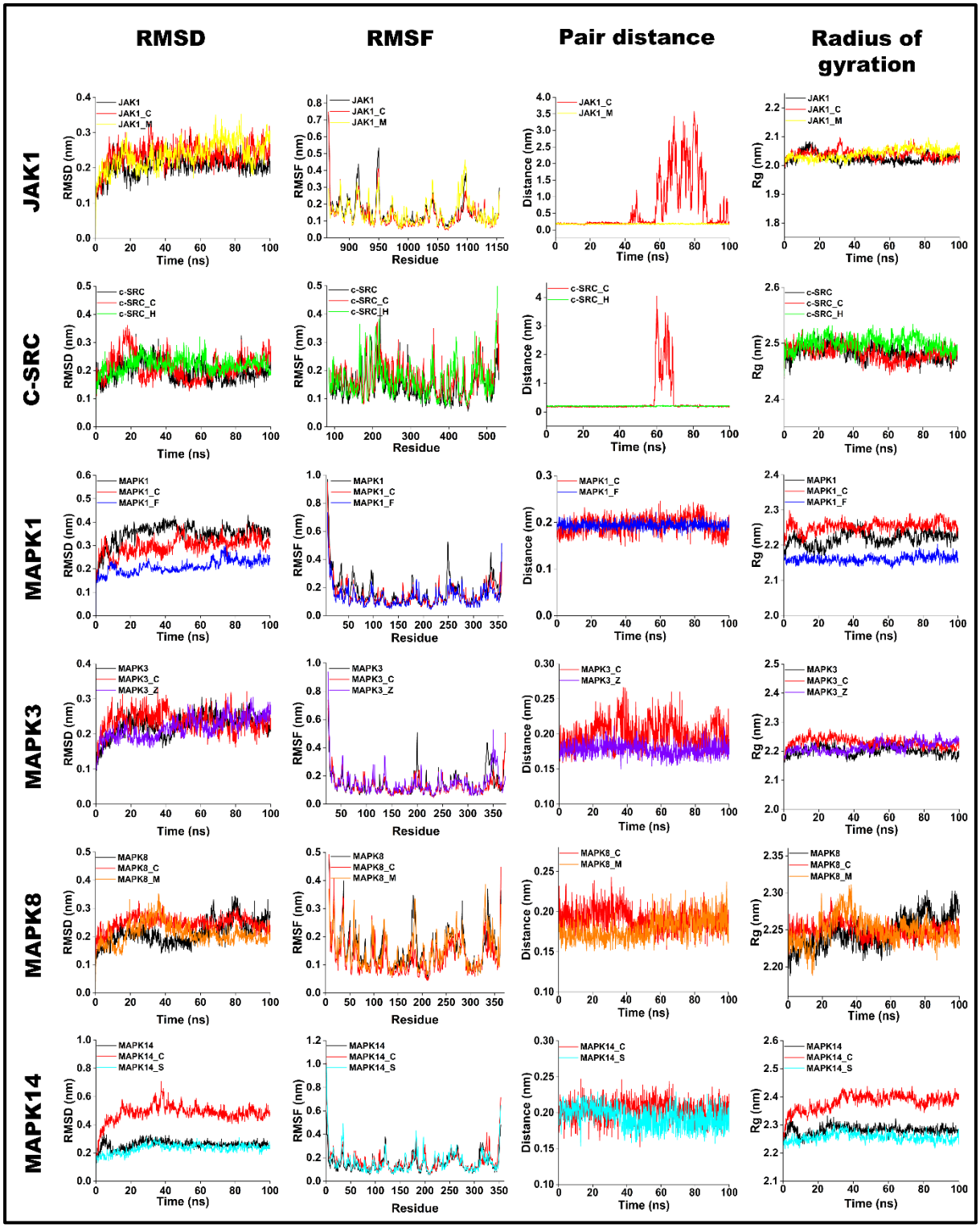

Figure 3.2.6. RMSD, RMSF, pair distance and radius of gyration of protein backbones, proteins with their known inhibitors and proteins with cytochalasin D

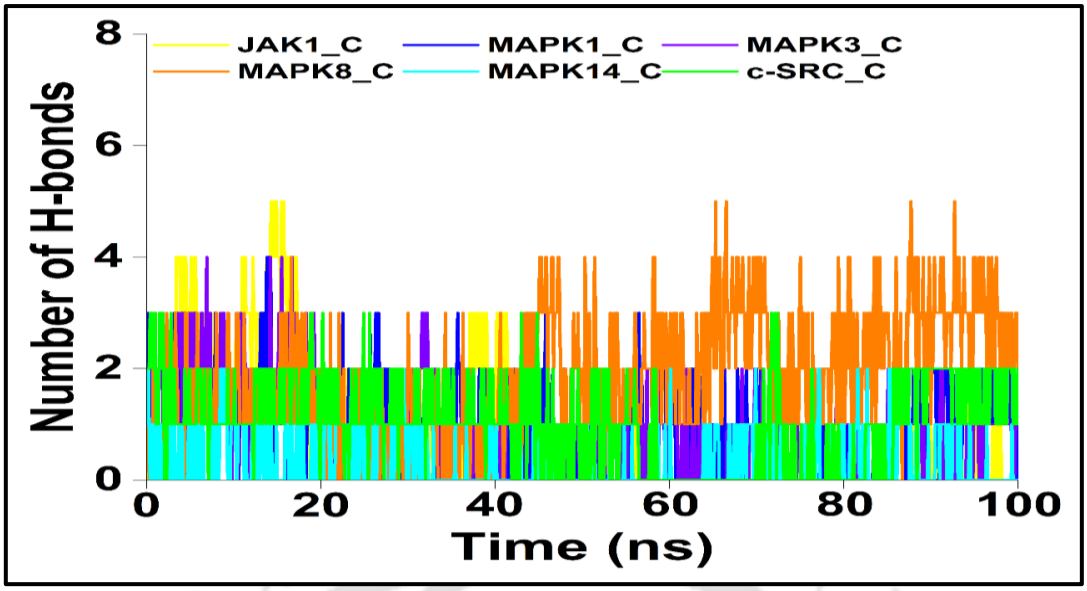

Figure 3.2.7. Average number of H-bonds between the target proteins with cytochalasin D

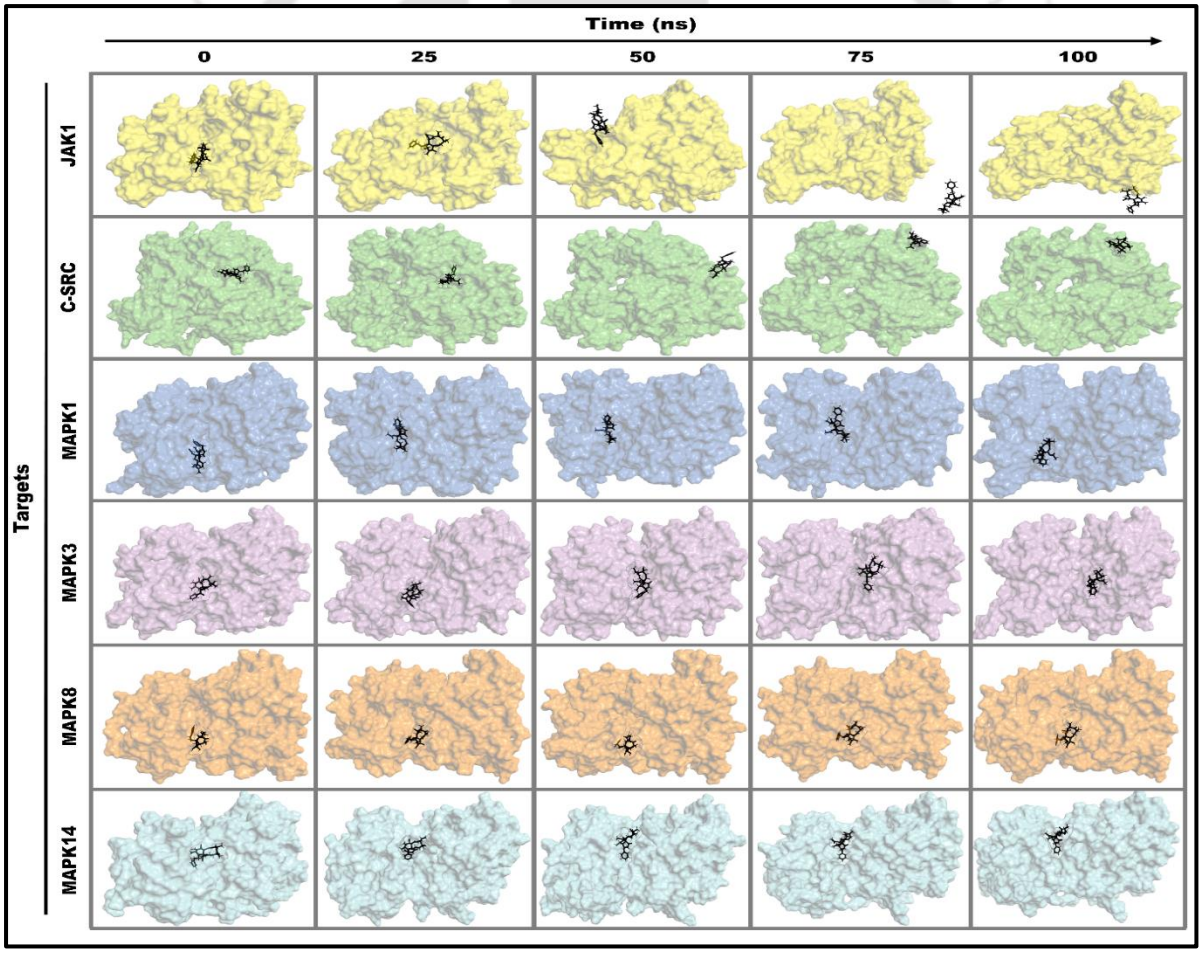

Figure 3.2.8. Still images of the 6 target proteins along with cytochalasin D after 100ns of MD simulation, taken at intervals of 25ns (0, 25, 50, 75, 100ns).

3.3. Discussion

The exploration of natural herbal products as potential candidates for cancer prevention and treatment has garnered significant attention in recent years, owing to their promising therapeutic properties and impactful role in modern medical strategies (Khan & Trivedi, 2023). Among these natural products, secondary metabolites derived from entomopathogenic fungi have emerged as particularly noteworthy due to their potent anticancer properties (L. Zhang et al., 2020). These bioactive compounds have demonstrated the ability to induce apoptosis, inhibit cancer cell proliferation, and selectively target critical signalling pathways involved in cancer progression (Shin et al., 2014). However, the journey from discovering novel anticancer agents within entomopathogenic fungi to developing them into effective drugs is tasking and time-consuming. The process involves several critical steps, including the isolation and purification of bioactive compounds, structural elucidation to determine their chemical nature, and extensive biological testing to evaluate their efficacy and safety (Xi et al., 2022). These steps are essential to ensure that the compounds are not only effective against cancer but also safe for therapeutic use.

Given the complexity of this drug discovery process, network pharmacology has emerged as a valuable tool to narrow-down and enhance the identification and characterization of potential anticancer agents. Network pharmacology provides a holistic approach by examining the multifaceted interactions and regulatory mechanisms of signalling pathways at a network level. This approach allows researchers to explore the interconnectedness and interdependence of drug targets, offering a comprehensive understanding of how a compound exerts its therapeutic effects across multiple biological pathways (Hopkins, 2008). By integrating network pharmacology into the drug discovery process, researchers can gain insights into the

multi-target mechanisms of innovative drugs. This approach not only aids in identifying potential drug candidates but also helps in understanding the broader implications of their interactions within complex biological systems. As a result, network pharmacology has become an indispensable tool in the development of novel therapeutic strategies, particularly in the field of cancer treatment, where multi-target approaches are often necessary to overcome the challenges posed by the disease's complexity and heterogeneity.

In this study, we applied network-based pharmacology to investigate the mechanisms underlying the cytotoxic effects of cytochalasin D, a bioactive compound derived from the entomopathogenic fungus *Metarhizium anisopliae*, on triple-negative breast cancer (TNBC) MDA-MB-231 cells. Our analysis identified 278 potential protein targets of cytochalasin D. KEGG pathway enrichment analysis revealed that these targets are involved in several crucial pathways, including those associated with cancer, neurodegeneration, the PI3K-Akt signalling pathway, and the MAPK signalling pathway.

Further examination through protein-protein interaction (PPI) analysis highlighted several genes with significant differential expression, such as SRC, FYN, MAPK1, LCK, MAPK3, LYN, JAK1, JAK2, PTK2, MAPK14, and MAPK8. Among these, MAPK1, MAPK3, MAPK8, and MAPK14 emerged as key targets, showing stable protein-ligand complexes during molecular dynamics (MD) simulations. These findings suggest that cytochalasin D may act as a potent inhibitor of the MAPK pathways. Binding energies calculated using MM-PBSA confirmed the stability of these complexes, reinforcing the potential efficacy of cytochalasin D as an inhibitor. Utilizing GROMACS 2023 and the CHARMM-GUI force field, our MD simulations provided an in-depth analysis of the dynamic interactions between cytochalasin D and

its target proteins. The simulations revealed critical insights into the structural stability, flexibility, and binding interactions of these complexes. The analysis of root mean square deviation (RMSD), root mean square fluctuation (RMSF), hydrogen bonding, bond lengths, and MM-PBSA binding energies contributed to a refined understanding of the molecular mechanisms driving cytochalasin D's interactions with its targets. Visualization of these results using QtGrace ensured clear and effective communication of our findings, supporting the overall conclusions of the study and emphasizing the potential of cytochalasin D as a therapeutic agent in cancer treatment.

3.4. Conclusion

Network pharmacology is fundamentally transforming drug discovery and development by acknowledging and leveraging the intricate, interconnected nature of biological systems. Traditional pharmacology typically follows a single-target paradigm, where a drug is designed to interact with one specific molecular target. This focused approach has indeed led to the development of numerous successful drugs. However, it often neglects the complex network of interactions within biological systems, where diseases are rarely attributable to a single factor but rather result from multiple, interrelated pathways. Network pharmacology, in contrast, considers the broader context of drug interactions within entire biological networks. By identifying and targeting multiple molecular nodes within these networks, this approach provides a more comprehensive strategy for disease intervention. It facilitates a deeper understanding of how drugs interact with various targets, potentially offering more effective and safer therapeutic options. Additionally, network pharmacology integrates with molecular dynamics (MD) simulation studies to further refine and validate potential drug targets.

By applying network pharmacology to investigate cytochalasin D, a bioactive compound derived from an entomopathogenic fungus, we have been able to identify and narrow down potential molecular targets involved in cancer progression. This method not only highlights the multiple targets cytochalasin D may interact with but also provides insights into its mechanisms of action and potential efficacy in treating cancer.

The subsequent chapter will build upon these findings by conducting a series of experimental studies using cytochalasin D against the triple-negative breast cancer (TNBC) cell line MDA-MB-231. These studies will aim to validate the molecular targets identified through network pharmacology and MD simulations, assessing the effectiveness and potential therapeutic benefits of cytochalasin D. By bridging computational predictions with empirical evidence, this chapter seeks to confirm the promising therapeutic potential of cytochalasin D in the context of TNBC treatment, thereby advancing the understanding and application of network pharmacology in cancer research.

Chapter 4

Cytotoxicity of Cytochalasin D against MDA-MB-231 cells

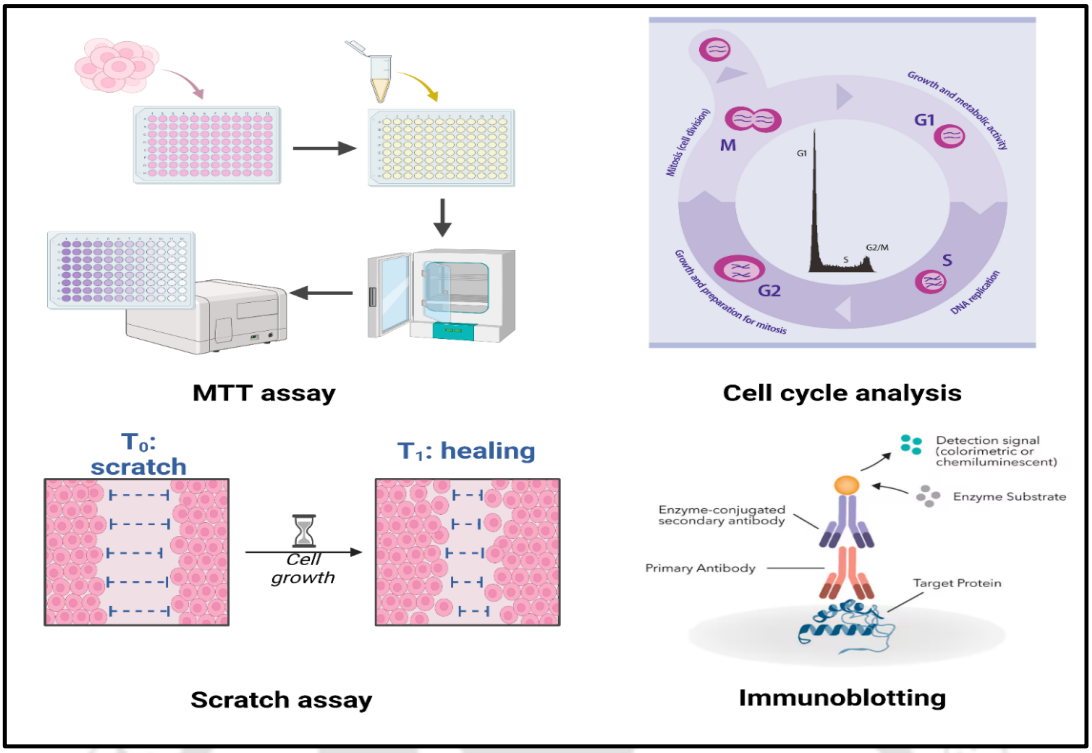

Scheme 4.1. Diagrammatic representation of *in vitro* assays of cytochalasin D against MDA-MB-231 cells

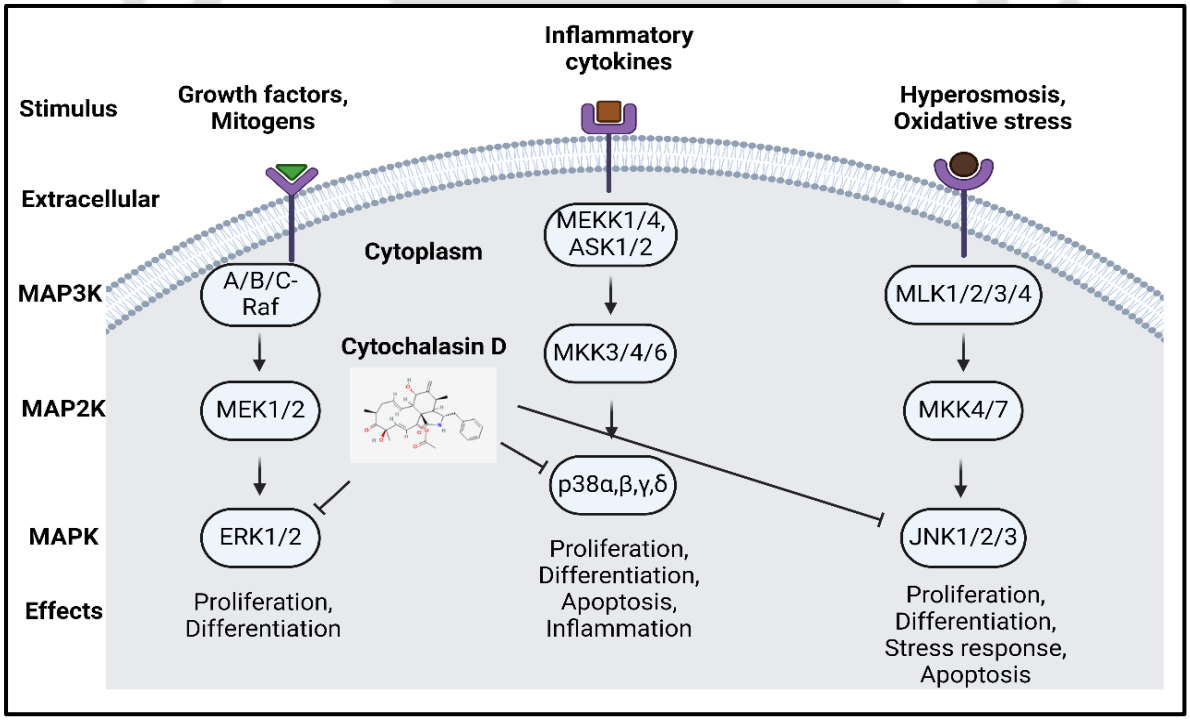

Scheme 4.2. Schematic representation of cytochalasin D's inhibitory effects on different members of MAPK signaling pathway

Abstract

Cytochalasin D, an alkaloid produced by various molds, has garnered significant attention for its potent anti-cancer properties. Initially recognized for its ability to inhibit actin polymerization, cytochalasin D disrupts cellular processes like cell division, motility, and morphology by binding to the barbed end of actin filaments. While early research focused on its effects on cell structure, recent studies have explored its broader therapeutic potential, particularly in cancer treatment. Cytochalasin D has been shown to induce apoptosis and arrest the cell cycle at the G1-S transition via p53-dependent pathways. Additionally, it inhibits macropinocytosis in tumor cells, affecting their survival. Despite its promise, the clinical application of cytochalasin D faces challenges due to non-specific toxicity. However, combinatorial therapies with drugs like doxorubicin and paclitaxel have demonstrated synergistic effects, particularly in multidrug-resistant cancers. In this study involving MDA-MB-231 cell line, cytochalasin D effectively inhibited cell migration, induced elevated ROS levels, and downregulated key MAP kinase proteins, underscoring its potential as a therapeutic agent in cancer treatment.

4.1. Introduction

Cytochalasin D, an alkaloid produced by various molds, belongs to a class of mycotoxins called cytochalasins (Aldridge et al., 1967; C Aldridge et al., 1967). Its isolation and characterization date back to the mid-20th century, when researchers began exploring natural products with biological activity. As discussed earlier in Chapter 1, it exhibits multiple therapeutic effects and has shown promising anti-cancerous properties when used alone or in conjugation with other drugs such as doxorubicin, paclitaxel and vinblastine (Trendowski, Christen, et al., 2015).

In initial days, research related to cytochalasin D was majorly focused on its effects on cell structure, motility and division, thanks to its actin inhibition property (Flanagan & Lin, 1980). It disrupts actin polymerization by binding to the barbed end of an elongating filament (Brown & Spudich, 1981; Goddette & Frieden, 1986; Trendowski, 2015). This alters cellular morphology and affects processes such as cell division and proliferation. But its activities aren't limited to just actin depolymerization and in the decade following its discovery the attention was shifted to decipher its molecular mechanism of action. Researchers utilized it to study various cellular processes dependent on the actin cytoskeleton, such as cell motility, intracellular trafficking, and cytokinesis. Its ability to induce changes in the cell's architecture made it invaluable for dissecting the roles of the actin cytoskeleton in these processes.

Current research surrounding cytochalasin D has shed light on its therapeutic properties with regard to cancer treatment. Its capacity to inhibit cell division and induce apoptosis has shown promise in preclinical models of various cancers. When checked for its effects on cell cycle machinery, cytochalasin D brought about an arrest at the G1-S transition via p53-dependent pathways (Trendowski, Mitchell, et al., 2015). Furthermore, it also inhibits macropinocytosis (a regulated form of endocytosis which

is dependent on actin filaments for uptake of solute molecules and nutrients) amongst tumour cells, hence affecting their survival (Qiu et al., 2022).

However, *in vivo* studies with cytochalasin D face the challenge of non-specific toxicity and hence current studies are more directed towards combinatorial therapy using cytochalasin D with other drugs such as doxorubicin and paclitaxel (Trendowski, Christen, et al., 2015). These drugs work in synergy and have proven to be very effective in case of multidrug-resistant neoplastic cells that overexpress drug efflux proteins.

The following section deals with the therapeutic properties of cytochalasin D against MDA-MB-231 cell line. The details of the methodology followed have been listed down in an earlier chapter (Chapter 2). Successful killing of the cells was observed when treated with cytochalasin D. It also inhibited migratory properties of the cells and brought about an arrest in the cell cycle machinery. Elevated ROS levels were also observed in the treated cells and immunoblotting experiments showed reduction in few members of the MAP kinase family proteins that are known to play crucial roles in cancer cell proliferation and tumour progression.

4.2. Results

4.2.1. Cytochalasin D exhibited cytotoxic effects on TNBC MDA-MB-231 cells

The half maximal inhibitory concentration (IC_{50}) of cytochalasin D was calculated based on the readings. The IC_{50} value represents the concentration of cytochalasin D required to inhibit 50% of cell viability compared to untreated control cells. In this study, the IC_{50} of cytochalasin D for the MDA-MB-231 cell line was determined to be 28.9 µg/mL. This value indicates the potency of cytochalasin D in reducing cell viability, providing a quantitative measure of its cytotoxic effects and suggests that cytochalasin D is effective at a moderate concentration in inhibiting the proliferation of

MDA-MB-231 cells, which is crucial for understanding its potential as a therapeutic agent in cancer treatment. (**Fig. 4.2.1**).

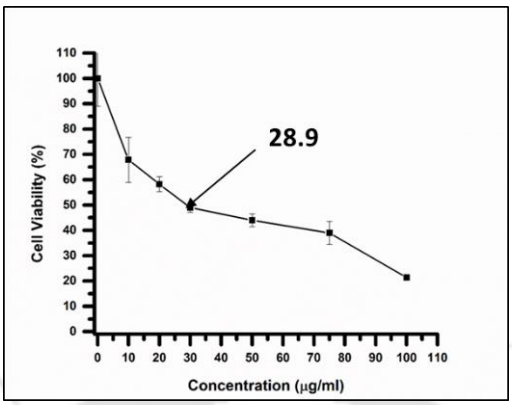

Figure 4.2.1. MTT assay using cytochalasin D against TNBC MDA-MB-231 cell line

4.2.2. Disruption of cell cycle machinery

Exposure to chemotherapeutic agents often triggers significant alterations in the cell cycle machinery due to the cellular stress these treatments impose (Sun et al., 2021). Stressed cells adapt and respond through various alternative pathways, including modifications in cell cycle progression (Caglar & Biray Avci, 2020). Understanding these changes is crucial for understanding the mechanisms of drug action and resistance in cancer cells. In the control group, the cell cycle distribution showed approximately 70% of the cell population was in the G1 phase, which is the phase where the cell grows and prepares for DNA synthesis. The remaining cells were equally distributed between the G2 and S phases, with 15% in each phase. The G2 phase is where the cell prepares for mitosis, and the S phase is where DNA replication occurs. Upon treating the MDA-MB-231 cells with cytochalasin D over a 48-hour period, we observed a dose-dependent alteration in the cell cycle distribution. Specifically, there was a significant increase in the percentage of cells in the S phase, indicating an arrest in this phase. At a concentration of 10 µg/mL of cytochalasin D, the proportion of cells in the S phase rose to 31%. This trend continued with higher concentrations: at 20 µg/mL, the S phase

population increased to 56%, and at 30 µg/mL, it slightly decreased to 54%, suggesting that the maximum effect of cytochalasin D on S phase arrest was achieved at 20 µg/mL. The arrest of cells in the S phase implies that cytochalasin D interferes with the cell's ability to complete DNA replication, thereby preventing progression to the G2 and M phases of the cell cycle. This S phase arrest is indicative of the drug's ability to halt cell proliferation, thereby exerting its cytotoxic effects. The plateau observed at the highest concentration suggests that beyond a certain point, increasing the concentration of cytochalasin D does not further enhance its effect on S phase arrest, possibly due to saturation of the drug's binding sites or maximum induction of the cellular stress response pathways. (**Fig. 4.2.2**).

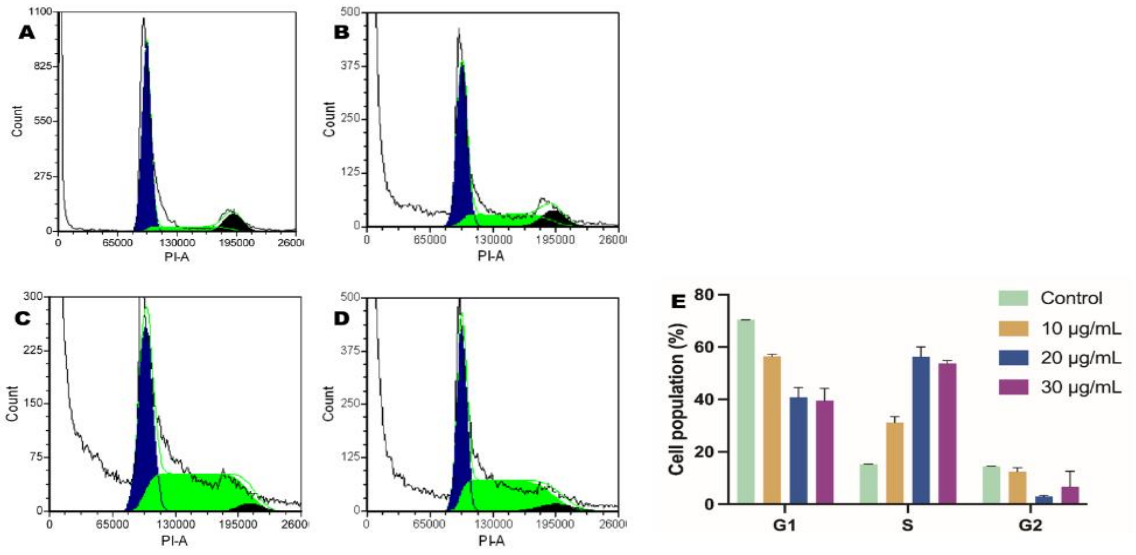

Figure 4.2.2. Cell cycle analysis with gradually increasing concentration of cytochalasin D **(A)** Untreated; **(B)** 10µg/mL; **(C)** 20µg/mL; **(D)** 30µg/mL; **(E)** Histogram representing cell populations in different phases of cell cycle with varying concentrations of cytochalasin D.

4.2.3. Exhibition of anti-migratory property

The wound healing assay, a commonly used method to evaluate the anti-migratory effects of compounds, was employed to assess the impact of cytochalasin D on the migratory capacity of MDA-MB-231 cells. In the control group, which did not receive any cytochalasin D treatment, a steady and progressive migration of the cells was observed from the initial time point up to 48 hours. The untreated cells demonstrated a significant reduction in the wound area within the first 24 hours, indicating robust migratory activity. By the 48-hour mark, the wound was completely filled, showcasing the cells' natural capacity for migration and healing. In contrast, the cells treated with cytochalasin D at the IC_{50} concentration (28.9 µg/mL) exhibited a markedly reduced rate of wound closure. The IC_{50} concentration, which is the concentration of cytochalasin D required to inhibit cell proliferation by 50%, was found to substantially impede the migratory ability of the cells. After 48 hours of treatment with cytochalasin D, only 54% of the wound area was covered, compared to the complete closure observed in the control group. The rate of migration for untreated cells was found to be 0.02 µm/h whereas, in treated cells it was found to be 0.01 µm/h, a 50% reduction. This significant reduction in wound closure highlights the potent anti-migratory effects of cytochalasin D. The results of this assay provide critical insights into the mechanism by which cytochalasin D exerts its effects on cancer cells. By inhibiting cell migration, cytochalasin D potentially prevents the spread and metastasis of cancer cells. Overall, the wound healing assay results reinforce the notion that cytochalasin D not only inhibits cell proliferation but also significantly impairs cell migration, making it a promising candidate for further investigation as an anti-metastatic agent in the treatment of aggressive cancers like triple-negative breast cancer. (**Fig. 4.2.3**).

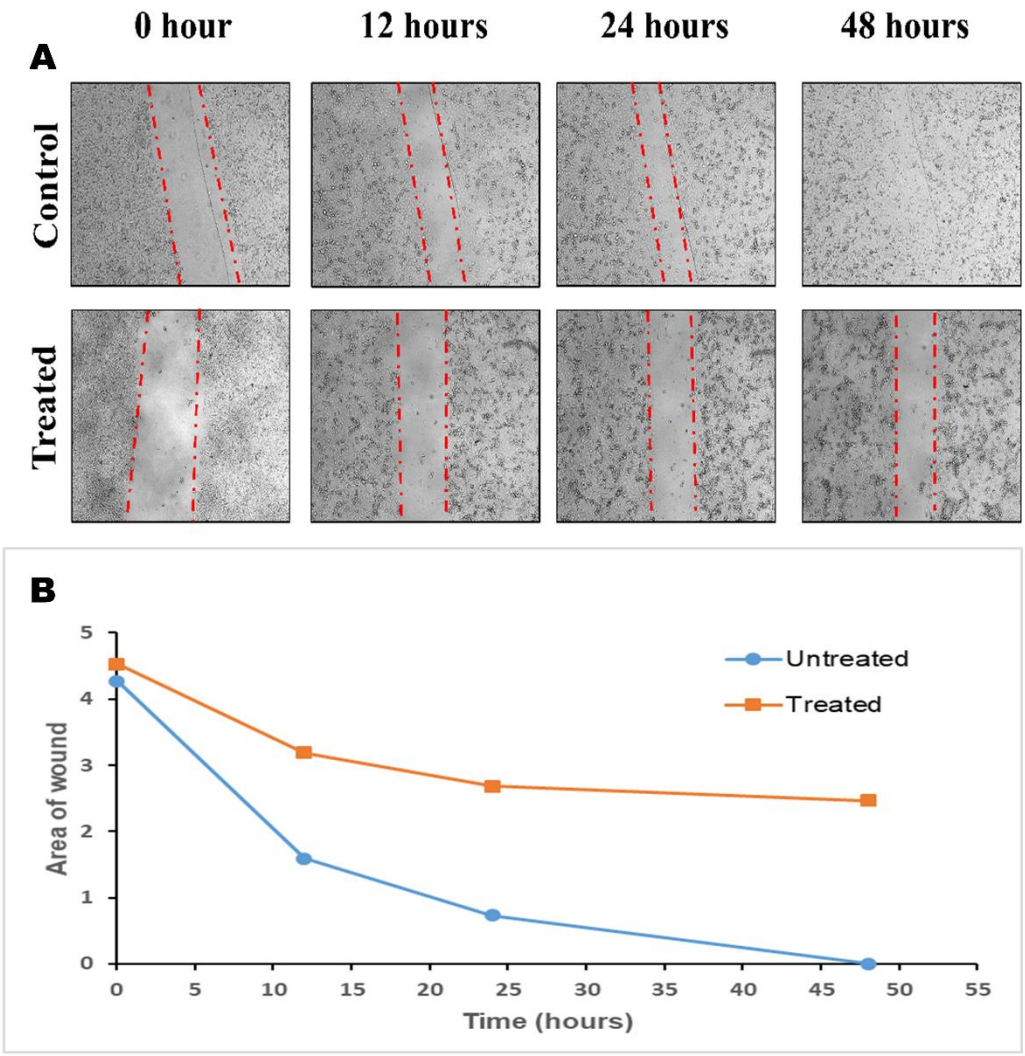

Figure 4.2.3. (A) Wound healing assay using IC_{50} of cytochalasin D (28.9 µg/mL); **(B)** Graph comparing wound area in treated and untreated MDA-MB-231 cells

4.2.4. Intra-cellular ROS detection

Reactive oxygen species (ROS) play a crucial role in various biological processes, including the induction of cytotoxicity in cancer cells (Eccleston, 2023). Elevated ROS levels can lead to oxidative stress, which damages cellular components such as proteins, lipids, and DNA, ultimately resulting in cell death (Padi et al., 2022). To investigate the impact of cytochalasin D on ROS levels, particularly hydrogen peroxide (H_2O_2), we conducted an assay using 2',7'-dichlorofluorescein diacetate (DCFDA), a fluorescent probe that detects ROS within cells. In our study, MDA-MB-231 cells were treated with

the half-maximal inhibitory concentration of cytochalasin D (28.9 µg/mL) for 4 hours. Following treatment, we observed a significant increase in DCF fluorescence intensity (**Fig. 4.2.4**). Specifically, there was a 4-fold increase in fluorescence intensity compared to the control cells. This substantial rise in ROS levels suggests that cytochalasin D induces oxidative stress in MDA-MB-231 cells. The increased ROS levels are likely contributing to the cytotoxic effects of cytochalasin D, as oxidative stress can trigger various cell death pathways, including apoptosis and necrosis. Furthermore, the elevated ROS may interfere with critical cellular signalling pathways, further inhibiting cell proliferation and promoting cell death.

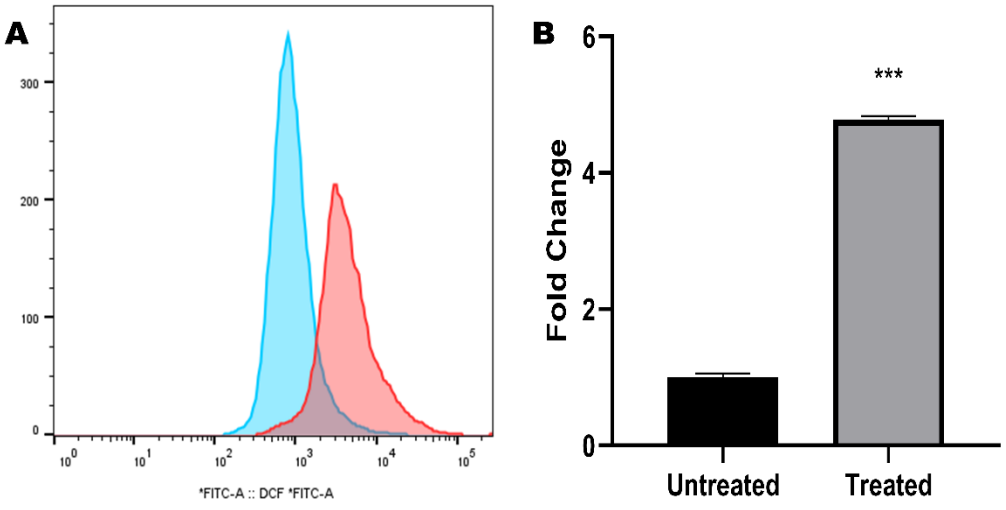

Figure 4.2.4. (A) ROS levels in MDA-MB-231 cells following cytochalasin D treatment; **(B)** Histogram showing 4-fold elevation in ROS levels in treated cells

4.2.5. Immunoblotting assay

Our *in-silico* analysis, which incorporated tools such as STRING, gene ontology, and molecular dynamics (MD) simulation, provides strong evidence that cytochalasin D could act as a potent inhibitor of mitogen-activated protein kinases (MAPKs). MAPKs, including ERK1/2, p38, and JNK, play crucial roles as effector proteins in the MAPK signalling cascade, influencing critical processes such as migration, invasion, and adhesion of aggressive cancer phenotypes like MDA-MB-231 (García-Hernández et

al., 2021). To investigate whether cytochalasin D treatment affects the expression levels of these key proteins, potentially disrupting the MAPK signalling pathway, we conducted western blot analysis using highly specific antibodies against ERK1/2, p38, and JNK. Our results showed a dose-dependent reduction in the levels of these proteins following 24 hours of cytochalasin D treatment, with the most significant decrease observed at a concentration of 30 µg/mL (**Fig. 4.2.5**). This substantial reduction in ERK1/2, p38, and JNK levels indicates a disruption of the MAPK signalling pathway, highlighting the impact of cytochalasin D on these critical signalling molecules. Additionally, we examined the effects of cytochalasin D on caspase 8, a key mediator of apoptosis. Our western blot analysis revealed a stark reduction in the expression levels of caspase 8 with increasing concentrations of cytochalasin D. This decrease in caspase 8 levels was consistent with the observed increase in the levels of cleaved caspase 8, the active form of the protein. The gradual increase in cleaved caspase 8 levels with higher concentrations of cytochalasin D directly confirms the activation of caspase 8, which is a hallmark of apoptosis induction. The results from our western blot analysis, combined with our in-silico findings, strongly suggest that cytochalasin D disrupts the MAPK signalling pathway by inhibiting key proteins such as ERK1/2, p38, and JNK. This disruption likely contributes to the observed cytotoxic effects in MDA-MB-231 cells. Furthermore, the activation of caspase 8 and the subsequent induction of apoptosis underscore the potential of cytochalasin D as a therapeutic agent in the treatment of triple-negative breast cancer. These findings pave the way for further exploration of cytochalasin D as a promising candidate in cancer therapy, particularly for targeting aggressive cancer phenotypes.

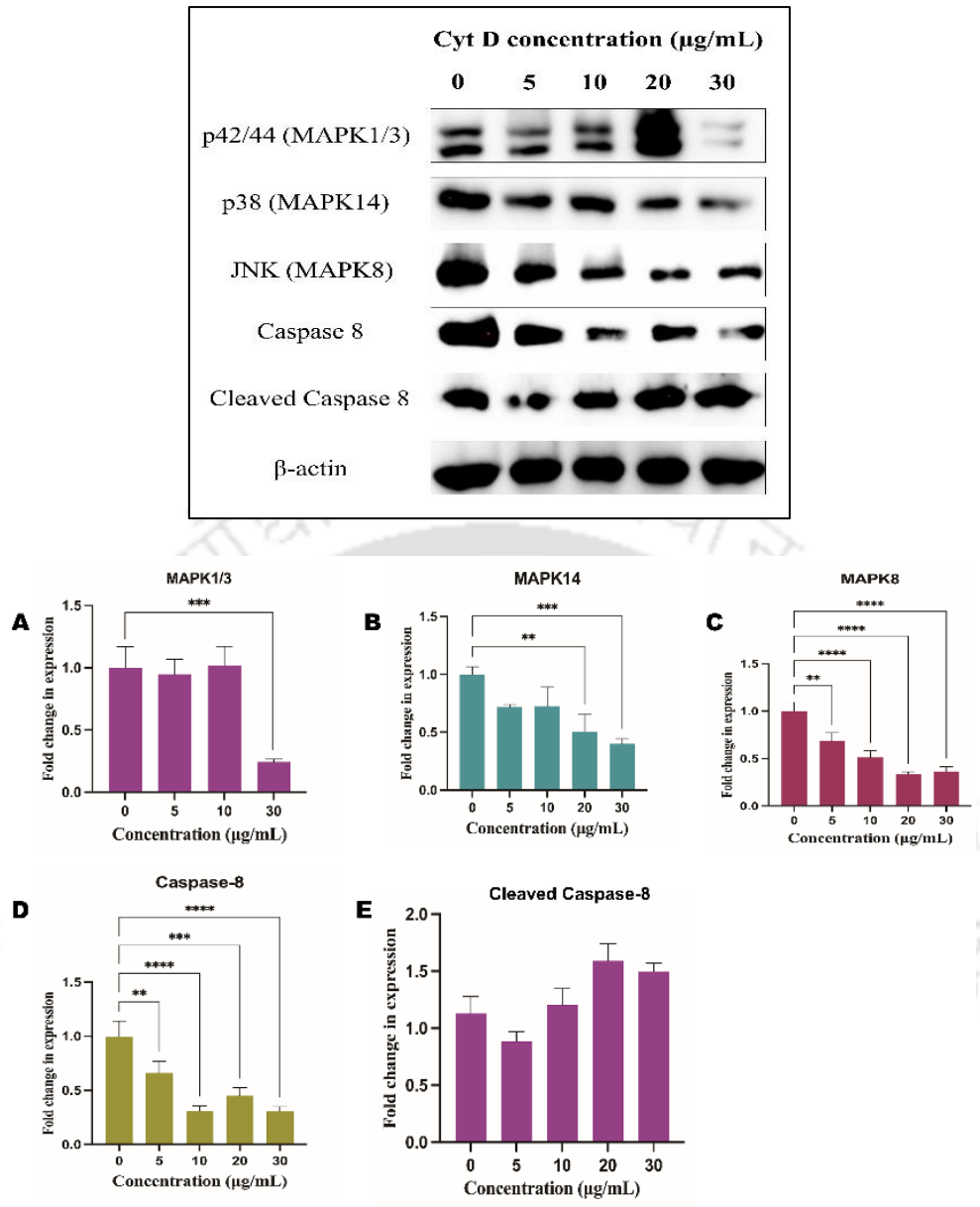

Figure 4.2.5. Expression levels of MAPK1, MAPK3, MAPK8, MAPK14 and Caspase 8 **(A)** MAPK1/3; **(B)** MAPK14; **(C)** MAPK8; **(D)** Caspase 8; **(E)** Cleaved caspase 8 in MDA-MB-231 cells treated with increasing levels of cytochalasin D (5,10,20, 30 µg/mL).

4.3. Discussion

The mitogen-activated protein kinase (MAPK) signalling pathway plays a pivotal role in regulating various biological processes essential for cellular function and survival, including cell proliferation, apoptosis, differentiation, migration, and invasion (Fang &

Richardson, 2005; Torres, 2003). This pathway is highly conserved across multicellular organisms and is crucial for the proper functioning of cells under normal physiological conditions. However, aberrant activation of the MAPK pathway is frequently observed in several types of human cancers, such as breast, colon, kidney, and lung carcinomas, where it significantly contributes to tumour progression and metastasis (Burotto et al., 2014). Specifically, the MAPK pathway is involved in the activation of proteolytic enzymes that degrade the basement membrane, a key step in promoting cancer cell migration and invasion. It also initiates the expression of various pro-survival genes that support the continuous growth and survival of cancer cells, making it a critical target for cancer therapy.

Cytochalasin D, a bioactive compound derived from fungi, has been studied for its potential anti-cancer properties, particularly against triple-negative breast cancer (TNBC), a highly aggressive subtype of breast cancer that lacks targeted therapies. In this study, the anti-cancer effects of cytochalasin D on the TNBC cell line MDA-MB-231 were systematically evaluated using multiple experimental approaches. The MTT cell viability assay, a standard method for assessing cell proliferation and viability, revealed that cytochalasin D has a potent cytotoxic effect on MDA-MB-231 cells, with an IC_{50} value of 28.9 µg/mL. This indicates that cytochalasin D is effective at inhibiting the growth of TNBC cells at relatively low concentrations. Further analysis using cell cycle assays demonstrated that cytochalasin D induces an arrest in the S phase of the cell cycle. This arrest leads to the formation of large, multi-nucleated cells, a phenotype that suggests significant disruption in cell division. Such cells are particularly vulnerable to nucleic acid-directed agents, making cytochalasin D a promising candidate for combination therapies aimed at exploiting these vulnerabilities. The wound healing assay, which measures the migratory capacity of cells, showed that

cytochalasin D significantly inhibits the migration of MDA-MB-231 cells. After 48 hours of treatment, only 54% of the wound area was covered in cytochalasin D-treated samples, compared to complete wound closure in untreated cells. This substantial reduction in cell migration underscores the potent anti-migratory effects of cytochalasin D, which could be particularly beneficial in preventing cancer metastasis. Additionally, the treated MDA-MB-231 cells exhibited a four-fold increase in reactive oxygen species (ROS) levels, suggesting that cytochalasin D induces apoptosis through oxidative stress. Elevated ROS levels can lead to cellular damage and trigger apoptotic pathways, further contributing to the anti-cancer effects of cytochalasin D.

Molecular dynamics (MD) simulations provided insights into the interactions between cytochalasin D and its molecular targets within the MAPK signalling pathway. These computational studies were complemented by western blotting analysis, which revealed a dose-dependent decrease in the expression levels of key MAPK proteins, including MAPK1, MAPK3, MAPK8, and MAPK14, upon treatment with cytochalasin D. This reduction in protein levels indicates that cytochalasin D effectively inhibits the MAPK pathway, thereby disrupting the signalling processes that promote cancer cell survival and proliferation. Furthermore, the role of cytochalasin D in inducing apoptosis was corroborated by analysing the activation of caspase 8, a critical mediator of the extrinsic apoptosis pathway. Western blot analysis showed a notable decrease in the expression of caspase 8, along with an increase in cleaved caspase 8, the active form of the enzyme. This suggests that cytochalasin D triggers apoptosis through the activation of the extrinsic pathway, leading to cancer cell death.

In summary, the study provides robust evidence that cytochalasin D disrupts the MAPK signalling pathway and induces apoptosis in MDA-MB-231 cells. These findings, supported by both in-silico and experimental data, underscore the potential of

cytochalasin D as a therapeutic agent in the treatment of aggressive breast cancer phenotypes. The integration of network pharmacology and molecular dynamic simulations was pivotal in uncovering the multi-target mechanisms of this novel anticancer compound.

4.4. Conclusion

In conclusion, this study provides comprehensive evidence that cytochalasin D is a potent anticancer agent with multi-target effects on the MAPK signalling pathway, cell migration, and apoptosis in MDA-MB-231 cells. The integration of network pharmacology and molecular dynamics simulations with experimental validation has unveiled the intricate mechanisms through which cytochalasin D exerts its effects. These findings not only underscore the therapeutic potential of cytochalasin D for TNBC but also open new avenues for its application in broader cancer treatment strategies. Given the aggressive nature and limited treatment options for TNBC, cytochalasin D's ability to inhibit cell migration, induce apoptosis, and disrupt key signalling pathways positions it as a promising candidate for further preclinical and clinical development. Future research could explore the potential of cytochalasin D in combination with other anticancer agents.

Although cytochalasin D has shown significant anticancer potential against TNBC cells, its clinical application faces challenges due to poor oral bioavailability and non-specific toxicity. Developing a suitable nanoparticle-based delivery system for cytochalasin D is a promising strategy to overcome these limitations. The following chapter will detail the preparation and characterization of cytochalasin D-loaded nanoparticles, as well as the evaluation of their safety and efficacy *in vitro*. This approach aims to enhance the therapeutic index of cytochalasin D, making it a viable

candidate for targeted cancer therapy and opening new avenues for the treatment of aggressive breast cancer phenotypes.

Chapter 5

Delivering Cytochalasin D using a suitable nano-carrier for hydrophobic drugs

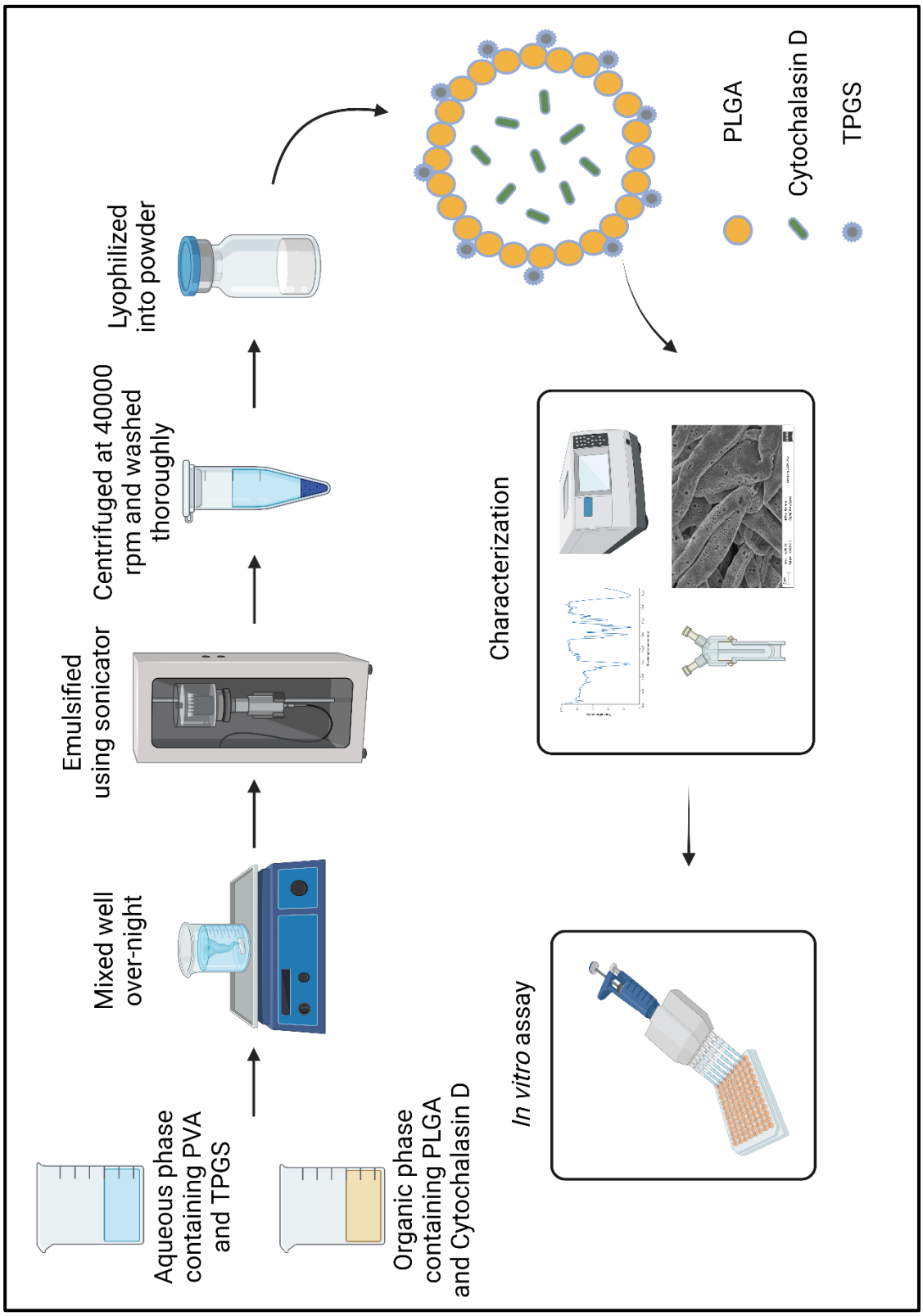

Scheme 5.1. Schematic representation of synthesis and characterization of void and cytochalasin D-loaded PLGA NPs along with *in vitro* assay against MDA-MB-231 cells

Abstract

The delivery of chemotherapeutic drugs is challenging due to their non-specific nature, leading to off-target effects and toxicity. Nanoparticle-mediated drug delivery has emerged as a solution, improving precision by targeting tumor sites. Nanocarriers protect drugs from degradation and increase the bioavailability. They enable both passive and active targeting, enhancing delivery to cancerous tissues. Polymeric nanoparticles, favored for their biocompatibility, are widely used and can be engineered for sustained drug release. These nanoparticles can also be functionalized with ligands to improve targeting. In this study, cytochalasin D-loaded PLGA NPs were employed to overcome the challenges faced by conventional use of cytochalasin D. Cytochalasin D-loaded PLGA NPs ranging from size 0-100nm were successfully synthesized and characterized using FESEM, FETEM and zeta potential. The entrapment efficiency of the synthesized NPs was found to be 60% and a burst release was observed in acidic buffer. The void PLGA NPs did not exhibit cytotoxicity in MTT assay against MDA-MB-231 cells, highlighting the biocompatible nature of the polymer. However, the drug loaded NPs exhibited an IC_{50} of 1.056 mg/mL. In summary, polymeric NPs offer significant improvements in targeted drug delivery, protection, and bioavailability, paving the way for more effective and safer cancer therapies.

5.1. Introduction

Nanoparticle (NP) drug delivery systems have revolutionized the field of medicine, particularly in the delivery of chemotherapeutic agents (Patra et al., 2018). These systems offer numerous advantages, including enhanced solubility and stability of drugs, controlled release profiles, improved bioavailability, and targeted delivery to specific tissues or cells (S. Singh, 2011; Yao et al., 2020). Such advantages are pivotal in addressing the challenges associated with conventional chemotherapy, such as systemic toxicity and non-specific distribution of drugs, which often lead to severe side effects and reduced therapeutic efficacy.

Among the various types of NPs, PLGA (poly(lactic-co-glycolic acid)) NPs have emerged as one of the most widely studied and utilized platforms for drug delivery (Zeb et al., 2022). PLGA is a biodegradable and biocompatible copolymer composed of lactic acid and glycolic acid monomers. These monomers are naturally metabolized in the body, ensuring the polymer's minimal toxicity and negligible long-term side effects. The degradation of PLGA occurs via hydrolysis, producing lactic acid and glycolic acid, which are subsequently eliminated as carbon dioxide and water. These unique properties of PLGA have led to its widespread approval by major regulatory agencies such as the Food and Drug Administration (FDA) and the European Medicines Agency (EMA) for various medical applications, including drug delivery, tissue engineering, etc. (Y. Wang et al., 2021). The biocompatibility and biodegradability of PLGA ensure that it is safe for use in the human body, making it an ideal material for developing NP drug delivery systems.

PLGA NPs offer several distinct advantages in drug delivery. Firstly, they provide controlled and sustained release of encapsulated drugs, which helps maintain therapeutic drug levels over extended periods and reduces the frequency of drug

administration. This controlled release is achieved by manipulating the ratio of lactic acid to glycolic acid in the copolymer and by altering the molecular weight of PLGA. Secondly, PLGA NPs protect encapsulated drugs from degradation and premature release, thereby enhancing their stability and bioavailability. This is particularly important for chemotherapeutic agents, which are often unstable and rapidly metabolized in the body. Additionally, PLGA NPs can be engineered to target specific tissues or cells by modifying their surface with ligands, antibodies, or other targeting moieties. This targeted delivery minimizes the exposure of healthy tissues to toxic drugs and enhances the accumulation of drugs in tumor tissues, thereby improving therapeutic outcomes and reducing side effects. The versatility of PLGA NPs allows for the encapsulation of a wide range of drugs, including hydrophobic and hydrophilic molecules, peptides, and proteins. These features, combined with the biocompatibility of PLGA polymer, makes these NPs ideal candidates for developing advanced drug delivery systems (Alvi et al., 2022).

In the following sections, we have prepared cytochalasin D loaded PLGA NPs alongside void PLGA NPs and checked for various physico-chemical properties of the NPs. We also checked the cytotoxicity of both the systems against MDA-MB-231 cell line. The details of the methodology followed have been covered in the second chapter.

5.2. Results

5.2.1. Physico-chemical properties of void and cytochalasin D loaded PLGA NPs

Zeta potential is a fundamental parameter in the characterization of NPs and colloidal systems. It provides insight into the surface charge and stability of NPs in a solution. NPs with high zeta potential (either positive or negative) tend to repel each other, leading to better colloidal stability and preventing aggregation. This stability is essential for maintaining the uniform distribution of NPs in a solution, which is particularly

important in drug delivery systems to ensure consistent dosing and efficacy. Our synthesized NPs exhibited higher negative zeta potential values. For the void PLGA nanoparticles (NPs), a zeta potential value of -16.8 mV was observed, while for the cytochalasin D loaded PLGA NPs, the value was -12.7 mV **(Fig. 5.2.1)**. The higher negative zeta potential of the synthesized nanoparticles is crucial as it ensures stable dispersion of the NPs in colloidal suspension. The stable and well-dispersed nanoparticles can efficiently circulate in the bloodstream, accumulate at the tumor site, and deliver the therapeutic payload, thereby enhancing the overall efficacy of the treatment.

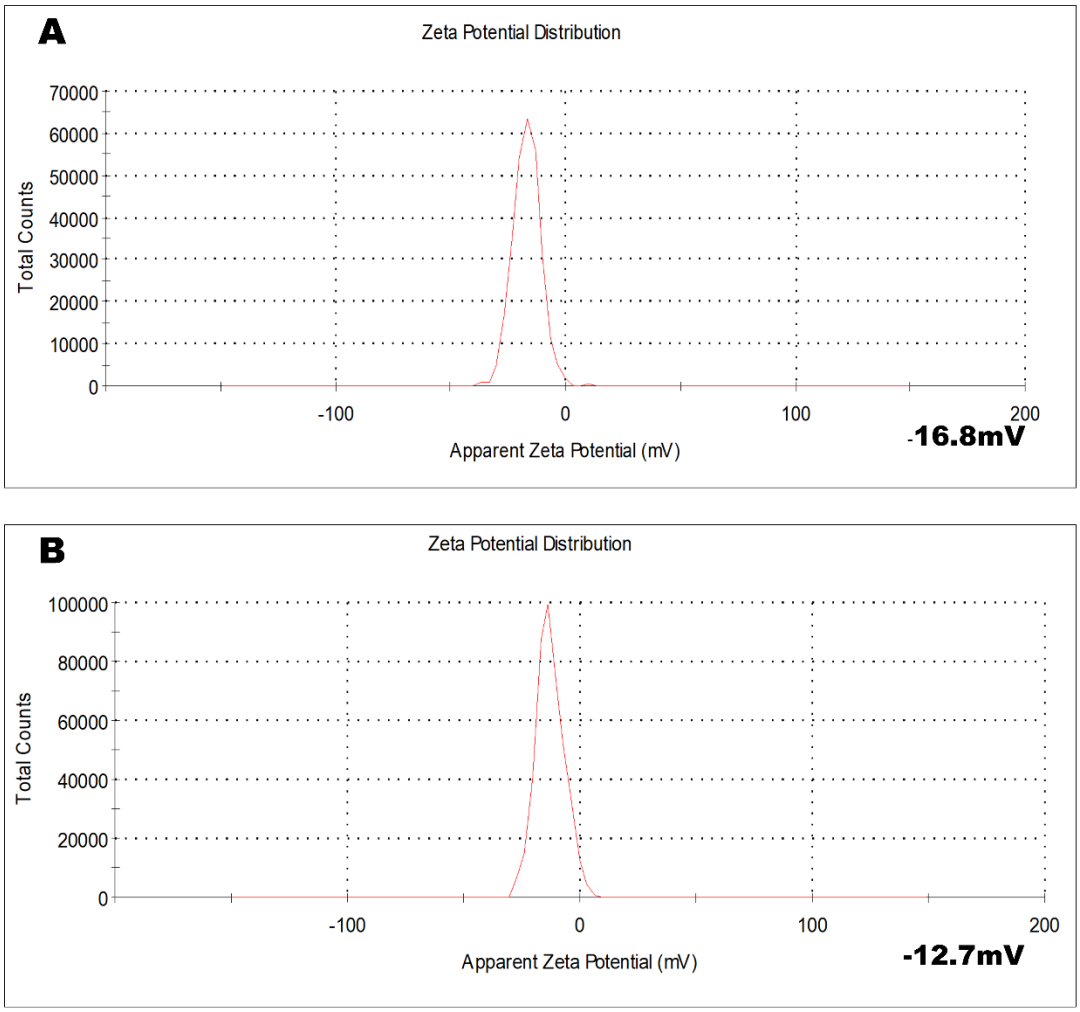

Figure 5.2.1. Zeta potential distribution of **(A)** void PLGA NPs (-16.8mV) and **(B)** cytochalasin D-loaded PLGA NPs (-12.7mV)

Further characterization of the nanoparticles was done using Field Emission Scanning Electron Microscopy (FESEM) and Field Emission Transmission Electron Microscopy (FETEM). These techniques provide detailed information about the morphology, size, structure, and surface properties of nanoparticles, which are crucial for understanding their behavior and performance in various applications, including drug delivery. This dual approach ensures a thorough understanding of the physical and chemical properties of nanoparticles. When visualized under FESEM, the NPs exhibited thread-like appendages, indicative of nanoparticle aggregates. These aggregates appeared as elongated structures, suggesting a certain degree of interaction and clustering among the nanoparticles. Upon further magnification, these thread-like appendages were found to consist of numerous spherical nanoparticles that were closely packed together **(Fig. 5.2.2)**. Detailed examination revealed that the majority of these spherical nanoparticles were within the size range of 100-200 nm.

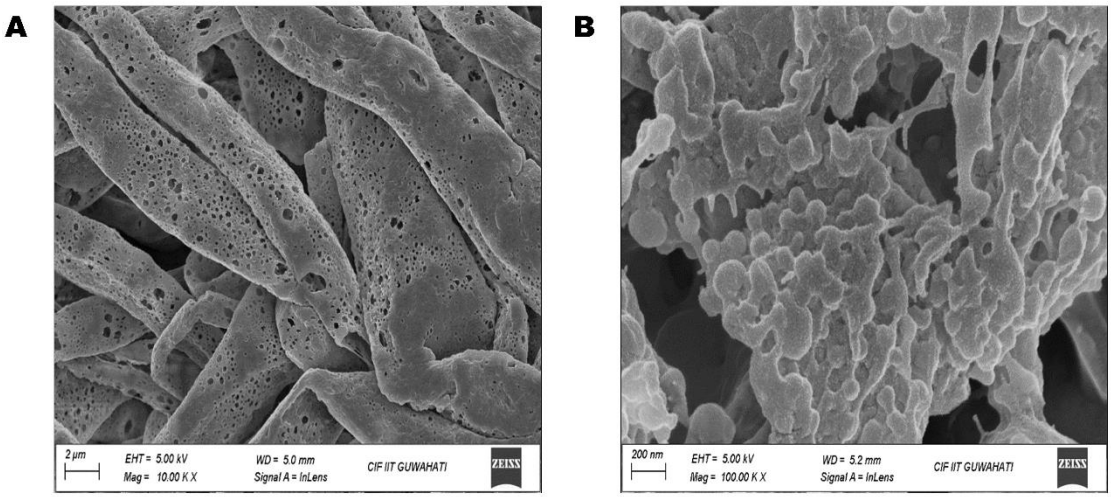

Figure 5.2.2. FESEM images of cytochalasin D-loaded PLGA NPs at different magnifications. **(A)** At 10,000X (thread-like appendages of aggregated NPs), **(B)** At 1,00,000X (spherical NPs in cluster)

However, when observed under FETEM, the NPs displayed a markedly different dispersion pattern. Unlike the aggregates seen in FESEM, the NPs appeared to be evenly dispersed, providing a more accurate representation of their individual sizes and shapes. This uniform dispersion is crucial for understanding the true size distribution and ensuring the consistency of the nanoparticle formulation. The mean average size diameter of the nanoparticles was found to be 54±21 nm **(Fig. 5.2.3)**. This size range is particularly advantageous for drug delivery, as particles smaller than 100 nm are known to have enhanced cellular uptake and improved penetration through biological barriers, such as the blood-brain barrier or tumor vasculature.

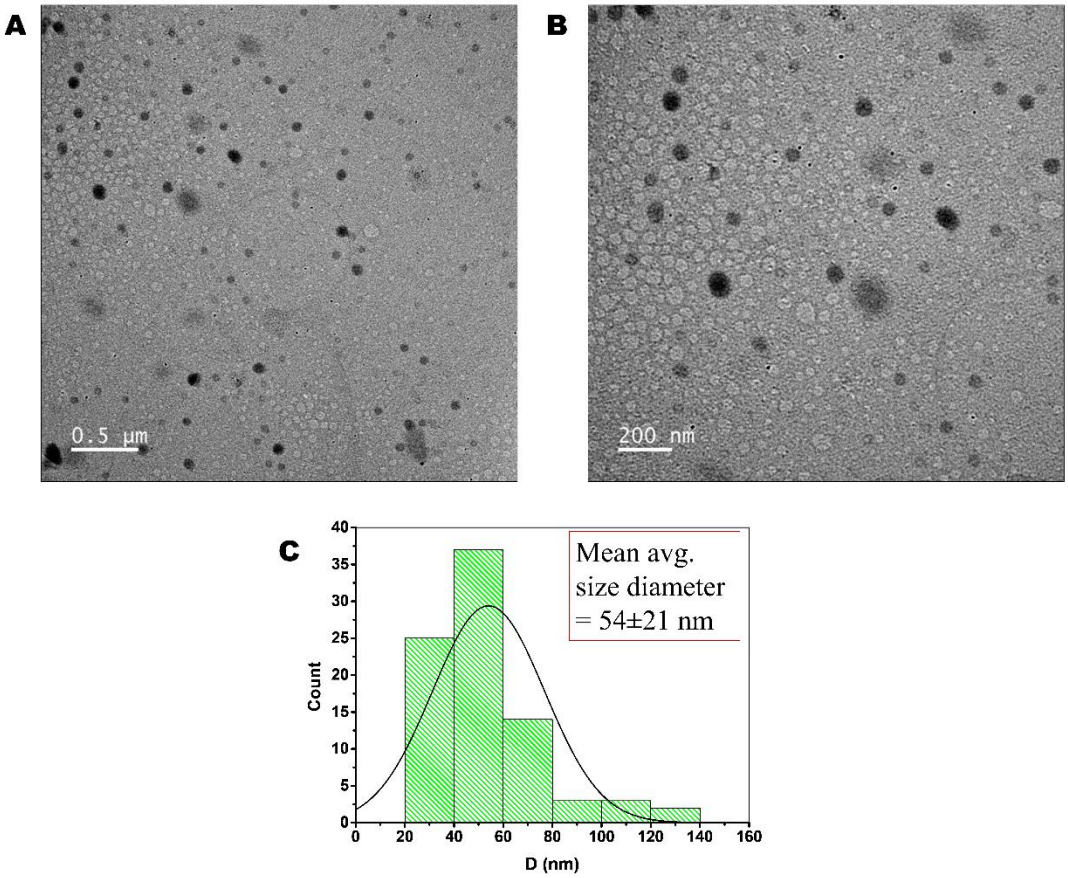

Figure 5.2.3. (A, B) FETEM images of cytochalasin D-loaded PLGA NPs; **(C)** size distribution curve of cytochalasin D-loaded PLGA NPs showing the mean average size diameter

5.2.2. Encapsulation efficiency and *in-vitro* drug release study

The encapsulation efficiency of NPs is a crucial parameter in evaluating the effectiveness of drug delivery systems. Upon checking the absorbance values of the supernatant obtained after synthesizing cytochalasin D-loaded NPs, the values corresponded to 40 µg/mL concentration indicating that 400 µg of the drug was present in 10 mL of the supernatant. So, nearly 60% of the drug got encapsulated **(Fig. 5.2.4)** indicating that a substantial portion of the drug has been successfully encapsulated within the PLGA NPs. This is important for ensuring that a sufficient amount of the therapeutic agent is delivered to the target site.

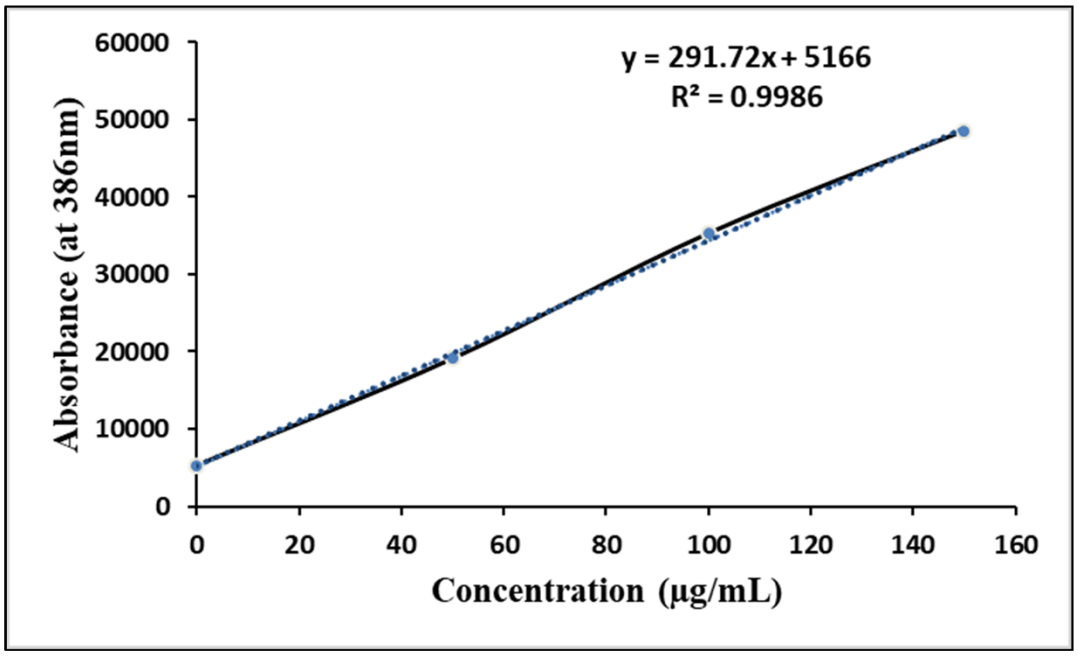

Figure 5.2.4. Standard curve of cytochalasin D to check the encapsulation efficiency of the synthesized PLGA NPs.

The release profile of entrapped cytochalasin D from the loaded PLGA nanoparticles was investigated in two different buffer solutions: phosphate-buffered saline (PBS) at pH 7.4, which simulates physiological conditions, and acetate buffer at pH 4, which mimics the acidic environment typically found in tumor tissues. The study was conducted over a period of 3 hours (180 minutes) to observe the release kinetics of the

drug under these varying conditions. At the 15-minute mark, a significant burst release of cytochalasin D was observed in the acetate buffer (pH 4). This rapid release can be attributed to the acidic environment, which likely causes the PLGA polymer to swell and degrade more quickly, thereby facilitating the faster release of the encapsulated drug. The lower pH accelerates the hydrolysis of the ester bonds in PLGA, leading to a quicker breakdown of the polymer matrix. Following the initial burst release in the acetate buffer, a steady and sustained release of cytochalasin D was observed over the remaining time period. This suggests that after the initial rapid release of surface-bound drug molecules, the remaining drug is released more gradually as the polymer matrix continues to degrade. In PBS buffer (pH 7.4), the release of cytochalasin D was more controlled from the beginning, without a significant burst. The near-neutral pH condition of PBS leads to a slower degradation rate of the PLGA matrix, resulting in a more gradual and sustained release of the drug **(Fig. 5.2.5)**.

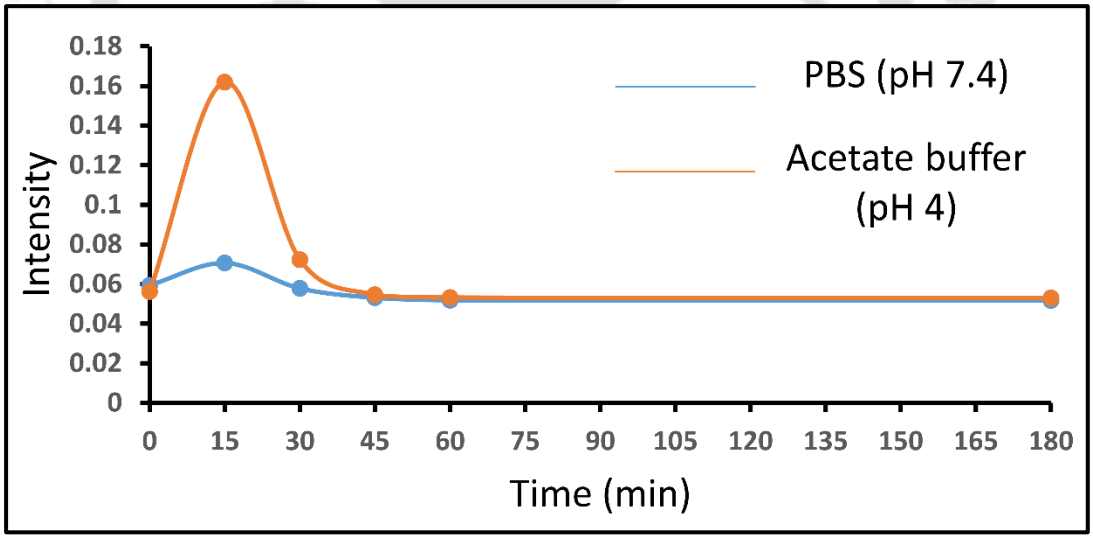

Figure 5.2.5. *In vitro* drug release profile under different pH conditions [PBS (pH 7.4) and Acetate buffer (pH 4)] showing burst release of cytochalasin D in acidic buffer

5.2.3. *In vitro* assessment of therapeutic activity of cytochalasin D loaded PLGA NPs

The cytotoxicity of both the void and cytochalasin D loaded PLGA NPs were checked against MDA-MB-231 cells. The void NPs didn't exhibit any cell mortality even at

higher concentrations of 3 mg/mL. The absence of cell mortality indicates that the PLGA carrier is biocompatible and does not induce adverse effects on the cancer cells, making it a safe vehicle for drug delivery. This biocompatibility is crucial as it ensures that any observed cytotoxic effects can be attributed to the encapsulated drug, rather than the nanoparticle carrier itself. However, the drug loaded NPs showed an IC_{50} concentration of 1.056 mg/mL **(Fig. 5.2.6)**. The enhanced cytotoxicity of the drug-loaded NPs, coupled with the biocompatibility of the PLGA carrier, highlights the promise of this approach in improving the therapeutic outcomes for cancer patients.

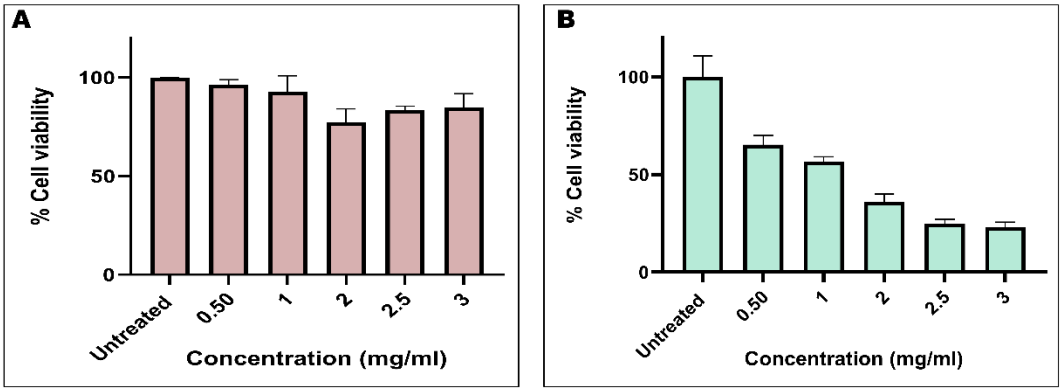

Figure 5.2.6. MTT assay with **(A)** void PLGA NPs and **(B)** cytochalasin D-loaded PLGA NPs against MDA-MB-231 cells

5.2.4. Generation of ROS following treatment with cytochalasin D loaded PLGA NPs

Following MTT assay, the treated MDA-MB-231 cells were checked for the presence of reactive oxygen species (ROS) upon treatment with the loaded NPs. An increase in the ROS population (nearly 2-fold) was observed in the treated cells compared to the untreated cells **(Fig. 5.2.7)**. ROS are highly reactive molecules that can damage various cellular components, including proteins, lipids, and DNA. The elevated ROS levels observed in the treated MDA-MB-231 cells suggest that cytochalasin D-loaded PLGA NPs induce oxidative stress, which can overwhelm the cell's antioxidant defenses and lead to apoptotic cell death.

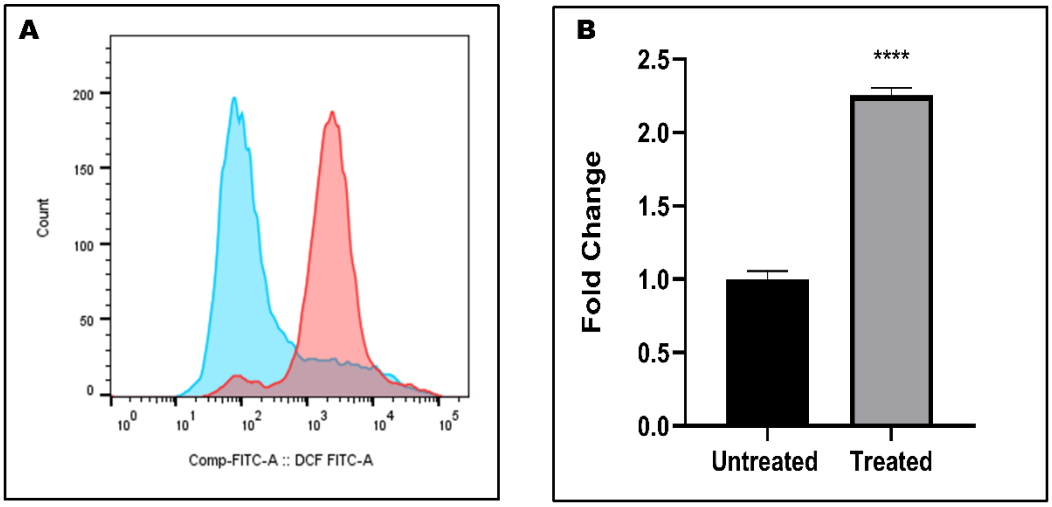

Figure 5.2.7. (A) Levels of ROS in MDA-MB-231 cells treated with cytochalasin D-loaded PLGA NPs; **(B)** Histogram showing 2.25-fold change in ROS in treated cells compared to untreated cells

5.3. Discussion

Among the various types of breast cancer, triple-negative breast cancer (TNBC) is the most aggressive form, characterized by the absence of HER2, progesterone, and estrogen receptors (Newton et al., 2022). This aggressiveness, combined with the lack of targeted therapies, makes TNBC a leading cause of death among women. TNBC accounts for 15-20% of all breast cancer cases (Li et al., 2022), and more than 50% of patients experience a relapse within 3 to 5 years of diagnosis. Chemotherapy is still the go-to treatment for triple-negative breast cancer (TNBC), however a number of problems can make it less effective, such as immune system suppression, toxicity to healthy cells, and the emergence of multi-drug resistance (MDR) (Dinakar et al., 2023). The field of cancer nanotherapeutics is developing at a very quick speed and has intriguing answers to many of the problems with traditional medication delivery methods. Conventional approaches frequently have drawbacks that can lower treatment efficacy and increase adverse effects, such as nonspecific biodistribution, insufficient targeting, poor water solubility, restricted oral bioavailability, and low therapeutic

indices (Cho et al., 2008). Nanoparticles, as a key component of cancer nanotherapeutics, have been extensively engineered to overcome these hurdles. They have the potential to enhance the therapeutic efficacy of drugs by efficiently traversing biological barriers while minimizing toxic effects on healthy cells (Dinakar et al., 2023; Jain et al., 2020; Parvez et al., 2022).

Over the years, researchers have explored a wide range of natural and synthetic polymers for the development of NPs. Among these, Poly(lactic acid) (PLA), Poly(glycolic acid) (PGA), and their copolymer Poly(lactic-co-glycolic acid) (PLGA) have garnered significant attention due to their exceptional biocompatibility and biodegradability (Misra et al., 2020; Moritz & Geszke-Moritz, 2015; Sur et al., 2019). These polymeric NPs also show versatility in delivering a wide range of chemotherapeutic agents such as secondary metabolites, immunomodulators, hormones and macromolecules (proteins, nucleic acids, peptides and antibodies) (Bala et al., 2004). In a nutshell, polymeric NPs, in comparison to lipid and inorganic NPs, offer a larger surface area, extended clearance time, lower toxicity, and improved control over particle size. These properties make them highly suitable for medical applications, particularly in drug delivery systems.

In this study, we successfully synthesized cytochalasin D-loaded PLGA NPs using the single emulsion solvent evaporation method, a well-established technique for creating polymer-based drug delivery systems. The resulting NPs exhibited an overall negative surface charge, which is a crucial factor in their stability and behavior in biological systems. The void (drug-free) NPs displayed a zeta potential of -16.8 mV, while the cytochalasin D-loaded NPs exhibited a slightly lower negative zeta potential of -12.7 mV. The higher absolute values of zeta potential, whether positive or negative, are indicative of strong electrostatic repulsion between particles (Williams, 2016). This

repulsion helps to prevent aggregation, ensuring that the nanoparticles remain well-dispersed within the desired system. A stable colloidal suspension is essential for effective drug delivery, as it ensures uniform distribution of the nanoparticles, reduces the risk of premature drug release, and facilitates better interaction with target cells or tissues (Bhattacharjee, 2016). The slight reduction in zeta potential upon drug loading could be attributed to the interaction of cytochalasin D with the PLGA matrix, which may influence the surface charge distribution. However, the negative surface charge remains sufficient to maintain nanoparticle stability and prevent aggregation, making these cytochalasin D-loaded PLGA nanoparticles a promising candidate for targeted drug delivery applications in cancer therapy.

Imaging of the synthesized NPs was carried out using Field Emission Scanning Electron Microscopy (FESEM) and Field Emission Transmission Electron Microscopy (FETEM), two powerful techniques that provide detailed insights into the morphology, size, and distribution of the NPs. When the cytochalasin D-loaded PLGA NPs were visualized under FESEM, the initial images revealed the presence of thread-like appendages. These appendages, upon closer examination and higher magnification, were identified as aggregates of spherical NPs. The observed aggregation could be due to the drying process during sample preparation for FESEM, where solvent evaporation can lead to the clustering of NPs. Despite this aggregation, the individual spherical NPs were predominantly within the size range of 100-200 nm. This size range is typical for PLGA-based NPs and is considered suitable for drug delivery purposes, as NPs within this range can efficiently penetrate biological barriers and are less likely to be cleared rapidly from the body. In contrast, the imaging of the same NPs using FETEM provided a more detailed and refined visualization. FETEM is known for its higher resolution and ability to provide more accurate size measurements. Under FETEM, the NPs were

observed to be thoroughly dispersed across the carbon mesh of the TEM grid, with no significant signs of aggregation. This thorough dispersion is critical as it indicates that in solution, the nanoparticles are less likely to form aggregates, ensuring better distribution and interaction with target cells or tissues in biological systems. Furthermore, the size distribution of the NPs was analyzed using the images obtained from FETEM. The size distribution curve generated from these images revealed that the average mean size diameter of the nanoparticles was 54±21 nm. This smaller average size, as compared to the range observed in FESEM, could be attributed to the different sample preparation techniques and the higher resolution of FETEM. The narrow size distribution and smaller average diameter are advantageous for drug delivery, as smaller NPs are generally more efficient in permeating through cellular membranes, ensuring better drug delivery to target sites. Additionally, the size uniformity is critical for consistent drug release profiles and predictable pharmacokinetics (Begines et al., 2020).

Entrapment efficiency is a critical parameter in drug delivery systems as it directly impacts the therapeutic efficacy of the nanoparticles. Higher entrapment efficiency means that more of the active drug is delivered to the target site, potentially enhancing the therapeutic outcome (Judefeind & de Villiers, 2009). The synthesized cytochalasin D-loaded PLGA NPs demonstrated an entrapment efficiency of 60%, indicating that a significant proportion of the drug was successfully encapsulated within the NPs during the formulation process.

The release profile of the encapsulated cytochalasin D from the PLGA NPs *in vitro*, was achieved using two different buffer solutions i.e. acetate buffer (pH 4) and phosphate-buffered saline (PBS, pH 7.4). These buffers were chosen to mimic the different pH environments that the nanoparticles might encounter within the body, such

as the acidic conditions in the tumor microenvironment and the near-neutral pH of the bloodstream. In the acetate buffer, the release profile exhibited a characteristic initial burst release around the 15-minute mark. This burst release is a common phenomenon observed in nanoparticle-based drug delivery systems and is often attributed to the rapid release of drug molecules that are either adsorbed on the surface of the nanoparticles or loosely bound within the outer layers of the polymer matrix (Son et al., 2017). The burst release can be beneficial in certain therapeutic contexts, such as achieving an immediate therapeutic effect by rapidly delivering a high concentration of the drug to the target site. Following the initial burst, the release profile in the acetate buffer transitioned into a sustained release phase, extending up to the 180-minute mark. During this phase, the drug molecules encapsulated deeper within the nanoparticle matrix were gradually released as the PLGA polymer underwent hydrolytic degradation. This sustained release is advantageous for maintaining therapeutic drug levels over an extended period, reducing the frequency of drug administration and minimizing potential side effects. In contrast, the release profile in the PBS buffer was more stable throughout the duration of the experiment. The absence of a significant burst release in PBS suggests that the nanoparticles maintained their integrity better in the neutral pH environment, with a more controlled and steady release of the encapsulated cytochalasin D. This controlled release in PBS is indicative of the robust encapsulation of the drug within the PLGA matrix, providing a consistent and prolonged drug release, which is essential for maintaining therapeutic efficacy over time.

The *in vitro* cytotoxicity of cytochalasin D-loaded PLGA NPs was thoroughly evaluated against the TNBC cell line MDA-MB-231 to assess the therapeutic potential of the formulated drug delivery system. The study aimed to determine the effectiveness of the drug-loaded NPs in inhibiting cancer cell viability, as well as to compare the

cytotoxic effects of the loaded NPs with that of the void NPs. The cytochalasin D-loaded PLGA NPs demonstrated significant cytotoxicity against the MDA-MB-231 cells, with an IC_{50} value of 1.056 mg/mL. The IC_{50} value, or the half-maximal inhibitory concentration, is a critical parameter that indicates the concentration of a substance required to inhibit 50% of the cell population under investigation. An IC_{50} of 1.056 mg/mL suggests that the loaded NPs were quite effective in exerting their anticancer effects at relatively low concentrations, which highlights the potential of cytochalasin D as a potent therapeutic agent when delivered via PLGA nanoparticles. However, the void PLGA NPs, which served as a control, exhibited no significant cytotoxic effects on the MDA-MB-231 cells, even at concentrations as high as 3 mg/mL. This observation is crucial because it underscores the biocompatibility and inert nature of the PLGA polymer itself. The lack of cytotoxicity from the void NPs confirms that the polymer matrix used for nanoparticle synthesis does not interfere with the viability of healthy cells or contribute to any adverse effects, which is essential for any drug delivery system intended for clinical use.

When the treated MDA-MB-231 cells were analyzed, a substantial increase in ROS generation was observed, with nearly a two-fold elevation in ROS levels compared to the untreated cells. This significant rise in ROS production upon treatment with cytochalasin D-loaded NPs suggests that the nanoparticles effectively induced oxidative stress within the cancer cells. Such an increase in ROS is often associated with mitochondrial dysfunction, DNA damage, and the activation of apoptotic pathways, ultimately leading to cell death. The untreated cells, however, maintained relatively low levels of ROS, consistent with the normal physiological state where ROS are tightly regulated to prevent cellular damage. The difference in ROS levels between treated and untreated cells underscores the specific cytotoxic action of the cytochalasin

D-loaded NPs. The nanoparticles likely enhance the intracellular accumulation of cytochalasin D, leading to the disruption of the cellular redox balance and a marked increase in oxidative stress. Elevated ROS levels in cancer cells can trigger various signaling pathways that culminate in apoptosis (Navaneetha Krishnan et al., 2021; Zaidieh et al., 2019), making ROS generation a critical mechanism by which cytochalasin D-loaded NPs exert their anticancer effects. The oxidative stress-induced by these NPs can overwhelm the cellular antioxidant defenses, leading to irreversible damage to vital cellular components, ultimately resulting in cell death.

5.4. Conclusion

Cytochalasin D-loaded PLGA NPs exhibit promising characteristics for targeted cancer therapy, including stability, effective drug encapsulation, controlled release, and significant cytotoxicity against TNBC cells, making them a potential candidate for further development in cancer treatment. Their ability to target TNBC cells specifically and effectively suggests that they could be developed into a powerful treatment option for this challenging form of breast cancer.

Chapter 6

Conclusion and future prospects

6.1. Conclusion

The thesis is primarily focused on establishing the role of cytochalasin D as a MAPK pathway inhibitor. Involvement of MAPK pathway in breast cancer tumor development, progression and subsequent resistance to therapies has been well established. Although cytochalasin D has been majorly studied as an inhibitor of actin microfilament, this thesis sheds light on its other therapeutic aspects that can facilitate the current chemotherapy scenario for breast cancer. By employing network pharmacology along with immunoblotting experiments, a rather novel aspect of cytochalasin D has been explored.

The research findings of the thesis have been summarised below-

***In silico* identification of molecular targets of cytochalasin D in breast cancer cells**

- By applying the principles of network pharmacology to investigate cytochalasin D, a potent bioactive compound derived from the entomopathogenic fungus *Metarhizium anisopliae*, a list of potential molecular targets that are critically involved in cancer progression have been refined. 278 potential protein targets of cytochalasin D in TNBC MDA-MB-231 cells were mapped using Cytoscape software
- KEGG pathway enrichment analysis showed that these targets are involved in critical pathways such as cancer, neurodegeneration, the PI3K-Akt signalling pathway, and the MAPK signalling pathway. PPI analysis highlighted key differentially expressed genes, including SRC, FYN, MAPK1, LCK, MAPK3, LYN, JAK1, JAK2, PTK2, MAPK14, and MAPK8, with MAPK1, MAPK3, MAPK8, and MAPK14 emerging as crucial targets.
- Cytochalasin D was suggested to act as a potent inhibitor of the MAPK pathways, based on stable protein-ligand complexes observed in MD simulations. Binding

energies calculated via MM-PBSA confirmed the stability of cytochalasin D complexes with its target proteins.

- MD simulations provided detailed insights into the structural stability, flexibility, and binding interactions of cytochalasin D with its targets. Analysis of RMSD, RMSF, hydrogen bonding, bond lengths, and MM-PBSA binding energies offered a comprehensive understanding of cytochalasin D's molecular mechanisms of action.

The study supports the potential of cytochalasin D as a therapeutic agent in cancer treatment, particularly in targeting the MAPK pathways in TNBC.

In-vitro therapeutic effects of Cytochalasin D against MDA-MB-231 cells

- Cytochalasin D demonstrated significant bioactivity against the TNBC cell line MDA-MB-231, with an IC50 of 28.9 µg/mL, inducing S-phase cell cycle arrest and inhibiting cell migration.
- In wound healing assays, cytochalasin D-treated cells showed a significant reduction in migration, and increased ROS levels suggested the induction of apoptosis via oxidative stress.
- Molecular dynamics simulations and western blot analysis revealed that cytochalasin D inhibits the MAPK signalling pathway by reducing the expression of key proteins (MAPK1, MAPK3, MAPK8, and MAPK14).
- Cytochalasin D also activated the extrinsic apoptosis pathway, as evidenced by decreased expression of caspase 8 and increased levels of cleaved caspase 8, further confirming its pro-apoptotic effects.

To summarize the findings, cytochalasin D inhibits the MAPK pathway, induces apoptosis, and significantly reduces migration in TNBC cells, highlighting its potential as an anti-cancer agent.

Nano-carrier mediated delivery of Cytochalasin D

- Cytochalasin D-loaded PLGA nanoparticles (NPs) were successfully synthesized using the single emulsion solvent evaporation method, resulting in NPs with a negative surface charge, which is crucial for stability and dispersion in biological systems.
- Field Emission Scanning Electron Microscopy (FESEM) and Field Emission Transmission Electron Microscopy (FETEM) revealed that the NPs had a size range of 100-200 nm, with an average mean size diameter of 54±21 nm, indicating suitability for drug delivery with good dispersion and minimal aggregation.
- The NPs demonstrated an entrapment efficiency of 40%, with a release profile showing an initial burst release in acidic conditions followed by sustained release, and a more stable, controlled release in neutral pH, indicating robust encapsulation and potential for prolonged therapeutic effects.
- Cytochalasin D-loaded PLGA NPs exhibited significant cytotoxicity against TNBC MDA-MB-231 cells with an IC50 of 1.056 mg/mL, inducing a substantial increase in ROS generation, leading to oxidative stress and apoptosis in cancer cells.
- The void (drug-free) PLGA NPs showed no significant cytotoxic effects on MDA-MB-231 cells, confirming the biocompatibility and inert nature of the PLGA polymer, making it a safe carrier for drug delivery.

Cytochalasin D-loaded PLGA nanoparticles demonstrate effective cytotoxicity against TNBC cells through ROS-induced apoptosis, with strong stability, controlled drug release, and biocompatibility, making them a promising candidate for targeted cancer therapy.

6.2. Future prospects

I. Combinatorial approach: Combining Cytochalasin D with nucleic acid-directed agents offers a promising approach for treating triple-negative breast cancer (TNBC). Cytochalasin D's ability to disrupt the actin cytoskeleton, leading to cell cycle arrest and apoptosis, complements the targeted action of nucleic acid-directed agents that interfere with DNA and RNA synthesis or repair. This synergy can enhance the therapeutic efficacy. Additionally, the combination may reduce the likelihood of drug resistance development and allow for lower doses of each drug, minimizing side effects while maximizing treatment outcomes.

II. Active targeting: Conjugating ligands on PLGA NPs offers a powerful strategy for enhancing the active targeting of TNBC cells. By attaching specific ligands to the surface of these NPs, the overexpression of certain receptors on TNBC cells such as epidermal growth factor receptor (EGFR), folate receptor, and transferrin receptor, can be exploited, guiding the drug-loaded nanoparticles directly to the cancerous tissue.

III. *In vivo* studies with both cytochalasin D and cytochalasin D loaded PLGA NPs can help solidify the role of this fungal secondary metabolite in the fight against TNBC.

PUBLICATIONS

From thesis work:

1. Mohanty, A., Saini, G.K. Cytochalasin D as a potential MAPK family inhibitor for treating Triple-Negative Breast Cancer. (Under review in Molecular simulation)

2. Mohanty, A., Saini, G.K. Physicochemical Characterization and Anticancer Efficacy of Cytochalasin D Loaded PLGA Nanoparticles. (Under review)

From collaborative work:

1. Nambiar, S.S., Mohanty, A., Patra, A. and Saini, G.K., 2022. Deciphering therapeutic efficacy of mycosynthesized silver nanoparticles using entomopathogenic fungi Metarhizium anisopliae against MCF-7 breast cancer cells *in vitro*. https://doi.org/10.1101/2022.08.25.505221

CONFERENCES

1. Participated in the workshop entitled Diagnostic Approaches in Virology; From 4th – 6th March, 2020; Organized by Department of Biosciences and Bioengineering, Indian Institute of Technology (IIT) Guwahati.
2. Participated in 20th INDO-US Flow Cytometry Symposium cum Workshop; From 13th- 16th March,2019; Organized by International Society for advancement of Cytometry (ISAC) and Department of Biosciences and Bioengineering, Indian Institute of Technology (IIT) Guwahati.

APPENDIX

Table A1: Buffer composition.

Buffers	Composition
10X PBS (1L)	1.37M NaCl 27mM KCl 100mM Na_2HPO_4 18mM KH_2PO_4
TBST	TBS + 0.1% Tween 20
Acetate buffer (1L)	1.8g $C_2H_3NaO_2$ 4.6g CH_3COOH HCl/NaOH (to adjust pH)
Tris buffer saline (TBS)	1500mM NaCl 200mM Tris base Adjust pH to 7.6 using HCl

Table A2: Protein- JAK1; Reported inhibitor- MI

	Protein	Protein + Inhibitor	Protein + Cytochalasin D
RMSD (nm)	0.2	0.23	0.24
RMSF (nm)	0.15	0.14	0.13
Radius of gyration (nm)	1.6	1.7	1.7
Pair distance (nm)		0.18	0.67

Table A3: Protein- c-SRC; Reported inhibitor- H8H

	Protein	Protein + Inhibitor	Protein + Cytochalasin D
RMSD (nm)	0.19	0.22	0.21
RMSF (nm)	0.14	0.16	0.17
Radius of gyration (nm)	2.1	2.02	1.9
Pair distance (nm)		0.2	0.37

Table A4: Protein- MAPK1; Reported inhibitor- frz

	Protein	Protein + Inhibitor	Protein + Cytochalasin D
RMSD (nm)	0.34	0.2	0.29
RMSF (nm)	0.17	0.13	0.14
Radius of gyration (nm)	1.9	1.6	1.7
Pair distance (nm)		0.19	0.19

Table A5: Protein- MAPK3; Reported inhibitor- 38Z

	Protein	Protein + Inhibitor	Protein + Cytochalasin D
RMSD (nm)	0.22	0.21	0.23
RMSF (nm)	0.14	0.14	0.13
Radius of gyration (nm)	1.6	1.8	1.8
Pair distance (nm)		0.17	0.19

Table A6: Protein- MAPK8; Reported inhibitor- Myu

	Protein	Protein + Inhibitor	Protein + Cytochalasin D
RMSD (nm)	0.21	0.21	0.24
RMSF (nm)	0.15	0.14	0.12
Radius of gyration (nm)	1.8	1.8	1.9
Pair distance (nm)		0.17	0.19

Table A7: Protein- MAPK14; Reported inhibitor- Skepinone

	Protein	Protein + Inhibitor	Protein + Cytochalasin D
RMSD (nm)	0.26	0.23	0.48
RMSF (nm)	0.14	0.16	0.17
Radius of gyration (nm)	1.9	1.8	1.9
Pair distance (nm)		0.19	0.2

BIBLIOGRAPHY

Abdel-Wareth, M. T. A. (2021). *Fungal Secondary Metabolites: Current Research, Commercial Aspects, and Applications* (pp. 299–346). https://doi.org/10.1007/978-3-030-85603-8_8

Ades, F., Zardavas, D., Bozovic-Spasojevic, I., Pugliano, L., Fumagalli, D., de Azambuja, E., Viale, G., Sotiriou, C., & Piccart, M. (2014). Luminal B Breast Cancer: Molecular Characterization, Clinical Management, and Future Perspectives. *Journal of Clinical Oncology*, *32*(25), 2794–2803. https://doi.org/10.1200/JCO.2013.54.1870

ADRIAENS, M., JAILLARD, M., WAAGMEESTER, A., COORT, S., PICO, A., & EVELO, C. (2008). The public road to high-quality curated biological pathways. *Drug Discovery Today*, *13*(19–20), 856–862. https://doi.org/10.1016/j.drudis.2008.06.013

Agus, D. B., Akita, R. W., Fox, W. D., Lewis, G. D., Higgins, B., Pisacane, P. I., Lofgren, J. A., Tindell, C., Evans, D. P., Maiese, K., Scher, H. I., & Sliwkowski, M. X. (2002). Targeting ligand-activated ErbB2 signaling inhibits breast and prostate tumor growth. *Cancer Cell*, *2*(2), 127–137. https://doi.org/10.1016/S1535-6108(02)00097-1

Albukhaty, S., Sulaiman, G. M., Al-Karagoly, H., Mohammed, H. A., Hassan, A. S., Alshammari, A. A. A., Ahmad, A. M., Madhi, R., Almalki, F. A., Khashan, K. S., Jabir, M. S., Yusuf, M., Al-aqbi, Z. T., Sasikumar, P., & Khan, R. A. (2024). Iron oxide nanoparticles: The versatility of the magnetic and functionalized nanomaterials in targeting drugs, and gene deliveries with effectual magnetofection. *Journal of Drug Delivery Science and Technology*, *99*, 105838. https://doi.org/10.1016/j.jddst.2024.105838

Aldridge, D. C., Armstrong, J. J., Speake, R. N., & Turner, W. B. (1967). The cytochalasins, a new class of biologically active mould metabolites. *Chemical Communications (London)*, *1*, 26. https://doi.org/10.1039/c19670000026

Alvi, M., Yaqoob, A., Rehman, K., Shoaib, S. M., & Akash, M. S. H. (2022). PLGA-based nanoparticles for the treatment of cancer: current strategies and perspectives. *AAPS Open*, *8*(1), 12. https://doi.org/10.1186/s41120-022-00060-7

Amin, A. R. M. R., Karpowicz, P. A., Carey, T. E., Arbiser, J., Nahta, R., Chen, Z. G., Dong, J.-T., Kucuk, O., Khan, G. N., Huang, G. S., Mi, S., Lee, H.-Y., Reichrath, J., Honoki, K., Georgakilas, A. G., Amedei, A., Amin, A., Helferich, B., Boosani, C. S., … Shin, D. M. (2015). Evasion of anti-growth signaling: A key step in tumorigenesis and potential target for treatment and prophylaxis by natural compounds. *Seminars in Cancer Biology*, *35*, S55–S77. https://doi.org/10.1016/j.semcancer.2015.02.005

Ashburner, M., Ball, C. A., Blake, J. A., Botstein, D., Butler, H., Cherry, J. M., Davis, A. P., Dolinski, K., Dwight, S. S., Eppig, J. T., Harris, M. A., Hill, D. P., Issel-Tarver, L., Kasarskis, A., Lewis, S., Matese, J. C., Richardson, J. E., Ringwald, M., Rubin, G. M., & Sherlock, G. (2000). Gene Ontology: tool for the unification of biology. *Nature Genetics*, *25*(1), 25–29. https://doi.org/10.1038/75556

Bala, I., Hariharan, S., & Kumar, M. R. (2004). PLGA Nanoparticles in Drug Delivery: The State of the Art; *Critical Reviews in Therapeutic Drug Carrier Systems*, *21*(5), 387–422. https://doi.org/10.1615/CritRevTherDrugCarrierSyst.v21.i5.20

Balogh, L. P. (Ed.). (2020). *Nano-Enabled Medical Applications*. Jenny Stanford Publishing. https://doi.org/10.1201/9780429399039

Begines, B., Ortiz, T., Pérez-Aranda, M., Martínez, G., Merinero, M., Argüelles-Arias, F., & Alcudia, A. (2020). Polymeric Nanoparticles for Drug Delivery: Recent Developments and Future Prospects. *Nanomaterials*, *10*(7), 1403. https://doi.org/10.3390/nano10071403

BERG, T., FROHOLM, L., & LALAND, S. (1965). THE BIOSYNTHESIS OF GRAMICIDIN S IN A CELL-FREE SYSTEM. *Biochemical Journal*, *96*(1), 43–52. https://doi.org/10.1042/bj0960043

Bhattacharjee, S. (2016). DLS and zeta potential – What they are and what they are not? *Journal of Controlled Release*, *235*, 337–351. https://doi.org/10.1016/j.jconrel.2016.06.017

Bianchini, G., De Angelis, C., Licata, L., & Gianni, L. (2022). Treatment landscape of triple-negative breast cancer — expanded options, evolving needs. *Nature Reviews Clinical Oncology*, *19*(2), 91–113. https://doi.org/10.1038/s41571-021-00565-2

Binder, M., & Tamm, C. (1973). The Cytochalasans: A New Class of Biologically Active Microbial Metabolites. *Angewandte Chemie International Edition in English*, *12*(5), 370–380. https://doi.org/10.1002/anie.197303701

Bitencourt-Ferreira, G., & de Azevedo, W. F. (2019). *Molegro Virtual Docker for Docking* (pp. 149–167). https://doi.org/10.1007/978-1-4939-9752-7_10

Bogyo, D., Fondy, S. R. E., Finster, L., Fondy, C., Patil, S., & Fondy, T. P. (1991). Cytochalasin-B-induced immunosuppression of murine allogeneic anti-tumor response and the effect of recombinant human interleukin-2. *Cancer Immunology Immunotherapy*, *32*(6), 400–405. https://doi.org/10.1007/BF01741335

Bollag, D. M. (1997). Epothilones: novel microtubule-stabilising agents. *Expert Opinion on Investigational Drugs*, *6*(7), 867–873. https://doi.org/10.1517/13543784.6.7.867

Borel, J. F., Feurer, C., Gubler, H. U., & Stähelin, H. (1994). Biological effects of cyclosporin A: A new antilymphocytic agent. *Agents and Actions*, *43*(3–4), 179–186. https://doi.org/10.1007/BF01986686

Bray, F., Laversanne, M., Sung, H., Ferlay, J., Siegel, R. L., Soerjomataram, I., & Jemal, A. (2024). Global cancer statistics 2022: GLOBOCAN estimates of incidence and mortality worldwide for 36 cancers in 185 countries. *CA: A Cancer Journal for Clinicians*, *74*(3), 229–263. https://doi.org/10.3322/caac.21834

Brown, S. S., & Spudich, J. A. (1979). Cytochalasin inhibits the rate of elongation of actin filament fragments. *Journal of Cell Biology*, *83*(3), 657–662. https://doi.org/10.1083/JCB.83.3.657

Brown, S. S., & Spudich, J. A. (1981). Mechanism of action of cytochalasin: evidence that it binds to actin filament ends. *The Journal of Cell Biology*, *88*(3), 487–491. https://doi.org/10.1083/jcb.88.3.487

Burotto, M., Chiou, V. L., Lee, J., & Kohn, E. C. (2014). The MAPK pathway across different malignancies: A new perspective. *Cancer*, *120*(22), 3446–3456. https://doi.org/10.1002/cncr.28864

Caglar, H. O., & Biray Avci, C. (2020). Alterations of cell cycle genes in cancer: unmasking the role of cancer stem cells. *Molecular Biology Reports*, *47*(4), 3065–3076. https://doi.org/10.1007/s11033-020-05341-6

C Aldridge, B. D., Turner, W. B., Aldridge, D. C., Armstrong, J. J., Speake, R. N., & Carter, S. B. (1967). Structures of cytochalasins C and D. *J. Chem. SOG. (C)*. https://doi.org/https://doi.org/10.1039/J39690000923

Cavalli, R., Caputo, O., & Gasco, M. R. (1993). Solid lipospheres of doxorubicin and idarubicin. *International Journal of Pharmaceutics*, *89*(1), R9–R12. https://doi.org/10.1016/0378-5173(93)90313-5

Chabner, B. A., & Roberts, T. G. (2005). Chemotherapy and the war on cancer. *Nature Reviews Cancer*, *5*(1), 65–72. https://doi.org/10.1038/nrc1529

Chandran, U., Mehendale, N., Patil, S., Chaguturu, R., & Patwardhan, B. (2017). Network Pharmacology. In *Innovative Approaches in Drug Discovery* (pp. 127–164). Elsevier. https://doi.org/10.1016/B978-0-12-801814-9.00005-2

CHENG, J., TEPLY, B., SHERIFI, I., SUNG, J., LUTHER, G., GU, F., LEVYNISSENBAUM, E., RADOVICMORENO, A., LANGER, R., & FAROKHZAD, O. (2007). Formulation of

functionalized PLGA–PEG nanoparticles for in vivo targeted drug delivery. *Biomaterials*, *28*(5), 869–876. https://doi.org/10.1016/j.biomaterials.2006.09.047

Chernova, O. B., Chernov, M. V., Agarwal, M. L., Taylor, W. R., & Stark, G. R. (1995). The role of p53 in regulating genomic stability when DNA and RNA synthesis are inhibited. *Trends in Biochemical Sciences*, *20*(10), 431–434. https://doi.org/10.1016/S0968-0004(00)89094-5

Cho, K., Wang, X., Nie, S., Chen, Z. (Georgia), & Shin, D. M. (2008). Therapeutic Nanoparticles for Drug Delivery in Cancer. *Clinical Cancer Research*, *14*(5), 1310–1316. https://doi.org/10.1158/1078-0432.CCR-07-1441

Chugh, H., Sood, D., Chandra, I., Tomar, V., Dhawan, G., & Chandra, R. (2018). Role of gold and silver nanoparticles in cancer nano-medicine. *Artificial Cells, Nanomedicine, and Biotechnology*, *46*(sup1), 1210–1220. https://doi.org/10.1080/21691401.2018.1449118

Cimini, D., Fioravanti, D., Tanzarella, C., & Degrassi, F. (1998). Simultaneous inhibition of contractile ring and central spindle formation in mammalian cells treated with cytochalasin B. *Chromosoma*, *107*(6–7), 479–485. https://doi.org/10.1007/s004120050332

Citron, M. L. (2008). Dose-Dense Chemotherapy: Principles, Clinical Results and Future Perspectives. *Breast Care*, *3*(4), 251–255. https://doi.org/10.1159/000148914

Colleoni, M., Nole', F., Minchella, I., Noberasco, C., Luini, A., Orecchia, A., Veronesi, P., Zurrida, S., Viale, G., & Goldhirsch, A. (1998). Pre-operative chemotherapy and radiotherapy in breast cancer. *European Journal of Cancer*, *34*(5), 641–645. https://doi.org/10.1016/S0959-8049(97)10091-0

Connor, E. E., Mwamuka, J., Gole, A., Murphy, C. J., & Wyatt, M. D. (2005). Gold Nanoparticles Are Taken Up by Human Cells but Do Not Cause Acute Cytotoxicity. *Small*, *1*(3), 325–327. https://doi.org/10.1002/smll.200400093

Cooper, J. A. (1987). Effects of cytochalasin and phalloidin on actin. *The Journal of Cell Biology*, *105*(4), 1473–1478. https://doi.org/10.1083/jcb.105.4.1473

Correa, P., Fox, J., Fontham, E., Ruiz, B., Lin, Y., Zavala, D., Taylor, N., Mackinley, D., De Lima, E., Portilla, H., & Zarama, G. (1990). Helicobacter pylori and gastric carcinoma: Serum antibody prevalence in populations with contrasting cancer risks. *Cancer*, *66*(12), 2569–2574. https://doi.org/10.1002/1097-0142(19901215)66:12<2569::AID-CNCR2820661220>3.0.CO;2-I

Cotlar, A. M., Dubose, J. J., & Rose, D. M. (2003). History of surgery for breast cancer: radical to the sublime. *Current Surgery*, *60*(3), 329–337. https://doi.org/10.1016/S0149-7944(02)00777-8

Creighton, C. (2012). The molecular profile of luminal B breast cancer. *Biologics: Targets and Therapy*, 289. https://doi.org/10.2147/BTT.S29923

Daina, A., Michielin, O., & Zoete, V. (2019). SwissTargetPrediction: updated data and new features for efficient prediction of protein targets of small molecules. *Nucleic Acids Research*, *47*(W1), W357–W364. https://doi.org/10.1093/nar/gkz382

Danaei, G., Vander Hoorn, S., Lopez, A. D., Murray, C. J., & Ezzati, M. (2005). Causes of cancer in the world: comparative risk assessment of nine behavioural and environmental risk factors. *The Lancet*, *366*(9499), 1784–1793. https://doi.org/10.1016/S0140-6736(05)67725-2

Das, A. P., & Agarwal, S. M. (2024). Recent advances in the area of plant-based anti-cancer drug discovery using computational approaches. *Molecular Diversity*, *28*(2), 901–925. https://doi.org/10.1007/s11030-022-10590-7

Debien, V., De Caluwé, A., Wang, X., Piccart-Gebhart, M., Tuohy, V. K., Romano, E., & Buisseret, L. (2023). Immunotherapy in breast cancer: an overview of current strategies and perspectives. *Npj Breast Cancer*, *9*(1), 7. https://doi.org/10.1038/s41523-023-00508-3

Della Rocca, J., & Lin, W. (2010). Nanoscale Metal–Organic Frameworks: Magnetic Resonance Imaging Contrast Agents and Beyond. *European Journal of Inorganic Chemistry*, *2010*(24), 3725–3734. https://doi.org/10.1002/ejic.201000496

De Spiegeleer, B., Verbeke, F., D'Hondt, M., Hendrix, A., Van De Wiele, C., Burvenich, C., Peremans, K., De Wever, O., Bracke, M., & Wynendaele, E. (2015). The Quorum Sensing Peptides PhrG, CSP and EDF Promote Angiogenesis and Invasion of Breast Cancer Cells In Vitro. *PLOS ONE*, *10*(3), e0119471. https://doi.org/10.1371/journal.pone.0119471

Dinakar, Y. H., Rajana, N., Kumari, N. U., Jain, V., & Mehra, N. K. (2023). Recent Advances of Multifunctional PLGA Nanocarriers in the Management of Triple-Negative Breast Cancer. *AAPS PharmSciTech*, *24*(8), 258. https://doi.org/10.1208/s12249-023-02712-7

Du, L., Sánchez, C., & Shen, B. (2001). Hybrid Peptide–Polyketide Natural Products: Biosynthesis and Prospects toward Engineering Novel Molecules. *Metabolic Engineering*, *3*(1), 78–95. https://doi.org/10.1006/mben.2000.0171

Eccleston, A. (2023). A ROS-mediated resistance pathway to anticancer drugs. *Nature Reviews Drug Discovery*, *22*(7), 534–534. https://doi.org/10.1038/d41573-023-00094-w

Espinosa Fernandez, J. R., Eckhardt, B. L., Lee, J., Lim, B., Pearson, T., Seitz, R. S., Hout, D. R., Schweitzer, B. L., Nielsen, T. J., Lawrence, O. R., Wang, Y., Rao, A., & Ueno, N. T. (2020). Identification of triple-negative breast cancer cell lines classified under the same molecular

subtype using different molecular characterization techniques: Implications for translational research. *PLOS ONE*, *15*(4), e0231953. https://doi.org/10.1371/journal.pone.0231953

Fang, J. Y., & Richardson, B. C. (2005). The MAPK signalling pathways and colorectal cancer. *The Lancet Oncology*, *6*(5), 322–327. https://doi.org/10.1016/S1470-2045(05)70168-6

Federico, A., Fratello, M., Scala, G., Möbus, L., Pavel, A., Del Giudice, G., Ceccarelli, M., Costa, V., Ciccodicola, A., Fortino, V., Serra, A., & Greco, D. (2022). Integrated Network Pharmacology Approach for Drug Combination Discovery: A Multi-Cancer Case Study. *Cancers*, *14*(8), 2043. https://doi.org/10.3390/CANCERS14082043/S1

Ferreira, D. dos S., Lopes, S. C. de A., Franco, M. S., & Oliveira, M. C. (2013). pH-sensitive Liposomes for Drug Delivery in Cancer Treatment. *Therapeutic Delivery*, *4*(9), 1099–1123. https://doi.org/10.4155/tde.13.80

Ferreri, A. J. M., Guidoboni, M., Ponzoni, M., De Conciliis, C., Dell'Oro, S., Fleischhauer, K., Caggiari, L., Lettini, A. A., Dal Cin, E., Ieri, R., Freschi, M., Villa, E., Boiocchi, M., & Dolcetti, R. (2004). Evidence for an Association Between Chlamydia psittaci and Ocular Adnexal Lymphomas. *JNCI Journal of the National Cancer Institute*, *96*(8), 586–594. https://doi.org/10.1093/jnci/djh102

Flanagan, M. D., & Lin, S. (1980). Cytochalasins block actin filament elongation by binding to high affinity sites associated with F-actin. *Journal of Biological Chemistry*, *255*(3), 835–838. https://doi.org/10.1016/S0021-9258(19)86105-7

Foissner, I., & Wasteneys, G. O. (2007). Wide-Ranging Effects of Eight Cytochalasins and Latrunculin A and B on Intracellular Motility and Actin Filament Reorganization in Characean Internodal Cells. *Plant and Cell Physiology*, *48*(4), 585–597. https://doi.org/10.1093/pcp/pcm030

Fujii, Y., Tani, H., Ichinoe, M., & Nakajima, H. (2000). Zygosporin D and Two New Cytochalasins Produced by the Fungus *Metarrhizium anisopliae*. *Journal of Natural Products*, *63*(1), 132–135. https://doi.org/10.1021/np990331t

Gabizon, A. A. (1995). Liposome circulation time and tumor targeting: implications for cancer chemotherapy. *Advanced Drug Delivery Reviews*, *16*(2–3), 285–294. https://doi.org/10.1016/0169-409X(95)00030-B

García-Hernández, L., García-Ortega, M. B., Ruiz-Alcalá, G., Carrillo, E., Marchal, J. A., & García, M. Á. (2021). The p38 MAPK Components and Modulators as Biomarkers and Molecular Targets in Cancer. *International Journal of Molecular Sciences*, *23*(1), 370. https://doi.org/10.3390/ijms23010370

Garg, A., & Grundy, S. M. (1988). Lovastatin for Lowering Cholesterol Levels in Non-Insulin-Dependent Diabetes Mellitus. *New England Journal of Medicine*, *318*(2), 81–86. https://doi.org/10.1056/NEJM198801143180204

Garrido-Castro, A. C., Lin, N. U., & Polyak, K. (2019). Insights into Molecular Classifications of Triple-Negative Breast Cancer: Improving Patient Selection for Treatment. *Cancer Discovery*, *9*(2), 176–198. https://doi.org/10.1158/2159-8290.CD-18-1177

Gaulton, A., Bellis, L. J., Bento, A. P., Chambers, J., Davies, M., Hersey, A., Light, Y., McGlinchey, S., Michalovich, D., Al-Lazikani, B., & Overington, J. P. (2012). ChEMBL: a large-scale bioactivity database for drug discovery. *Nucleic Acids Research*, *40*(D1), D1100–D1107. https://doi.org/10.1093/nar/gkr777

Gene Ontology Consortium. (2004). The Gene Ontology (GO) database and informatics resource. *Nucleic Acids Research*, *32*(90001), 258D – 261. https://doi.org/10.1093/nar/gkh036

Ghosh, R., Narasanna, A., Wang, S. E., Liu, S., Chakrabarty, A., Balko, J. M., González-Angulo, A. M., Mills, G. B., Penuel, E., Winslow, J., Sperinde, J., Dua, R., Pidaparthi, S., Mukherjee, A., Leitzel, K., Kostler, W. J., Lipton, A., Bates, M., & Arteaga, C. L. (2011). Trastuzumab Has Preferential Activity against Breast Cancers Driven by HER2 Homodimers. *Cancer Research*, *71*(5), 1871–1882. https://doi.org/10.1158/0008-5472.CAN-10-1872

Gilson, M. K., Liu, T., Baitaluk, M., Nicola, G., Hwang, L., & Chong, J. (2016). BindingDB in 2015: A public database for medicinal chemistry, computational chemistry and systems pharmacology. *Nucleic Acids Research*, *44*(D1), D1045–D1053. https://doi.org/10.1093/nar/gkv1072

Glaviano, A., Foo, A. S. C., Lam, H. Y., Yap, K. C. H., Jacot, W., Jones, R. H., Eng, H., Nair, M. G., Makvandi, P., Geoerger, B., Kulke, M. H., Baird, R. D., Prabhu, J. S., Carbone, D., Pecoraro, C., Teh, D. B. L., Sethi, G., Cavalieri, V., Lin, K. H., … Kumar, A. P. (2023). PI3K/AKT/mTOR signaling transduction pathway and targeted therapies in cancer. *Molecular Cancer*, *22*(1), 138. https://doi.org/10.1186/s12943-023-01827-6

Goddette, D. W., & Frieden, C. (1986). Actin polymerization. The mechanism of action of cytochalasin D. *Journal of Biological Chemistry*, *261*(34), 15974–15980. https://doi.org/10.1016/S0021-9258(18)66662-1

González-Hernández, R. A., Valdez-Cruz, N. A., Macías-Rubalcava, M. L., & Trujillo-Roldán, M. A. (2023). Overview of fungal terpene synthases and their regulation. *World Journal of Microbiology and Biotechnology*, *39*(7), 194. https://doi.org/10.1007/s11274-023-03635-y

Goto, T., Kakisawa, H., & Hirata, Y. (1963). The structure of grifolin, an antibiotic from a basidiomycete. *Tetrahedron*, *19*(12), 2079–2083. https://doi.org/10.1016/0040-4020(63)85023-1

Grimm, L. J., & Mazurowski, M. A. (2020). Breast Cancer Radiogenomics: Current Status and Future Directions. *Academic Radiology*, *27*(1), 39–46. https://doi.org/10.1016/j.acra.2019.09.012

Gulhati, P., Bowen, K. A., Liu, J., Stevens, P. D., Rychahou, P. G., Chen, M., Lee, E. Y., Weiss, H. L., O'Connor, K. L., Gao, T., & Evers, B. M. (2011). mTORC1 and mTORC2 Regulate EMT, Motility, and Metastasis of Colorectal Cancer via RhoA and Rac1 Signaling Pathways. *Cancer Research*, *71*(9), 3246–3256. https://doi.org/10.1158/0008-5472.CAN-10-4058

Gupta, A. K., & Gupta, M. (2005). Synthesis and surface engineering of iron oxide nanoparticles for biomedical applications. *Biomaterials*, *26*(18), 3995–4021. https://doi.org/10.1016/j.biomaterials.2004.10.012

Gupta, P. K., Tripathi, D., Kulkarni, S., & Rajan, M. G. R. (2016). Mycobacterium tuberculosis H37Rv infected THP-1 cells induce epithelial mesenchymal transition (EMT) in lung adenocarcinoma epithelial cell line (A549). *Cellular Immunology*, *300*, 33–40. https://doi.org/10.1016/j.cellimm.2015.11.007

Guy, R. H. (2010). *Transdermal Drug Delivery* (pp. 399–410). https://doi.org/10.1007/978-3-642-00477-3_13

Hädener, A., Roth, P., & Tamm, C. (1989). Biosynthesis of Cytochalasans. XI. New Results on the Incorporation of Phenylalanine into Cytochalasin D by Zygosporium masonii [1]. *Zeitschrift Für Naturforschung C*, *44*(1–2), 19–32. https://doi.org/10.1515/znc-1989-1-205

Halling-Brown, M. D., Bulusu, K. C., Patel, M., Tym, J. E., & Al-Lazikani, B. (2012). canSAR: an integrated cancer public translational research and drug discovery resource. *Nucleic Acids Research*, *40*(D1), D947–D956. https://doi.org/10.1093/nar/gkr881

Hansen, R., & Oren, M. (1997). p53; from inductive signal to cellular effect. *Current Opinion in Genetics & Development*, *7*(1), 46–51. https://doi.org/10.1016/S0959-437X(97)80108-6

Haussmann, J., Corradini, S., Nestle-Kraemling, C., Bölke, E., Njanang, F. J. D., Tamaskovics, B., Orth, K., Ruckhaeberle, E., Fehm, T., Mohrmann, S., Simiantonakis, I., Budach, W., & Matuschek, C. (2020). Recent advances in radiotherapy of breast cancer. *Radiation Oncology*, *15*(1), 71. https://doi.org/10.1186/s13014-020-01501-x

Hayot, C., Debeir, O., Van Ham, P., Van Damme, M., Kiss, R., & Decaestecker, C. (2006). Characterization of the activities of actin-affecting drugs on tumor cell migration. *Toxicology and Applied Pharmacology*, *211*(1), 30–40. https://doi.org/10.1016/j.taap.2005.06.006

Higgins, M. J., & Baselga, J. (2011). Targeted therapies for breast cancer. *Journal of Clinical Investigation*, *121*(10), 3797–3803. https://doi.org/10.1172/JCI57152

Hollingsworth, S. A., & Dror, R. O. (2018). Molecular Dynamics Simulation for All. *Neuron*, *99*(6), 1129–1143. https://doi.org/10.1016/j.neuron.2018.08.011

Hopkins, A. L. (2008). Network pharmacology: the next paradigm in drug discovery. *Nature Chemical Biology 2008 4:11*, *4*(11), 682–690. https://doi.org/10.1038/nchembio.118

Horn, D., & Rieger, J. (2001). Organic Nanoparticles in the Aqueous Phase—Theory, Experiment, and Use. *Angewandte Chemie International Edition*, *40*(23), 4330. https://doi.org/10.1002/1521-3773(20011203)40:23<4330::AID-ANIE4330>3.0.CO;2-W

Huang, F.-Y., Li, Y.-N., Mei, W.-L., Dai, H.-F., Zhou, P., & Tan, G.-H. (2012). Cytochalasin D, a tropical fungal metabolite, inhibits CT26 tumor growth and angiogenesis. *Asian Pacific Journal of Tropical Medicine*, *5*(3), 169–174. https://doi.org/10.1016/S1995-7645(12)60019-4

Huang, F. Y., Mei, W. L., Li, Y. N., Tan, G. H., Dai, H. F., Guo, J. L., Wang, H., Huang, Y. H., Zhao, H. G., Zhou, S. L., Li, L., & Lin, Y. Y. (2012). The antitumour activities induced by pegylated liposomal cytochalasin D in murine models. *European Journal of Cancer*, *48*(14), 2260–2269. https://doi.org/10.1016/J.EJCA.2011.12.018

Huang, M., Lu, J.-J., & Ding, J. (2021). Natural Products in Cancer Therapy: Past, Present and Future. *Natural Products and Bioprospecting*, *11*(1), 5–13. https://doi.org/10.1007/s13659-020-00293-7

HWANG, J., YI, M., ZHANG, X., XU, Y., JUNG, J. H., & KIM, D.-K. (2013). Cytochalasin B induces apoptosis through the mitochondrial apoptotic pathway in HeLa human cervical carcinoma cells. *Oncology Reports*, *30*(4), 1929–1935. https://doi.org/10.3892/or.2013.2617

Isakoff, S. J. (2010). Triple-Negative Breast Cancer. *The Cancer Journal*, *16*(1), 53–61. https://doi.org/10.1097/PPO.0b013e3181d24ff7

Jain, V., Kumar, H., Anod, H. V., Chand, P., Gupta, N. V., Dey, S., & Kesharwani, S. S. (2020). A review of nanotechnology-based approaches for breast cancer and triple-negative breast cancer. *Journal of Controlled Release*, *326*, 628–647. https://doi.org/10.1016/j.jconrel.2020.07.003

Jakubczyk, D., & Dussart, F. (2020). Selected Fungal Natural Products with Antimicrobial Properties. *Molecules*, *25*(4), 911. https://doi.org/10.3390/molecules25040911

Judefeind, A., & de Villiers, M. M. (2009). Drug Loading into and In Vitro Release from Nanosized Drug Delivery Systems. In *Nanotechnology in Drug Delivery* (pp. 129–162). Springer New York. https://doi.org/10.1007/978-0-387-77668-2_5

Kanehisa, M. (2000). KEGG: Kyoto Encyclopedia of Genes and Genomes. *Nucleic Acids Research*, *28*(1), 27–30. https://doi.org/10.1093/nar/28.1.27

Karplus, M., & McCammon, J. A. (2002). Molecular dynamics simulations of biomolecules. *Nature Structural Biology*, *9*(9), 646–652. https://doi.org/10.1038/nsb0902-646

Khan, M. R. U. Z., & Trivedi, V. (2023). Molecular modelling, docking and network analysis of phytochemicals from Haritaki churna: role of protein cross-talks for their action. *Journal of Biomolecular Structure and Dynamics*. https://doi.org/10.1080/07391102.2023.2220036

Kim, S., Chen, J., Cheng, T., Gindulyte, A., He, J., He, S., Li, Q., Shoemaker, B. A., Thiessen, P. A., Yu, B., Zaslavsky, L., Zhang, J., & Bolton, E. E. (2023). PubChem 2023 update. *Nucleic Acids Research*, *51*(D1), D1373–D1380. https://doi.org/10.1093/nar/gkac956

Kim, S., Thiessen, P. A., Bolton, E. E., Chen, J., Fu, G., Gindulyte, A., Han, L., He, J., He, S., Shoemaker, B. A., Wang, J., Yu, B., Zhang, J., & Bryant, S. H. (2016). PubChem Substance and Compound databases. *Nucleic Acids Research*, *44*(D1), D1202–D1213. https://doi.org/10.1093/nar/gkv951

Klocker, E. V., Balic, M., & Steger, G. (2022). Molecular profiling leading to personalized treatment in breast cancer. *Memo - Magazine of European Medical Oncology*, *15*(3), 196–200. https://doi.org/10.1007/s12254-021-00792-4

Knox, C., Wilson, M., Klinger, C. M., Franklin, M., Oler, E., Wilson, A., Pon, A., Cox, J., Chin, N. E. (Lucy), Strawbridge, S. A., Garcia-Patino, M., Kruger, R., Sivakumaran, A., Sanford, S., Doshi, R., Khetarpal, N., Fatokun, O., Doucet, D., Zubkowski, A., … Wishart, D. S. (2024). DrugBank 6.0: the DrugBank Knowledgebase for 2024. *Nucleic Acids Research*, *52*(D1), D1265–D1275. https://doi.org/10.1093/nar/gkad976

Koohi Moftakhari Esfahani, M., Alavi, S. E., Cabot, P. J., Islam, N., & Izake, E. L. (2022). Application of Mesoporous Silica Nanoparticles in Cancer Therapy and Delivery of Repurposed Anthelmintics for Cancer Therapy. *Pharmaceutics*, *14*(8), 1579. https://doi.org/10.3390/pharmaceutics14081579

Kowalski, R. J., Giannakakou, P., & Hamel, E. (1997). Activities of the Microtubule-stabilizing Agents Epothilones A and B with Purified Tubulin and in Cells Resistant to Paclitaxel (Taxol®). *Journal of Biological Chemistry*, *272*(4), 2534–2541. https://doi.org/10.1074/jbc.272.4.2534

Kuerbitz, S. J., Plunkett, B. S., Walsh, W. V, & Kastan, M. B. (1992). Wild-type p53 is a cell cycle checkpoint determinant following irradiation. *Proceedings of the National Academy of Sciences*, *89*(16), 7491–7495. https://doi.org/10.1073/pnas.89.16.7491

Kuhn, M., Letunic, I., Jensen, L. J., & Bork, P. (2016). The SIDER database of drugs and side effects. *Nucleic Acids Research*, *44*(D1), D1075–D1079. https://doi.org/10.1093/nar/gkv1075

Kuhn, M., von Mering, C., Campillos, M., Jensen, L. J., & Bork, P. (2007). STITCH: interaction networks of chemicals and proteins. *Nucleic Acids Research*, *36*(Database), D684–D688. https://doi.org/10.1093/nar/gkm795

Kumar, P., & Aggarwal, R. (2016). An overview of triple-negative breast cancer. *Archives of Gynecology and Obstetrics*, *293*(2), 247–269. https://doi.org/10.1007/s00404-015-3859-y

Lee, J., Yi, J.-M., Kim, H., Lee, Y. J., Park, J.-S., Bang, O.-S., & Kim, N. S. (2014). Cytochalasin H, an Active Anti-angiogenic Constituent of the Ethanol Extract of <i>Gleditsia sinensis</i> Thorns. *Biological and Pharmaceutical Bulletin*, *37*(1), 6–12. https://doi.org/10.1248/bpb.b13-00318

Lee, Y.-M., Oh, M. H., Go, J.-H., Han, K., & Choi, S.-Y. (2020). Molecular subtypes of triple-negative breast cancer: understanding of subtype categories and clinical implication. *Genes & Genomics*, *42*(12), 1381–1387. https://doi.org/10.1007/s13258-020-01014-7

Levine, A. J. (1997). p53, the Cellular Gatekeeper for Growth and Division. *Cell*, *88*(3), 323–331. https://doi.org/10.1016/S0092-8674(00)81871-1

Lin, W., Rieter, W. J., & Taylor, K. M. L. (2009). Modular Synthesis of Functional Nanoscale Coordination Polymers. *Angewandte Chemie International Edition*, *48*(4), 650–658. https://doi.org/10.1002/anie.200803387

Li, S. (Ed.). (2021). *Network Pharmacology*. Springer Singapore. https://doi.org/10.1007/978-981-16-0753-0

Liu, J., Tian, R., Sun, C., Guo, Y., Dong, L., Li, Y., & Song, X. (2023). Microbial metabolites are involved in tumorigenesis and development by regulating immune responses. *Frontiers in Immunology*, *14*. https://doi.org/10.3389/fimmu.2023.1290414

Li, Y., Zhang, H., Merkher, Y., Chen, L., Liu, N., Leonov, S., & Chen, Y. (2022). Recent advances in therapeutic strategies for triple-negative breast cancer. *Journal of Hematology & Oncology*, *15*(1), 121. https://doi.org/10.1186/s13045-022-01341-0

Loty, S., Forest, N., Boulekbache, H., & Sautier, J. (1995). Cytochalasin D induces changes in cell shape and promotes in vitro chondrogenesis: A morphological study. *Biology of the Cell*, *83*(2–3), 149–161. https://doi.org/10.1016/0248-4900(96)81303-7

Magnuson, B. L., Clifford, T. M., Hoskins, L. A., & Bernard, A. C. (2005). Enteral Nutrition and Drug Administration, Interactions, and Complications. *Nutrition in Clinical Practice*, *20*(6), 618–624. https://doi.org/10.1177/0115426505020006618

Ma, J.-Q., Zhang, Y.-J., & Tian, Z.-K. (2021). Anti-oxidant, anti-inflammatory and anti-fibrosis effects of ganoderic acid A on carbon tetrachloride induced nephrotoxicity by regulating the Trx/TrxR and JAK/ROCK pathway. *Chemico-Biological Interactions*, *344*, 109529. https://doi.org/10.1016/j.cbi.2021.109529

Małecki, J. M., Bentke, A., Ostrowska, B., & Laidler, P. (2010). Cytochalasin D, LY294002 and olomoucine synergize in promoting death of melanoma cells through activation of caspase-3 and apoptosis. *Melanoma Research*, *20*(1), 52–58. https://doi.org/10.1097/CMR.0b013e328332f1e6

Malone, E. R., Oliva, M., Sabatini, P. J. B., Stockley, T. L., & Siu, L. L. (2020). Molecular profiling for precision cancer therapies. *Genome Medicine*, *12*(1), 8. https://doi.org/10.1186/s13073-019-0703-1

Mani, S., Hande, A., & Boichuk, S. (2022). Triple-Negative Breast Cancer: the Current Aspects of Pathogenesis and Therapies. *BioNanoScience*, *12*(4), 1404–1435. https://doi.org/10.1007/s12668-022-00991-1

Masoudi-Sobhanzadeh, Y., Omidi, Y., Amanlou, M., & Masoudi-Nejad, A. (2020). Drug databases and their contributions to drug repurposing. *Genomics*, *112*(2), 1087–1095. https://doi.org/10.1016/j.ygeno.2019.06.021

Massova, I., & Kollman, P. A. (2000). Combined molecular mechanical and continuum solvent approach (MM-PBSA/GBSA) to predict ligand binding. *Perspectives in Drug Discovery and Design*, *18*(1), 113–135. https://doi.org/10.1023/A:1008763014207

Ma, Y., Xiu, Z., Zhou, Z., Huang, B., Liu, J., Wu, X., Li, S., & Tang, X. (2019). Cytochalasin H Inhibits Angiogenesis *via* the Suppression of HIF-1α Protein Accumulation and VEGF Expression through PI3K/AKT/P70S6K and ERK1/2 Signaling Pathways in Non-Small Cell Lung Cancer Cells. *Journal of Cancer*, *10*(9), 1997–2005. https://doi.org/10.7150/jca.29933

Medina, M. A., Oza, G., Sharma, A., Arriaga, L. G., Hernández Hernández, J. M., Rotello, V. M., & Ramirez, J. T. (2020). Triple-Negative Breast Cancer: A Review of Conventional and Advanced Therapeutic Strategies. *International Journal of Environmental Research and Public Health*, *17*(6), 2078. https://doi.org/10.3390/ijerph17062078

Medina, O., Zhu, Y., & Kairemo, K. (2004). Targeted Liposomal Drug Delivery in Cancer. *Current Pharmaceutical Design*, *10*(24), 2981–2989. https://doi.org/10.2174/1381612043383467

Mesnard, B., De Vroey, B., Maunoury, V., & Lecuit, M. (2012). Immunoproliferative small intestinal disease associated with Campylobacter jejuni. *Digestive and Liver Disease*, *44*(9), 799–800. https://doi.org/10.1016/j.dld.2012.03.020

Misra, R., Patra, B., Varadharaj, S., & Verma, R. S. (2020). Establishing the promising role of novel combination of triple therapeutics delivery using polymeric nanoparticles for Triple negative breast cancer therapy. *BioImpacts*, *11*(3), 199–207. https://doi.org/10.34172/bi.2021.27

Mokri, N., Sepehri, Z., Faninam, F., Khaleghi, S., Kazemi, N. M., & Hashemi, M. (2022). Chitosan-coated Zn-metal-organic framework nanocomposites for effective targeted delivery of LNA-antisense miR-224 to colon tumor: in vitro studies. *Gene Therapy*, *29*(12), 680–690. https://doi.org/10.1038/s41434-021-00265-7

Moraes, D. F. C., de Mesquita, L. S. S., do Amaral, F. M. M., de Sousa Ribeiro, M. N., & Malik, S. (2017). Anticancer Drugs from Plants. In *Biotechnology and Production of Anti-Cancer Compounds* (pp. 121–142). Springer International Publishing. https://doi.org/10.1007/978-3-319-53880-8_5

Moritz, M., & Geszke-Moritz, M. (2015). Recent Developments in Application of Polymeric Nanoparticles as Drug Carriers. *Advances in Clinical and Experimental Medicine*, *24*(5), 749–758. https://doi.org/10.17219/acem/31802

Morris, G. M., Goodsell, D. S., Halliday, R. S., Huey, R., Hart, W. E., Belew, R. K., & Olson, A. J. (1998). Automated docking using a Lamarckian genetic algorithm and an empirical binding free energy function. *Journal of Computational Chemistry*, *19*(14), 1639–1662. https://doi.org/10.1002/(SICI)1096-987X(19981115)19:14<1639::AID-JCC10>3.0.CO;2-B

Nakamura, K., Shinozuka, K., & Yoshikawa, N. (2015). Anticancer and antimetastatic effects of cordycepin, an active component of Cordyceps sinensis. *Journal of Pharmacological Sciences*, *127*(1), 53–56. https://doi.org/10.1016/j.jphs.2014.09.001

NavaneethaKrishnan, S., Rosales, J. L., & Lee, K.-Y. (2021). ROS-Mediated Apoptosis in Cancer. In *Handbook of Oxidative Stress in Cancer: Mechanistic Aspects* (pp. 1–20). Springer Singapore. https://doi.org/10.1007/978-981-15-4501-6_48-1

Noor, F., Rehman, A., Ashfaq, U. A., Saleem, M. H., Okla, M. K., Al-Hashimi, A., Abdelgawad, H., & Aslam, S. (2022). Integrating Network Pharmacology and Molecular Docking Approaches to Decipher the Multi-Target Pharmacological Mechanism of Abrus precatorius L. Acting on Diabetes. *Pharmaceuticals*, *15*(4), 414. https://doi.org/10.3390/PH15040414/S1

Obidiro, O., Battogtokh, G., & Akala, E. O. (2023). Triple Negative Breast Cancer Treatment Options and Limitations: Future Outlook. *Pharmaceutics*, *15*(7), 1796. https://doi.org/10.3390/pharmaceutics15071796

Okrój, M., Kamysz, W., Slominska, E. M., Mysliwski, A., & Bigda, J. (2005). A novel mechanism of action of the fumagillin analog, TNP-470, in the B16F10 murine melanoma cell line. *Anti-Cancer Drugs*, *16*(8), 817–823. https://doi.org/10.1097/01.cad.0000172835.60142.a5

Onishi, Y., Azuma, Y., Sato, Y., Mizuno, Y., Tadakuma, T., & Kizaki, H. (1993). Topoisomerase inhibitors induce apoptosis in thymocytes. *Biochimica et Biophysica Acta (BBA) - Molecular Cell Research*, *1175*(2), 147–154. https://doi.org/10.1016/0167-4889(93)90017-J

Padi, S. K. R., Chauhan, S. S., & Singh, N. (2022). ROS Induced by Chemo- and Targeted Therapy Promote Apoptosis in Cancer Cells. In *Handbook of Oxidative Stress in Cancer: Mechanistic Aspects* (pp. 583–598). Springer Nature Singapore. https://doi.org/10.1007/978-981-15-9411-3_47

Palmerston Mendes, L., Pan, J., & Torchilin, V. (2017). Dendrimers as Nanocarriers for Nucleic Acid and Drug Delivery in Cancer Therapy. *Molecules*, *22*(9), 1401. https://doi.org/10.3390/molecules22091401

Parvez, S., Karole, A., Dinakar, Y. H., & Mudavath, S. L. (2022). Nanoformulation mediated silencing of P-gp efflux protein for the efficient oral delivery of anti-leishmanial drugs. *Journal of Drug Delivery Science and Technology*, *78*, 103959. https://doi.org/10.1016/j.jddst.2022.103959

Patra, J. K., Das, G., Fraceto, L. F., Campos, E. V. R., Rodriguez-Torres, M. del P., Acosta-Torres, L. S., Diaz-Torres, L. A., Grillo, R., Swamy, M. K., Sharma, S., Habtemariam, S., & Shin, H.-S. (2018). Nano based drug delivery systems: recent developments and future prospects. *Journal of Nanobiotechnology*, *16*(1), 71. https://doi.org/10.1186/s12951-018-0392-8

Paul, W., & Sharma, C. P. (2020). Inorganic nanoparticles for targeted drug delivery. In *Biointegration of Medical Implant Materials* (pp. 333–373). Elsevier. https://doi.org/10.1016/B978-0-08-102680-9.00013-5

Pinzi, L., & Rastelli, G. (2019). Molecular Docking: Shifting Paradigms in Drug Discovery. *International Journal of Molecular Sciences*, *20*(18), 4331. https://doi.org/10.3390/ijms20184331

Porta, C., Paglino, C., & Mosca, A. (2014). Targeting PI3K/Akt/mTOR Signaling in Cancer. *Frontiers in Oncology*, *4*. https://doi.org/10.3389/fonc.2014.00064

Prado-Alonso, L., Pérez-Victoria, I., Malmierca, M. G., Montero, I., Rioja-Blanco, E., Martín, J., Reyes, F., Méndez, C., Salas, J. A., & Olano, C. (2022). Colibrimycins, Novel Halogenated Hybrid Polyketide Synthase-Nonribosomal Peptide Synthetase (PKS-NRPS) Compounds Produced by *Streptomyces* sp. Strain CS147. *Applied and Environmental Microbiology*, *88*(1). https://doi.org/10.1128/AEM.01839-21

Puszkin, E., Puszkin, S., Lo, L. W., & Tanenbaum, S. W. (1973). Binding of Cytochalasin D to Platelet and Muscle Myosin. *Journal of Biological Chemistry*, *248*(22), 7754–7761. https://doi.org/10.1016/S0021-9258(19)43253-5

Qiao, K., Chooi, Y.-H., & Tang, Y. (2011). Identification and engineering of the cytochalasin gene cluster from Aspergillus clavatus NRRL 1. *Metabolic Engineering*, *13*(6), 723–732. https://doi.org/10.1016/j.ymben.2011.09.008

Qiu, Z., Liu, W., Zhu, Q., Ke, K., Zhu, Q., Jin, W., Yu, S., Yang, Z., Li, L., Sun, X., Ren, S., Liu, Y., Zhu, Z., Zeng, J., Huang, X., Huang, Y., Wei, L., Ma, M., Lu, J., … Sui, X. (2022). The Role and Therapeutic Potential of Macropinocytosis in Cancer. *Frontiers in Pharmacology*, *13*. https://doi.org/10.3389/fphar.2022.919819

Quiñonero, F., Ortigosa-Palomo, A., Ortiz, R., Melguizo, C., & Prados, J. (2024). Fungi-Derived Bioactive Compounds as Potential Therapeutic Agents for Pancreatic Cancer: A Systematic Review. *Microorganisms*, *12*(8), 1527. https://doi.org/10.3390/microorganisms12081527

Rai, N., Gupta, P., Keshri, P. K., Verma, A., Mishra, P., Kumar, D., Kumar, A., Singh, S. K., & Gautam, V. (2022). Fungal Endophytes: an Accessible Source of Bioactive Compounds with Potential Anticancer Activity. *Applied Biochemistry and Biotechnology*, *194*(7), 3296–3319. https://doi.org/10.1007/s12010-022-03872-1

Rangan, P., & Mondino, A. (2022). Microbial short-chain fatty acids: a strategy to tune adoptive T cell therapy. *Journal for ImmunoTherapy of Cancer*, *10*(7), e004147. https://doi.org/10.1136/jitc-2021-004147

Rarey, M., Kramer, B., Lengauer, T., & Klebe, G. (1996). A Fast Flexible Docking Method using an Incremental Construction Algorithm. *Journal of Molecular Biology*, *261*(3), 470–489. https://doi.org/10.1006/jmbi.1996.0477

Reis-Sobreiro, M., Teixeira da Mota, A., Jardim, C., & Serre, K. (2021). Bringing Macrophages to the Frontline against Cancer: Current Immunotherapies Targeting Macrophages. *Cells*, *10*(9), 2364. https://doi.org/10.3390/cells10092364

Ren, W., Luo, Z., Pan, F., Liu, J., Sun, Q., Luo, G., Wang, R., Zhao, H., Bian, B., Xiao, X., Pu, Q., Yang, S., & Yu, G. (2020). Integrated network pharmacology and molecular docking

approaches to reveal the synergistic mechanism of multiple components in *Venenum Bufonis* for ameliorating heart failure. *PeerJ*, *8*, e10107. https://doi.org/10.7717/peerj.10107

Ren, X., Yan, C.-X., Zhai, R.-X., Xu, K., Li, H., & Fu, X.-J. (2023). Comprehensive survey of target prediction web servers for Traditional Chinese Medicine. *Heliyon*, *9*(8), e19151. https://doi.org/10.1016/j.heliyon.2023.e19151

Riley, D. S. (Ed.). (2022). *Materia Medica of New and Old Homeopathic Medicines*. Springer International Publishing. https://doi.org/10.1007/978-3-030-65920-2

Roulin, D., Cerantola, Y., Dormond-Meuwly, A., Demartines, N., & Dormond, O. (2010). Targeting mTORC2 inhibits colon cancer cell proliferation in vitro and tumor formation in vivo. *Molecular Cancer*, *9*(1), 57. https://doi.org/10.1186/1476-4598-9-57

Roy, A., Ahuja, S., & Garg, S. (2021). *Fungal Secondary Metabolites: Biological Activity and Potential Applications* (pp. 159–188). https://doi.org/10.1007/978-3-030-60659-6_7

Rubtsova, S. N., Kondratov, R. V., Kopnin, P. B., Chumakov, P. M., Kopnin, B. P., & Vasiliev, J. M. (1998). Disruption of actin microfilaments by cytochalasin D leads to activation of p53. *FEBS Letters*, *430*(3), 353–357. https://doi.org/10.1016/S0014-5793(98)00692-9

Ru, J., Li, P., Wang, J., Zhou, W., Li, B., Huang, C., Li, P., Guo, Z., Tao, W., Yang, Y., Xu, X., Li, Y., Wang, Y., & Yang, L. (2014). TCMSP: a database of systems pharmacology for drug discovery from herbal medicines. *Journal of Cheminformatics*, *6*(1), 13. https://doi.org/10.1186/1758-2946-6-13

Sabbahi, R., Hock, V., Azzaoui, K., Saoiabi, S., & Hammouti, B. (2022). A global perspective of entomopathogens as microbial biocontrol agents of insect pests. *Journal of Agriculture and Food Research*, *10*, 100376. https://doi.org/10.1016/j.jafr.2022.100376

Saito, R., Smoot, M. E., Ono, K., Ruscheinski, J., Wang, P.-L., Lotia, S., Pico, A. R., Bader, G. D., & Ideker, T. (2012). A travel guide to Cytoscape plugins. *Nature Methods*, *9*(11), 1069–1076. https://doi.org/10.1038/nmeth.2212

SCHWARTZMAN, R. A., & CIDLOWSKI, J. A. (1993). Apoptosis: The Biochemistry and Molecular Biology of Programmed Cell Death*. *Endocrine Reviews*, *14*(2), 133–151. https://doi.org/10.1210/edrv-14-2-133

Sen, P., Kandasamy, T., & Ghosh, S. S. (2022). In-silico evidence of ADAM metalloproteinase pathology in cancer signaling networks. *Journal of Biomolecular Structure and Dynamics*, *40*(22), 11771–11786. https://doi.org/10.1080/07391102.2021.1964602

Serrano, M., Lin, A. W., McCurrach, M. E., Beach, D., & Lowe, S. W. (1997). Oncogenic ras Provokes Premature Cell Senescence Associated with Accumulation of p53 and p16INK4a. *Cell*, *88*(5), 593–602. https://doi.org/10.1016/S0092-8674(00)81902-9

Shaikh, F., Tai, H. K., Desai, N., & Siu, S. W. I. (2021). LigTMap: ligand and structure-based target identification and activity prediction for small molecular compounds. *Journal of Cheminformatics*, *13*(1), 44. https://doi.org/10.1186/s13321-021-00523-1

Shankar, J., & Nabi, I. R. (2015). Actin Cytoskeleton Regulation of Epithelial Mesenchymal Transition in Metastatic Cancer Cells. *PLOS ONE*, *10*(3), e0119954. https://doi.org/10.1371/journal.pone.0119954

Shannon, P., Markiel, A., Ozier, O., Baliga, N. S., Wang, J. T., Ramage, D., Amin, N., Schwikowski, B., & Ideker, T. (2003). Cytoscape: A Software Environment for Integrated Models of Biomolecular Interaction Networks. *Genome Research*, *13*(11), 2498–2504. https://doi.org/10.1101/gr.1239303

Shatrohan Lal, R. K. (2014). Synthesis of Organic Nanoparticles and their Applications in Drug Delivery and Food Nanotechnology: A Review. *Journal of Nanomaterials & Molecular Nanotechnology*, *03*(04). https://doi.org/10.4172/2324-8777.1000150

Shen, B., Du, L., Sanchez, C., Edwards, D. J., Chen, M., & Murrell, J. M. (2001). The biosynthetic gene cluster for the anticancer drug bleomycin from Streptomyces verticillus ATCC15003 as a model for hybrid peptide-polyketide natural product biosynthesis. *Journal of Industrial Microbiology and Biotechnology*, *27*(6), 378–385. https://doi.org/10.1038/sj.jim.7000194

Sherman, B. T., Hao, M., Qiu, J., Jiao, X., Baseler, M. W., Lane, H. C., Imamichi, T., & Chang, W. (2022). DAVID: a web server for functional enrichment analysis and functional annotation of gene lists (2021 update). *Nucleic Acids Research*, *50*(W1), W216–W221. https://doi.org/10.1093/nar/gkac194

Shin, T. Y., Bae, S. M., Choi, J. B., & Woo, S. D. (2014). Simple and rapid screening of entomopathogenic fungi having radical-scavenging and anticancer activities. *Journal of Asia-Pacific Entomology*, *17*(3), 543–547. https://doi.org/10.1016/j.aspen.2014.05.002

Singh, P., & Sahoo, S. K. (2022). Piperlongumine loaded PLGA nanoparticles inhibit cancer stem-like cells through modulation of STAT3 in mammosphere model of triple negative breast cancer. *International Journal of Pharmaceutics*, *616*, 121526. https://doi.org/10.1016/j.ijpharm.2022.121526

Singh, S. (2011). Nanoparticle based drug delivery system: Advantages and applications. *Indian Journal of Science and Technology*, *4*(3), 177–184. https://doi.org/10.17485/ijst/2011/v4i3.16

Son, G.-H., Lee, B.-J., & Cho, C.-W. (2017). Mechanisms of drug release from advanced drug formulations such as polymeric-based drug-delivery systems and lipid nanoparticles. *Journal of Pharmaceutical Investigation*, *47*(4), 287–296. https://doi.org/10.1007/s40005-017-0320-1

Song, S., Vuai, M. S., & Zhong, M. (2018). The role of bacteria in cancer therapy – enemies in the past, but allies at present. *Infectious Agents and Cancer*, *13*(1), 9. https://doi.org/10.1186/s13027-018-0180-y

Souto, E. B., Almeida, A. J., & Müller, R. H. (2007). Lipid Nanoparticles (SLN®, NLC®) for Cutaneous Drug Delivery:Structure, Protection and Skin Effects. *Journal of Biomedical Nanotechnology*, *3*(4), 317–331. https://doi.org/10.1166/jbn.2007.049

Spratt, B. G. (1980). Biochemical and genetical approaches to the mechanism of action of penicillin. *Philosophical Transactions of the Royal Society of London. B, Biological Sciences*, *289*(1036), 273–283. https://doi.org/10.1098/rstb.1980.0045

Spudich, J. A., & Lin, S. (1972). Cytochalasin B, Its Interaction with Actin and Actomyosin from Muscle. *Proceedings of the National Academy of Sciences*, *69*(2), 442–446. https://doi.org/10.1073/pnas.69.2.442

Stehn, J., Schevzov, G., O'Neill, G., & Gunning, P. (2006). Specialisation of the Tropomyosin Composition of Actin Filaments Provides New Potential Targets for Chemotherapy. *Current Cancer Drug Targets*, *6*(3), 245–256. https://doi.org/10.2174/156800906776842948

Sun, Y., Liu, Y., Ma, X., & Hu, H. (2021). The Influence of Cell Cycle Regulation on Chemotherapy. *International Journal of Molecular Sciences*, *22*(13), 6923. https://doi.org/10.3390/ijms22136923

Sur, S., Rathore, A., Dave, V., Reddy, K. R., Chouhan, R. S., & Sadhu, V. (2019). Recent developments in functionalized polymer nanoparticles for efficient drug delivery system. *Nano-Structures & Nano-Objects*, *20*, 100397. https://doi.org/10.1016/j.nanoso.2019.100397

Su, X., Zhang, L., Kang, H., Zhang, B., Bao, G., & Wang, J. (2018). Mechanical, nanomorphological and biological reconstruction of early-stage apoptosis in HeLa cells induced by cytochalasin﷿B. *Oncology Reports*. https://doi.org/10.3892/or.2018.6921

Szklarczyk, D., Franceschini, A., Wyder, S., Forslund, K., Heller, D., Huerta-Cepas, J., Simonovic, M., Roth, A., Santos, A., Tsafou, K. P., Kuhn, M., Bork, P., Jensen, L. J., & von Mering, C. (2015). STRING v10: protein–protein interaction networks, integrated over the tree of life. *Nucleic Acids Research*, *43*(D1), D447–D452. https://doi.org/10.1093/nar/gku1003

Tacar, O., Sriamornsak, P., & Dass, C. R. (2012). Doxorubicin: an update on anticancer molecular action, toxicity and novel drug delivery systems. *Journal of Pharmacy and Pharmacology*, *65*(2), 157–170. https://doi.org/10.1111/j.2042-7158.2012.01567.x

Torres, M. (2003). Mitogen-activated protein kinase pathways in redox signaling. *Frontiers in Bioscience*, *8*(4), 999. https://doi.org/10.2741/999

Touwaide, A., & Appetiti, E. (2013). Knowledge of Eastern materia medica (Indian and Chinese) in pre-modern Mediterranean medical traditions: A study in comparative historical ethnopharmacology. *Journal of Ethnopharmacology*, *148*(2), 361–378. https://doi.org/10.1016/j.jep.2013.03.068

Trendowski, M. (2015). Using Cytochalasins to Improve Current Chemotherapeutic Approaches. *Anti-Cancer Agents in Medicinal Chemistry*, *15*(3), 327. https://doi.org/10.2174/1871520614666141016164335

Trendowski, M., Christen, T. D., Acquafondata, C., & Fondy, T. P. (2015). Effects of cytochalasin congeners, microtubule-directed agents, and doxorubicin alone or in combination against human ovarian carcinoma cell lines in vitro. *BMC Cancer*, *15*(1), 632. https://doi.org/10.1186/s12885-015-1619-9

Trendowski, M., Mitchell, J. M., Corsette, C. M., Acquafondata, C., & Fondy, T. P. (2015). Chemotherapy with cytochalasin congeners in vitro and in vivo against murine models. *Investigational New Drugs*, *33*(2), 290–299. https://doi.org/10.1007/s10637-014-0203-5

Trott, O., & Olson, A. J. (2010). AutoDock Vina: Improving the speed and accuracy of docking with a new scoring function, efficient optimization, and multithreading. *Journal of Computational Chemistry*, *31*(2), 455–461. https://doi.org/10.1002/jcc.21334

Tsoutsou, P. G., Zaman, K., Martin Lluesma, S., Cagnon, L., Kandalaft, L., & Vozenin, M.-C. (2018). Emerging Opportunities of Radiotherapy Combined With Immunotherapy in the Era of Breast Cancer Heterogeneity. *Frontiers in Oncology*, *8*. https://doi.org/10.3389/fonc.2018.00609

Upadhayay, A., Pal, D., & Kumar, A. (2022). Salmonella typhi induced oncogenesis in gallbladder cancer: Co-relation and progression. *Advances in Cancer Biology - Metastasis*, *4*, 100032. https://doi.org/10.1016/j.adcanc.2022.100032

Vilcinskas, A., Matha, V., & Götz, P. (1997). Effects of the entomopathogenic fungus Metarhizium anisopliae and its secondary metabolites on morphology and cytoskeleton of plasmatocytes isolated from the greater wax moth, Galleria mellonella. *Journal of Insect Physiology*, *43*(12), 1149–1159. https://doi.org/10.1016/S0022-1910(97)00066-8

Vitetta, E. S., Krolick, K. A., Miyama-Inaba, M., Cushley, W., & Uhr, J. W. (1983). Immunotoxins: A New Approach to Cancer Therapy. *Science*, *219*(4585), 644–650. https://doi.org/10.1126/science.6218613

Wang, H., Zhang, C., Li, M., Liu, C., Wang, J., Ou, X., & Han, Y. (2022). Antimicrobial Peptides Mediate Apoptosis by Changing Mitochondrial Membrane Permeability. *International Journal of Molecular Sciences*, *23*(21), 12732. https://doi.org/10.3390/ijms232112732

Wang, Y., Qin, B., Xia, G., & Choi, S. H. (2021). FDA's Poly (Lactic-Co-Glycolic Acid) Research Program and Regulatory Outcomes. *The AAPS Journal*, *23*(4), 92. https://doi.org/10.1208/s12248-021-00611-y

Wassermann, A. M., & Bajorath, J. (2011). BindingDB and ChEMBL: online compound databases for drug discovery. *Expert Opinion on Drug Discovery*, *6*(7), 683–687. https://doi.org/10.1517/17460441.2011.579100

Weber-Stiehl, S., Järke, L., Castrillón-Betancur, J. C., Gilbert, F., & Sommer, F. (2022). Mitochondrial Function and Microbial Metabolites as Central Regulators of Intestinal Immune Responses and Cancer. *Frontiers in Microbiology*, *13*. https://doi.org/10.3389/fmicb.2022.919424

Weinberg, R. A. (n.d.). *How Cancer Arises on JSTOR*. Retrieved March 1, 2024, from https://www.jstor.org/stable/24993349?seq=2

White, S. R., Williams, P., Wojcik, K. R., Sun, S., Hiemstra, P. S., Rabe, K. F., & Dorscheid, D. R. (2001). Initiation of Apoptosis by Actin Cytoskeletal Derangement in Human Airway Epithelial Cells. *American Journal of Respiratory Cell and Molecular Biology*, *24*(3), 282–294. https://doi.org/10.1165/ajrcmb.24.3.3995

Williams, P. M. (2016). Zeta Potential. In *Encyclopedia of Membranes* (pp. 2063–2064). Springer Berlin Heidelberg. https://doi.org/10.1007/978-3-662-44324-8_612

Wishart, D. S. (2008). DrugBank and its Relevance to Pharmacogenomics. *Pharmacogenomics*, *9*(8), 1155–1162. https://doi.org/10.2217/14622416.9.8.1155

Xi, P., Niu, Y., Zhang, Y., Li, W., Gao, F., Gu, W., Kui, F., Liu, Z., Lu, L., & Du, G. (2022). The mechanism of dioscin preventing lung cancer based on network pharmacology and experimental validation. *Journal of Ethnopharmacology*, *292*, 115138. https://doi.org/10.1016/J.JEP.2022.115138

Yang, P. wen, Xu, P. ling, Cheng, C. shan, Jiao, J. ying, Wu, Y., Dong, S., Xie, J., & Zhu, X. yan. (2022). Integrating network pharmacology and experimental models to investigate the efficacy of

QYHJ on pancreatic cancer. *Journal of Ethnopharmacology*, *297*, 115516. https://doi.org/10.1016/J.JEP.2022.115516

Yao, Y., Zhou, Y., Liu, L., Xu, Y., Chen, Q., Wang, Y., Wu, S., Deng, Y., Zhang, J., & Shao, A. (2020). Nanoparticle-Based Drug Delivery in Cancer Therapy and Its Role in Overcoming Drug Resistance. *Frontiers in Molecular Biosciences*, *7*. https://doi.org/10.3389/fmolb.2020.00193

Yogeswari, S., Kamalraj, S., & Jayabaskaran, C. (2023). A Potential Source of Medicines from Fungi: An Overview of Biologically Active Secondary Metabolites. In *Fungal Resources for Sustainable Economy* (pp. 459–477). Springer Nature Singapore. https://doi.org/10.1007/978-981-19-9103-5_17

Yue, Y.-C., Yang, B.-Y., Lu, J., Zhang, S.-W., Liu, L., Nassar, K., Xu, X.-X., Pang, X.-Y., & Lv, J.-P. (2020). Metabolite secretions of Lactobacillus plantarum YYC-3 may inhibit colon cancer cell metastasis by suppressing the VEGF-MMP2/9 signaling pathway. *Microbial Cell Factories*, *19*(1), 213. https://doi.org/10.1186/s12934-020-01466-2

Zagami, P., & Carey, L. A. (2022). Triple negative breast cancer: Pitfalls and progress. *Npj Breast Cancer*, *8*(1), 95. https://doi.org/10.1038/s41523-022-00468-0

Zaidieh, T., Smith, J. R., Ball, K. E., & An, Q. (2019). ROS as a novel indicator to predict anticancer drug efficacy. *BMC Cancer*, *19*(1), 1224. https://doi.org/10.1186/s12885-019-6438-y

Zardecki, C., Dutta, S., Goodsell, D. S., Lowe, R., Voigt, M., & Burley, S. K. (2022). PDB-101: Educational resources supporting molecular explorations through biology and medicine. *Protein Science*, *31*(1), 129–140. https://doi.org/10.1002/pro.4200

Zeb, A., Gul, M., Nguyen, T.-T.-L., & Maeng, H.-J. (2022). Controlled release and targeted drug delivery with poly(lactic-co-glycolic acid) nanoparticles: reviewing two decades of research. *Journal of Pharmaceutical Investigation*, *52*(6), 683–724. https://doi.org/10.1007/s40005-022-00584-w

Zeeshan Bhatti, M., Ismail, H., & Khan Kayani, W. (2022). Plant Secondary Metabolites: Therapeutic Potential and Pharmacological Properties. In *Secondary Metabolites - Trends and Reviews*. IntechOpen. https://doi.org/10.5772/intechopen.103698

Zhang, H., Yee, D., & Wang, C. (2008). Quantum Dots for Cancer Diagnosis and Therapy: Biological and Clinical Perspectives. *Nanomedicine*, *3*(1), 83–91. https://doi.org/10.2217/17435889.3.1.83

Zhang, L., Chen, Z., Wang, H., Wu, S., Zhao, K., Sun, H., Kong, D., Wang, C., Leng, X., & Zhu, D. (2016). Preparation and evaluation of PCL–PEG–PCL polymeric nanoparticles for doxorubicin

delivery against breast cancer. *RSC Advances*, *6*(60), 54727–54737. https://doi.org/10.1039/C6RA04687H

Zhang, L., Fasoyin, O. E., Molnár, I., & Xu, Y. (2020). Secondary metabolites from hypocrealean entomopathogenic fungi: novel bioactive compounds. *Natural Product Reports*, *37*(9), 1181–1206. https://doi.org/10.1039/C9NP00065H

Zhang, P., Zhang, D., Zhou, W., Wang, L., Wang, B., Zhang, T., & Li, S. (2023). Network pharmacology: towards the artificial intelligence-based precision traditional Chinese medicine. *Briefings in Bioinformatics*, *25*(1). https://doi.org/10.1093/bib/bbad518

Zhao, S., & Li, S. (2010). Network-Based Relating Pharmacological and Genomic Spaces for Drug Target Identification. *PLoS ONE*, *5*(7), e11764. https://doi.org/10.1371/journal.pone.0011764

Zhao, Z., Guo, P., & Brand, E. (2018). A concise classification of bencao (materia medica). *Chinese Medicine*, *13*(1), 18. https://doi.org/10.1186/s13020-018-0176-y

Zhu, D., Tao, W., Zhang, H., Liu, G., Wang, T., Zhang, L., Zeng, X., & Mei, L. (2016). Docetaxel (DTX)-loaded polydopamine-modified TPGS-PLA nanoparticles as a targeted drug delivery system for the treatment of liver cancer. *Acta Biomaterialia*, *30*, 144–154. https://doi.org/10.1016/j.actbio.2015.11.031

Zhu, H., Sarkar, S., Scott, L., Danelisen, I., Trush, M., Jia, Z., & Li, Y. R. (2016). Doxorubicin Redox Biology: Redox Cycling, Topoisomerase Inhibition, and Oxidative Stress. *Reactive Oxygen Species*, 189–198. https://doi.org/10.20455/ros.2016.835

Zhu, S., Wu, Y., Song, B., Yi, M., Yan, Y., Mei, Q., & Wu, K. (2023). Recent advances in targeted strategies for triple-negative breast cancer. *Journal of Hematology & Oncology*, *16*(1), 100. https://doi.org/10.1186/s13045-023-01497-3